47

DYNAMIC RESPONSE OF THIN-WALLED FRAMES

A Thesis

By

NANI BUSHAN ROY

Submitted to the Department of Civil Engineering of Bangladesh University of Engineering and Technology, Dhaka in partial fulfilment of the requirements for the degree

of

MASTER OF SCIENCE IN CIVIL ENGINEERING

বাংলাদেশ প্রকৌশল বিশ্ববিদ্যালয়
নং 75709
তাং 24-10-89
লাইব্রেরী, ঢাকা

September, 1989

#75709#

690.1
1989
ROY

DYNAMIC RESPONSE OF THIN-WALLED FRAMES

A Thesis
By
NANI BUSHAN ROY

Approved as to style and content By:

(Dr. A.M.M. Taufiqul Anwar)
Associate Professor,
Dept. of Civil Engineering,
BUET, Dhaka.
— Chairman

(Dr. Alamgir M. Hoque)
Professor and Head,
Dept. of Civil Engineering,
BUET, Dhaka.
— Member

(Dr. Alamgir Habib)
Professor,
Dept. of Civil Engineering,
BUET, Dhaka.
— Member

(Dr. M. Mizanul Huq)
Managing Director
NEW ERA Consultant Ltd.
Dhaka.
— Member (External)

September, 1989

ABSTRACT

The thesis work presents a general solution scheme for the dynamic response analysis of thin-walled frames subjected to simultaneous action of static and dynamic loads. Consideration of influence of axial forces by introducing geometric stiffness matrix for stiffness modification provides further scope of determining the critical load factor. The investigation takes care of the specific characters of thin-walled sections e.g. the inapplicability of Navier's hypothesis and deviation from Saint-Venant's principle. Property formulation of thin-walled members using finite element approach has been based on introduction of a seventh degree of freedom at each node to take care of the warping of thin-walled sections. The thin-walled frames have been treated as MDOF systems and the response analysis has been carried out by using the Duhamel integral solution and step-by-step integration method separately. The critical buckling load and frequencies have been determined by standard eigen problem solution. A general computer program has been developed for realization of the theoretical solution scheme to provide solution of numerical problems.

Using the developed computer program various numerical examples concerning the dynamic response, critical load and frequency analysis of plane and space framed systems have been solved. A parametric study has been carried out in order to investigate the influence of structure geometry, load increment factor etc. on the displacement response, free vibration frequency and stability of thin-walled plane and space frames. Frequencies of thin-walled systems have been observed to decrease with the increase of static load factor and increasing structure height. The lowest frequency has been found to vanish at a certain load factor termed as critical load factor showing the system to be no more oscillatory beyond this load level. The displacement response on the other hand increases with the increase of static load factor and structure dimensions.

ACKNOWLEDGEMENT

The author expresses his sincere gratitude to Dr. A.M.M. Taufiqul Anwar, Associate Professor of the Department of Civl Engineering, Bangladesh University of Engineering and Technology, Dhaka, under whose supervision this thesis work was carried out. Dr. Anwar extended his helping hand by providing constant guidance, offering valuable suggestions, encouragement and inspiration at every stage of this investigation and in preparation and writing of the thesis. The author wishes to thank Dr. Alamgir M. Hoque, Professor and Head, Department of Civil Engineering for his encouragement and co-operation.

The author is also indebted to Computer Centre staff for their co-operation. The assistance of Mr. M.A. Malek in preparing the thesis is gratefully acknowledged.

NOTATIONS

A	=	Area of cross-section
a	=	Nodal displaement matrix
a_x, a_y	=	Co-ordinates along x and y axis
b	=	Bay width of structure
b_x, b_y	=	Coordinates of torsion center
C	=	Damping matrix of structure
C_{E1}, C_{E2}, etc	=	Components of element damping matrix
C_n	=	Generalized damping
C_x, C_y, C_z	=	Direction cosines of the member axes
C_w	=	Warping constant
d	=	Width of member
d_x, d_y	=	Co-ordinates of pole
E	=	Modulus of elasticity
e_y, e_z	=	Ecentricity of applied load in y and z direction
F_D	=	Damping force vector
F_I	=	Inertia force vector
F_E	=	Elastic force vector
F_x	=	Axial load along x-axis
G	=	Modulus of rigidity
H_k	=	Moment due to nonuniform tangential stress
h	=	Height of structure
I_o	=	Polar moment of inertia

I_y, I_z	=	Moment of inertia about y and z-axes
J	=	Saint Venant's torsion constant
J_1, J_2 etc	=	Nodal forces of joint j
K	=	Overall structure stiffness matrix
$\bar{K}$	=	Combined stiffness matrix
K_E	=	Element stiffness matrix
K_G	=	Geometric stiffness matrix
K_n	=	Generalized stiffness
$k(t)$	=	Incremental stiffness matrix
K_{E1}, K_{E2} etc	=	Components of element stiffness matrix
k_{G1}, k_{G2} etc	=	Components of geometric stiffness matrix
k	=	Relative horizontal and vertical load factor
L	=	Span of beam element
M_n	=	Generalized mass
M_x	=	Twisting moment about shear center axis
M_y, M_z	=	Applied moment about the principal axes
M_{y1}, M_{y2}	=	Nodal moments about y-axis
M_{z1}, M_{z2}	=	Nodal moments about z-axis
m	=	Structure mass matrix
m_E	=	Element mass matrix
m_{E1}, m_{E2} etc.	=	Components of element mass matrix
N_i	=	Shape functions
P	=	Applied static load
P_n	=	Generalized load
$P(t)$	=	Dynamic load

P_{cr}	= Critical value of the applied load
Q_{y1}, Q_{y2}	= Nodal forces along y-axis
Q_{z1}, Q_{z2}	= Nodal forces along z-axis
R	= Component of transformation matrix
T	= Transformation matrix
t	= Time
U	= Strain energy of the system
u,v,w	= Displacement along the three coordinate axes
V	= Potential of the applied loads
V_1	= Potential of the applied loads in the prebuckling deformations
V_2	= Potential of the applied loads in the adjacent equilibrium position.
v(t)	= Dynamic displacement
w'	= Frequency
x,y,z	= The rectangular co-ordinate system
α	= Angle of inclination of the local x and z-axes with the corresponding global axes.
β	= Inclination of local axes with global axes
δ	= Thickness of member
ε	= Damping ratio
ρ	= Density
θ	= Rotation about z-axis = dv/dx
Ψ	= Rotation about y-axis = dw/dx
χ	= $d\phi/dx$

λ	= Load factor
λ_{cr}	= Critical load factor
μ	= Percentage of mass matrix
ϕ	= Angle of twist
σ	= Normal stress
τ	= Shearing stress

CONTENTS

		Page
ABSTRACT		i
ACKNOWLEDGEMENT		iii
NOTATIONS		iv
Chapter 1	GENERAL INTRODUCTION	
1.1	Introduction	1
1.2	Classification of Elements According to Spatial Character	3
1.3	Distinctive Features of Thin-walled Beams	7
1.4	A Review in the Analysis of Structures of Thinwalled Sections.	14
1.5	Objectives of the Study	25
1.6	Scope of the Work	26
Chapter 2	DYNAMIC RESPONSE OF THIN-WALLED FRAMES	
2.1	Introduction	27
2.2	Equation of Motion for MDOF System	28
	2.2.1 Dynamic Equilibrium Condition	29
	2.2.2 Axial force Effects	36
2.3	Evaluation of Structural Property Matrices	38
	2.3.1 Analytical Model of Thin-walled Space Frame Element	39

2.3.2 Elastic Stiffness Matrix 44

2.3.3 Mass Properties 47

2.3.3.1 Consistent Mass Matrix 48

2.3.3.2 Lumped Mass Matrix 59

2.3.4 Damping Properties 61

2.3.5 Geometric Stiffness Matrix 67

2.4 Prebuckling Elastic Analysis 72

2.5 Analysis of Vibration Frequencies 73

2.6 Influence of Axial Forces 76

2.7 Buckling Load 77

2.8 Analysis of Dynamic Response 79

2.8.1 Mode Superposition Method 80

2.8.1.1 Duhamel Integral 84

2.8.2 Step-by-Step Integration Method 85

2.8.2.1 Incremental Equations of Equilibrium 87

Chapter 3 THE COMPUTER PROGRAM

3.1 Introduction 96

3.2 The Solution Scheme 96

3.3 Numbering System for Displacement 99

3.4 Transformation of Axes 104

3.5 Components of the Computer Program 108

3.6 The Subroutines 108

Chapter 4 NUMERICAL ANALYSIS AND DISCUSSIONS

4.1 Introduction 123

4.2 Convergence of the Solution 124

4.2.1 Concentrated Load at Middle of Simply supported Beam 125
4.2.2 Lateral Buckling of a Cantilever Beam 127
4.2.3 Buckling by Pure Torsion 129
4.3 Comparison of Solutions by Step-by-Step Integration and Duhamel Integral 131
4.4 Effect of Axial Force on Dynamic Response 132
4.5 Effect of Damping Ratio on Dynamic Response 136
4.6 Effect of Static Load Factor 139
4.6.1 Effect of Load Factor on Frequency 140
4.6.2 Effect of Load Factor on Response 147
4.7 Influence of Structure Height 151
4.7.1 Plane Framework 152
4.7.2 Portal Frame with Degrees of Freedom Unrestrained in three Dimensions 158
4.7.3 Thin-walled Space Framework 162
4.8 Effect of Simultaneous Variation of Bay Width and Height 167
4.8.1 Effect on Frequency 168
4.8.2 Effect on Critical Load 174
4.8.3 Effect on Dynamic Response 179
4.9 Effect of Relative Vertical and Horizontal Loading 182
4.9.1 Effect on Frequency 183
4.9.2 Effect on Critical Load 186
4.9.3 Effect on Displacement Response 189

4.10 Influence of Warping on Dynamic Response 193

Chapter 5 CONCLUSIONS AND RECOMMENDATIONS FOR FUTURE STUDY

5.1 Conclusions 196

5.2 Recommendations for Future Study 197

REFERENCES 198

CHAPTER 1

GENERAL INTRODUCTION

1.1 INTRODUCTION

Steel frameworks often constitute sections which are not prismatic in nature. These may be better described as thin-walled open or closed sections. The behaviour of such sections essentially differs from that of prismatic ones. The differentiation of the response of framed systems composed of thin-walled open sections from those of prismatic sections needs proper attention and constitutes a subject of special investigation.

The members of any steel framework must be designed for the largest moments, shears, and, in the case of columns, axial loads which can reasonably be expected to occur during the life time of the structure. The axial forces, when large, may tend to cause buckling of the system. The effect of large axial forces on the stiffness of a structure may be significant. In case of thin-walled sections, in addition to the axial forces, the transverse loads acting in planes of maximum rigidity also can modify the stiffness in a sig-

nificant manner. This is due to the tendency of such sections to a out of plane buckling in the plane of minimum rigidity. It is well known that the out of plane deformation of a thin-walled section is featured by a combination of both torsion and flexure. Hence the stiffness modification due to large axial forces and transverse loads in thin-walled members of a framed system is an important factor to be catered. An investigation into the effect of this stiffness modification on the overall response of such structures is a matter of both research interest and practical significance.

The loads, that are generally imposed on structures are either static or dynamic. Standard methods of structural analysis are more concerned with the first type of loading. In one sense static-loading condition may be looked upon merely as a special form of dynamic loading. Dynamic forces may act on a structure in many different ways. For example, a structure supporting an oscillating machinary, a bridge under moving loads or a structure subjected to suddenly applied dynamic forces such as blast or wind gust are all dynamically loaded. Sudden disturbance to a building foundation by some random earthquake activity is also a dynamic load for the building. The analysis of structures for response to the time varying forces is more involved than

that for static loading and this subject needs much work of investigation. In this work, the response analysis of thin-walled space frameworks subjected to arbitrary dynamic loading is undertaken. Investigation has been carried out to study the effect of stiffness modification on response due to high axial forces. Specific behaviour of thin-walled sections in difference to prismatic ones is taken care of.

In what follows, in this chapter distinctive characteristics of thin-walled sections are briefly described. The present state of dynamic analysis of structures composed of thin-walled sections is carefully reviewed in order to formulate the objectives of the present research.

1.2 CLASSIFICATION OF ELEMENTS ACCORDING TO SPATIAL CHARACTER

Conventional engineering structures may be looked upon as an assemblage of structural elements interconnected at a discrete number of nodal points. The basic structural elements can be divided into several categories according to their spatial character. Vlassov (41) has visualized this division by introducing four classes: (1) massive bodies, (2) plates and shells, (3) solid beams, and (4) thin-walled beams.

The first class comprises bodies whose three dimensions are comparable e.g. a sphere, a cube, an ellipsoid or a parallelepiped, in other words an elastic continuum filling all space or a half space.

The second class comprises bodies having one dimension small compared to other two which are of same order of magnitude. Examples are plates, thin slabs, shells of various shapes with wide applications in structural engineering, ship building and aviation industry. The general theory of plates and shells, which includes problems of strength and vibration, is based on geometrical hypotheses, valid for thin deformable bodies within a certain degree of approximation.

Member of the third class identified as solid beams are characterized in that two of their dimensions are of the same order of magnitude and very small compared with the third dimension. A slender parallelepiped may be considered as a solid beam when its two cross-sectional dimensions, width and height do not differ much. To simplify the analysis in investigating the phenomena of flexure and torsion in solid beams, a number of geometrical hypotheses are generally introduced. For example, in case of a beam

deformed by transverse bending and longitudinal extension, of the six components of the strain tensor only one is preserved, corresponding to elongation in the direction parallel to the beam axis. The other five components of the strain tensor are taken to vanish. The law of plane sections popularly known as Navier's hypothesis, which forms the basis of the elementary theory of bending of beams, is a consequence of these geometrical hypotheses. This law states that any cross-section of a beam which is initially plane remains plane after deformation.

In investigating the torsion phenomenon, the so called theory of pure torsion is usually assumed to be valid. The theory is based on the hypothesis that there is no extension or shearing strain in the plane of the cross-section and no longitudinal extension occurs. As a result only shearing stresses arise in the cross-sections of the beam.

The general theory of axial deformation, flexure and pure torsion of beams of solid sections essentially recognizes the applicability of Saint-Venant's principle. Based on this principle and the adopted hypotheses, the resultant vector of all internal forces acting on any cross section may be replaced by an equivalent system of statically equipolent forces without changing the stress or state of strain of the

mathematical model adopted for the solid beams.

It is, therefore, implied that the analysis of all derived structures comprising of beam elements such as two dimensional or three dimensional frames is based on the validity of law of plane sections and pure torsion.

The fourth class of structural elements according of Vlassov comprises bodies which have the form of long prismatic shells. They are characterized by the fact that their three dimensions are all of different order of magnitude. The thickness is small compared with any characteristic dimension of the cross section, and the cross sectional dimensions are smaller compared with the length of the member. These bodies have been grouped separately by Vlassov and were called as thin-walled beams. Rolled, welded, or riveted metallic beams, columns, elements of girders and frames etc. comprises this group. Many spatial engineering structures have such proportions that they can be considered as thin-walled beam structure. Examples are certain types of girder bridges and arched bridges with sufficiently rigid cross ties, suspension bridges having a roadway with a channel or I-section, long reinforced-concrete ribbed, cylindrical or prismatic shell arches, bunkers, pipelines, etc. Metal stringers, frames and other structural members of aircraft

and of ships can also be considered as thin-walled beams.

1.3 DISTINCTIVE FEATURES OF THINWALLED BEAMS

Thin-walled beams differ from the beams of solid sections in that they can undergo longitudinal extension as a result of torsion. The resulting longitudinal strains cause longitudinal normal stresses proportional to them. This leads to an internal equilibrium of the longitudinal forces in each cross section. These complementary longitudinal normal stresses, which arise as a result of the relative warping of the section and which are ignored in the theory of pure torsion, can attain very large values in thin-walled beams with open (rigid or flexible) cross sections and also in beams with closed flexible cross sections. However, a thin-walled beam which has a rigid closed cross section can, in many cases, be considered to behave more like solid beams under combined flexure and torsion. The longitudinal normal stresses due to longitudinal extensions in such beams have a local character. These stresses fall off very rapidly along the beam dictated by Saint-Venant's, principle. If the thin-walled beam has a flexible cross section of closed contour, allowance for complementary stresses associated with the distortion of the section must be made.

The cross-sections of the thin-walled beams do not remain plane after deformation. These beams rather behave as thin-walled space systems undergoing longitudinal deformations due to both bending and torsion. The resulting complementary sectorial stresses may become very high, a fact which causes the thin-walled open sections to have a very low torsional rigidity and therefore specially prone to torsional buckling. Thus torsion associated with sectorial stresses in the cross-sections plays an important role in the destabilization of thin-walled beams by twisting. A thin-walled bar subjected to uniform axial compression may buckle torsionally while its longitudinal axis remains straight. This happens at a load well below its Euler critical load. A pure torsional buckling by uniform axial compression has been illustrated in the example of a doubly symmetric bar in Fig. 1.1. Combined bending and twisting also may occur in axially loaded members whose shear center axis and centroidal axis do not coincide. Example is the axial compression of members such as angles, channels, etc. which lack double symmetry. Due to noncoincidence of the centroid and shear center, the torsion and flexure interact. This again leads to a critical value of load below that for pure Euler buckling case in plane of minimum rigidity.

Combined bending and twisting also occurs in transversely loaded beams when the compression flange becomes unstable and wants to buckle laterally at the same time that the tension flange is stable and wants to remain straight. The net effect is that the entire section rotates and moves laterally as shown in Fig. 1.2. A thin-walled beam loaded in the plane of greatest flexural rigidity buckles laterally at a certain limiting value of P. This limiting value P is its critical value in the sense that it is the smallest load at which the beam can be maintained in equilibrium in a slightly deflected and twisted form.

Vlassov (41) developed a comprehensive theory for the analysis of beams and columns of thin-walled open sections. Vlassov's theory is based on the following geometric and kinematic hypotheses:

i) a thin-walled beam of open section can be considered as a shell of rigid (undeformable) section.

ii) the shearing deformations of the middle surface (characterizing the change in the angle between the coordinate line z = constant, and s = constant) can be assumed to vanish.

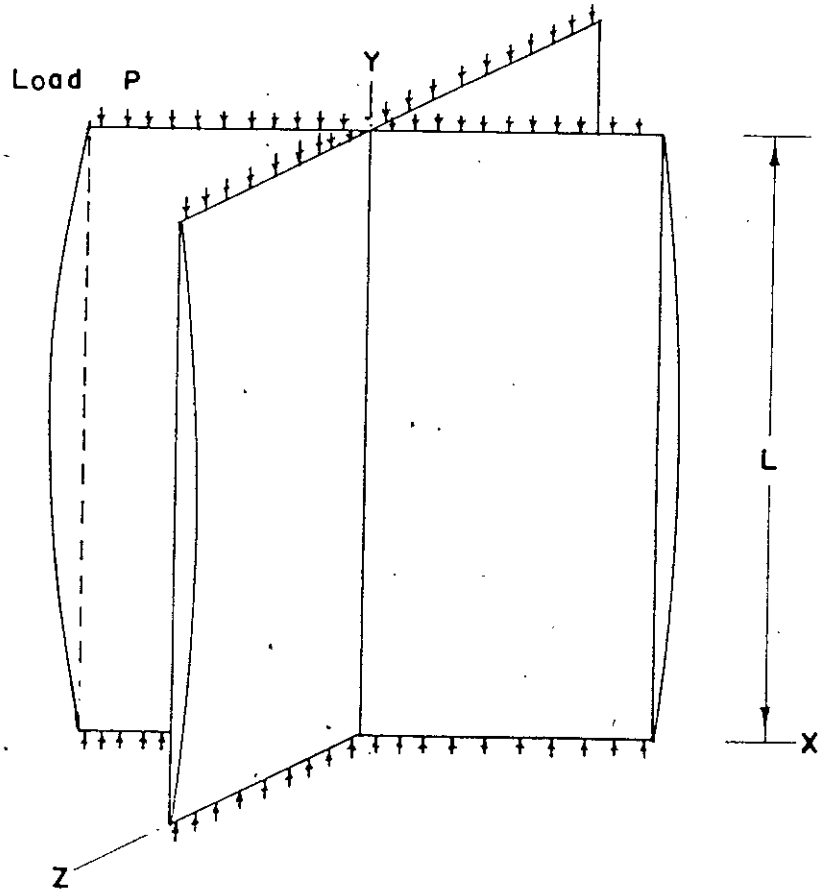

FIG.: 1·1 PURE TORSIONAL BUCKLING OF DOUBLY SYMMETRIC BAR.

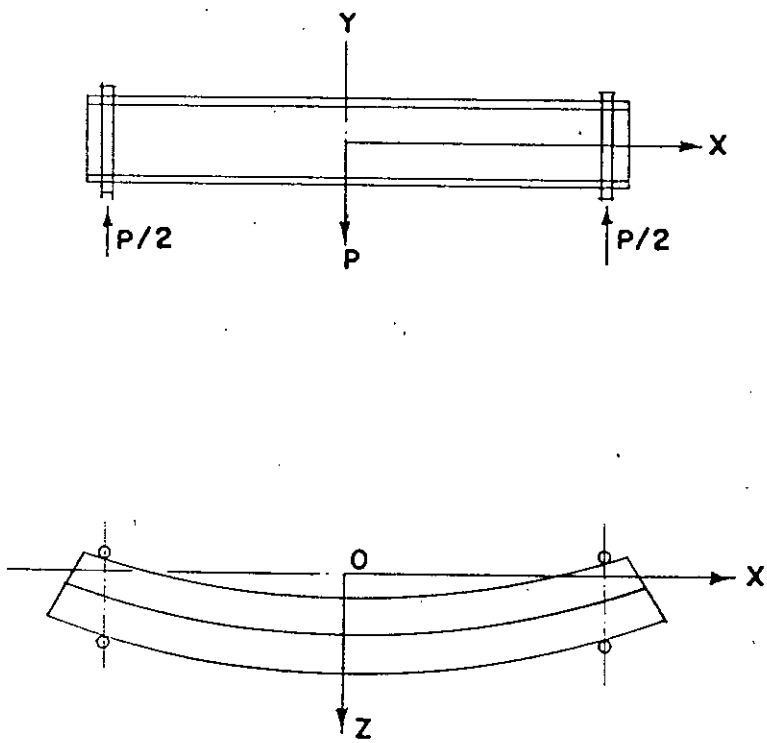

FIG. 1.2 LATERAL BUCKLING OF SIMPLY SUPPORTED BEAM.

iii) the normal stresses are constant over the thickness of the beam and the shearing stresses vary linearly over the wall thickness.

Based on these hypotheses, the normal and shearing stresses were expressed as:

$$\sigma = E(\zeta' - \xi''x - \eta''y - \theta''w)$$

$$\tau(z,s) = [S_0(z) - \int p_z ds - \int \partial\sigma/\partial z \, ds]/\delta$$

and the normal strain as

$$\xi = \zeta' - C\theta'' - [\xi'' + (a_y - d_y)\theta'']x - [\eta'' - (a_x - d_x)\theta'']y - \theta''w_0$$

Vlassov put forward a set of differential equations of motion for vibration of beams of thin-walled open section. These equations are combined for the general case of motion and may be expressed as

$$EJ_y \quad \partial^4\xi/\partial z^4 - \gamma J_y/g \ \partial^4\xi/\partial z^2\partial t^2 + \gamma F/g \ \partial^2\xi/\partial t^2$$

$$+ a_y \gamma F \partial^2\theta/g \partial t^2 = q_x(z,t)$$

$$EJ_x \partial^4\eta/\partial z_4 - \gamma J_x/g \partial^4\eta/\partial z^2\partial t^2 + \gamma F/g \ \partial^2\eta/\partial t^2$$

$$- a_y \gamma F \partial^2\eta/g \ \partial t^2 = q_y(z,t)$$

$$a_y\gamma F\partial^2\xi/g\partial t^2 - a_x\gamma\partial^2\eta/g\partial t^2 + EJ_w\partial^4\theta/\partial z^4 - GJ_d\partial^2\theta/\partial z^2$$

$$- \gamma J_w\partial^4\theta/ g\partial z^2\partial t^2 + \gamma F\partial^2\theta/g\partial t^2 = m_B(z,t)$$

The influence of just described distinctive features of thin-walled sections in the dynamic analysis of framed systems composed of such sections has not yet been given proper attention in existing literature. The present research is devoted to this study.

1.4 A REVIEW IN THE ANALYSIS OF STRUCTURES OF THIN-WALLED SECTIONS

The circumference of knowledge for the structural analysis is continually increasing day by day keeping pace with the development of advanced technology. Engineering structures are required to be designed for strength and checked for stability, so that they are capable enough to carry the external loads safely. The structural analyses, that are mostly performed, are static, stability, and dynamic.
Extreme attention has been given to the static analysis of framed systems from the very beginning such systems came into use and proved its economic usefulness in the engineering field. Now advanced methods and computational techniques are available for the analysis of such systems. Moreover, after the advent of finite element technique, these analyses can be performed most easily by using computers. Framed structures composed of thin-walled members can as well be analysed for static load using this method.

Attention has also been given to the development of stability analysis of structures in general. The stability analysis of thin-walled members of different cross section contours was studied by Vlassov (41) and Timoshenko (37).

They derived differential equations and presented solution techniques for stability analysis of individual thin-walled members of various cross sections subjected to different types of external loads. However, their solutions were confined to simple cases of boundary conditions due to non-availability of suitable displacement functions satisfying complicated boundary conditions. It was further restricted by lack of adequate computational facilities. Essentially, solutions for structures composed of several thin-walled members could not be adequately covered by classical literature.

It is well known that engineering structures are significantly influenced by the dynamic loads caused by wind velocity, wave action, impact effect, bomb blast, earthquake forces etc. The total structural response is developed due to the combined action of static and dynamic loads. So it is required to be able to analyse structures for dynamic loads which is commonly known as dynamic analysis. The dynamic analysis of thin-walled structures has not yet received adequate attention though dynamic analysis of engineering structures in general is drawing more and more attention. As the thin-walled structures are now popularly being used from the economic point of view, it is necessary to extend the scope of dynamic analysis over structures composed of such

members. It is also desirable to give full consideration to their distinctive characters in such analyses.

In what follows, a brief review of historical development in research work for static, stability, and dynamic analysis of framed structures with particular reference to those composed of thin-walled sections is presented.

It has just been mentioned that considerable progress has been achieved in the static analysis of frame structures and the literature covering this aspect is extremely extensive. Many analytical and numerical methods are now available for such analysis. However, the analysis of framed systems subjected to the static load became much easier after the introduction of matrix method of solution. The matrix method of static analysis is mainly based on the formulation of stiffness matrix and consistency of deformation of the structure. Moreover, after the advent of computer facilities and introduction of finite element concept, many works on static analysis started to be published covering solutions of complicated structure.

In 1970, Krajcinovic (25) worked on static analysis of framed systems composed of thin-walled sections. The flexibility, transformation and equilibrium matrices were

derived and two different techniques of matrix force method was presented. He opined that the procedure is applicable for the general case of solid beam assemblage through a limiting process (when the torsional rigidity approaches zero).

In 1981, Vasquer and Riddill (40) presented the stiffness matrix of a thin-walled open section element including the effect of shear strains due to warping. They presented closed form solution for the stiffness coefficients for the case of negligible torsional stiffness.

The analysis of framed systems composed of prismatic sections has been widely covered so far. A detail review of such work will not be presented here. In 1984, for example, Sulata (36) worked on the static analysis problem of reinforced concrete frames subjected to vertical end lateral loadings. A solution technique, based on the finite element method was also presented. The method considers nonlinear behaviour of reinforced concrete plane frames arising out of material nonlinearity and large displacements.

The elastic stability analysis of single beam-columns has been carried out for a long period. During the early stages of tweenteeth century Engessar and Chwalla studied the elas-

tic stability of individual members. Timoshenko (37) and Vlassov (41) have given the earliest solutions for lateral buckling of I-beams. Many researchers like Bleich (19), Khalifa (22), Trahair (39) also studied the stability problem of thin-walled members of different cross sections under different types of loading.

However, the stability analysis of beam-columns and framed systems became more easier after the advent of finite element technique and computer facilities. The finite element buckling analysis of space structures composed of thin-walled members was originally presented by Krajcinovic (24), Barosonm and Gallaghar (5) and Powel and Klinger (30), Krajeinovic based his stiffness and stability matrices upon the solutions of the governing differential equations describing the flexural and torsional behaviour of the linear problem. In other two papers a cubic polynomial was used to describe the lateral displacement and longitudinal axis rotation of beam-column.

In 1970, Powell and Klinger (30) developed a computer program able to determine the elastic critical loads for single continuous wide flange beam for general support conditions, load and variation of cross section. The numerical results were in good agreements with those from test

made by Trahair (39).

The finite element method found its application in the works of Hancock & Trahair (18), Kitipornchai & Ritcher (23), and Hassan (19) to study the buckling behaviour of thin-walled members of different cross sections under various types of loading. In 1985, Hassan developed a computer program for buckling analysis of thin-walled members and showed that the results are in good agreement with the experiments made by him. He also extended his solution for stability analysis of curved thin-walled beams and arches.

Buckling analysis of framed systems with prismatic sections had been given wide attention by many researchers. For example, in 1964, R. Emilio (31) developed some methods for analysis of frames under combined action of vertical and lateral forces and for computation of buckling loads. These methods were generalized and extended further for application to space frame problems and to nonlinear frames for buckling analysis.

In 1965, Le-Wa-Lu (28) studied inelastic buckling of steel frames and showed that a symmetrically loaded frame may buckle in an antisymmetric configuration under critical load. At this instant, the frame losses its resistance to

imposed lateral forces or deformation and failure by buckling thus terminates the load carrying capacity of it.

In 1968, Halldorssan and Wang (17) worked on the stability analysis of rigid frame works by using matrix method of solution. They developed a computer programme with matrix formulation for the solution of buckling load of frames under axial load in the primary condition.

Gold berg (16), in 1968 presented an approximate theory of buckling analysis for multistory frames having shear bracing in the form of a vertical truss. He derived some governing equations considering the effects of shear stiffness of bracing and flexural stiffness of girder. Solutions to the system of governing equations were given in closed form for the case in which the frame and the loading have certain regular characteristics. These solutions lead to formulae for the required girder stiffness when the bracing stiffness column sizes and axial loads are prescribed.

In 1980, Razzaq & Mossa (34) studied instability of rigid jointed, unbraced, single story, single bay orthogonal space frames subjected to static load at column top. The columns were assumed to be fixed at the base. They investigated the influence on the frame behaviour of the relative magnitude

of the load multiplication factors for the columns and the orientation of the principle axes of the column cross section. The instability loads are also compared with those obtained approximately using the effective lengths approach.

Charles & Jerome (11) studied the different factors influencing the stability limit load of structural steel building frames. The manner in which these can be accounted in formulating the structural stiffness matrix are described, so that an evaluation of the determinant of this matrix may be a better index of frame stability.

The history of dynamic analysis started through the development of vibration analysis concept. Now advanced methods and solution techniques are available based on the use of continually developing computer facilities. The dynamic analysis of framed systems may be performed considering it as an assemblage of individual members. Findings of some recent works on dynamic analysis of individual members and framed systems are summarized here.

Valassov (41) derived the governing differential equation for forced vibration of thin walled members using the free vibration concept. He used an element of thin-walled cross section and derived the differential equation giving proper

consideration for warping displacement. Timoshenko (37), in 1955, also worked on vibration analysis of isolated members. Frequencies and displacements were computed by solving the governing differential equations.

In 1960, Snitko (35) worked on the dynamic analysis of rigid frames by using force method suggested by Prager. However, he did not put forward any solution for dynamic resposne analysis of rigid frames. In 1963, Levien & Hurtz (27) used this force method for the dynamic analysis. They modified the force method and extended it to the dynamic analysis of multistory rigid frames.

In 1963, Burch (10) worked on dynamic analysis of framed systems in general by using the stiffness method. He used the finite element concept to develop the stiffness matrix and the dynamic problem was solved by using digital computer. The stiffness method of dynamic analysis has also been used by Clough (12) in 1962 for MDOF systems.

In 1964, Arthur, Sing, & Johon (2) analyzed the dynamic response of multistory elastic plastic frames. The equations of motion were solved by a single step forward numerical procedure.

In 1963, Bailey (4) studied the problem of dynamic bending of a elastic pin-ended column using the large deflection theory and including axial inertia terms. Equations were derived for the motion of a column that was initially slightly curved with one end displaced axially towards the other and Numerical solutions of these equations were obtained by solving corresponding differential equations on a digital computer.

In 1964, Rawlings (33) analysed a rigid portal steel frame subjected to a pulse of loading assuming the material to have rigid plastic characteristics. He examined the influence of strain hardening of the material and of large changes of structural geometry on the motion.

In 1970, Leimbach & Donald (26) worked on free vibration of two dimensional frame works considering concentrated masses and inertias at the joints. For spacific boundary conditions transcendental equations for the free vibration frequencies and solutions for model functions were obtained in the form of discrete trigonometric functions.

Using the lumped mass system, Arthur (1), in 1970, determined the dynamic response of floodlight tower subjected to time varing wind load. All computations were performed on a

digital computer and the computed results compared fairly well with observed responses.

Basu, Nagpal & Nagar (6), in 1981, worked on frame wall systems subjected to dynamic loading. The results of the analysis have been obtained by the exact numerical solution of the resulting differential equation interms of lateral displacement.

Maison and Neuss (29) worked on dynamic analysis of an existing 44 story steel frame high rise building to study the influence of various modeling aspects on the predicted dynamic properties and computed seismic response behaviour.

In 1985, Torkamoni (32) performed an analysis of dynamic response of 15-story building subjected to wind loading to study the importance of torsional dynamic response coupled with translation response. He used finite element modeling to assemble the stiffness matrix of the structure. He studied the comparison between the finite element and equivalent cantilever model.

It was observed from the review above that the dynamic analysis of rigid frames of prismatic sections have drawn attention of different researchers. However, the available

now literature do not give answers to many problems related to dynamic analysis of thin-walled beam assemblages including framed systems composed of thin-walled sections.

1.5 OBJECTIVES OF THE STUDY

The purpose of the present work is to develop a solution scheme for the dynamic response analysis of thin-walled plane and space frame works using finite element approach. It is also intended to undertake a parametric study including axial force effect in members of such systems. The principal objectives are:

1) To formulate a theoretical approach for the dynamic response analysis of loaded thin-walled space frame works.

2) To develop a general computer program for the response analysis of thin-walled space frameworks subjected to static and dynamic loads.

3) To study the influence of axial and lateral forces on the response by introducing the geometric stiffness of thin-walled system and to determine the critical load factor.

4) To investigate the effect of different parameters such as

structure geometry, load increment factor, etc. on the dynamic response and free vibration frequency.

1.6 SCOPE OF THE WORK

Based on the finite element method, the structural property matrices for thin-walled space frame elements are formulated. Using these structural property matrices, the theoretical approach for dynamic response of thin-walled space frame works, considering it as a multidegree of freedom system, is developed in chapter 2. The determination of dynamic response by using the Duhamel integral and step-by-step integration method is also discussed in this chatper. Based on the theoretical derivations in chapter 2, a general computer program for dynamic analysis of thin-walled space frameworks is developed in chapter 3. The influence of static load factor, structural property etc. on the dynamic response is investigated and their graphical representations are shown in chapter 4.

Finally, from the investigations, carried out in chapter 4, conclusions, and recommendations for future study of dynamic response of thin-walled space frameworks are given in chapter 5.

CHAPTER 2

DYNAMIC RESPONSE OF THIN-WALLED FRAMES

2.1 INTRODUCTION

From the review of the available works presented in Chapter 1, it is seen that the problem of dynamic response of thin-walled framed systems deserves proper attention. The partial differential equations of motion presented by Vlassov and discussed in detail in the preceeding chapter are applicable only to the dynamic problems of individual thin-walled members. Moreover, the equations have serious drawback in that they can be solved only for a limited cases of boundary conditions. This is because, choosing appropriate displacement functions, satisfying all given static and kinematic boundary conditions at a time is an extremely difficult job and mostly a formiddable one. With this limitation, the differential equations of motion for thin-walled beams can not be directly used for solving complicated sytems composed of considerable number of thin-walled members. It will be therefore appropriate to treat a space framework composed of thin-walled members as a discrete multiple degree of freedom system. If the structural property matrices of an individual member can be formulated first, the remaining part of the solution

will be to follow standard procedure for a MDOF system. In this chapter, the job of formulating the structural property matrices for thin-walled framed systems is undertaken. This includes the formulation of the elastic stiffness matrix, the geometric stiffness matrix, the mass matrix, and the damping matrix. The geometric matrix is formulated to take care of the axial force effect which plays an important role in causing the instability of thin-walled members in particular. The property matrices are obtained by choosing appropriate shape functions and then following a finite element procedure. Dynamic displacements of thin-walled space frame-works can be determined by the dynamic response analysis procedure described in this chapter. The method of determining the vibration frequencies and buckling loads for such frameworks is also formulated.

2.2 EQUATION OF MOTION FOR MDOF SYSTEM

If the physical property of the system is such that its motion can be defined by a single co-ordinate then it actually is a SDOF system and the dynamic response of such a SDOF system can be evaluated by the solution of a single differential equation of motion. However, if the structure has more than one possible mode of displacement i.e if the structure is considered as a multiple degrees of freedom system, then the dynamic response analysis can be performed using a set of equations of motion and the total

number of such equations will be the same as the number of degrees of freedom of the structure. Each equation is formulated corresponding to each degree of freedom. One of the greatest disadvantage of the single degree of freedom approximation is that it is difficult to assess the reliability of the result obtained from it.

In general, the dynamic response of a structure can not be described adequately by a single degree of freedom model; usually the response includes time variation of the displacement shape as well as its amplitude. Such behaviour can be described only in-terms of more than one displacement coordinate, that is, the motion must be represented by more than one degree of freedom. As noted earlier, the degrees of freedom in a discrete parameter system may be taken as the displacement amplitudes of certain selected points in the structure, or they may be generalized coordinates representing the amplitude of a specified set of displacement patterns. In the present discussion, the procedure of development of equations of motion of a MDOF system is illustrated.

2.2.1 Dynamic Equilibrium Condition

In deriving the equations of motion of a general multiple degrees of freedom system, it will be convenient to refer to the general

simple beam shown in Fig. 2.1 as a typical example. The discussion applies equally to any type of structure, but the visualization of the physical factors involved in evaluating all the forces acting is simplified for the type of structure shown here. The motion of this structure will be assumed to be defined by the displacements of a set of discrete points $v_1(t)$, $v_2(t)$ ...$v_i(t)$ ..... $v_n(t)$, on the beam. In principle, these points may be located arbitrarily on the structure, in practice, they should be associated with some significant specified features of the physical properties and should be distributed so as to provide a good representation of the deflected shape. The number of degrees of freedom to be considered depends upon the degree of accuracy desired; greater numbers provide better approximation of the true dynamic behaviour. In the beam of Fig. 2.1, only one displacement component has been associated with each nodal point of the beam. It should be noted, however, that several displacement components could be identified with each point; e.g. the rotation and longitudinal motions might be used as addition of degrees of freedom at each node.

The equation of motion of the system of Fig. 2.1 can be formulated by expressing the equilibrium of the effective forces associated with each of its degree of freedom. In general, four types of forces will be involved at any point i, the externally applied force $P_i(t)$ and the forces resulting from the motion,

that is F_{Ii}, damping force F_{Di} and elastic force F_{Si}. Thus for each of the several degrees of freedom the dynamic equilibrium conditions may be expressed as

$$
\begin{aligned}
F_{I1} + F_{D1} + F_{S1} &= P_1(t) \\
F_{I2} + F_{D2} + F_{S2} &= P_2(t) \\
F_{I3} + F_{D3} + F_{S3} &= P_3(t)
\end{aligned}
\qquad (2.1)
$$

or when the force vectors are represented in matrix form the above equations may be combinedly expressed as

$$F_I + F_D + F_S = P(t) \qquad (2.2)$$

Each of the resisting forces may be expressed most conveniently by means of an appropriate set of influence co-efficients. When for example, the elastic force component developed at point 1 be considered, this depends, in general, upon the displacement components developed at all points of structure. Thus

$$F_{S1} = K_{11}v_1 + K_{12}\ v_2 \ldots\ldots + K_{1N}v_N \qquad (2.3a)$$

Similarly, the elastic force corresponding to degree of freedom v_2 is

$$F_{S2} = K_{21}v_1 + K_{22}v_2 + \dots\dots\dots + K_{2N}v_N \qquad (2.3b)$$

and in general

$$F_{Si} = K_{i1}v_2 + K_{i2}v_2 + \dots\dots\dots + K_{iN}v_N \qquad (2.3c)$$

In these expressions it has been assumed that the structural behaviour is linear, so that the principle of superposition applies. The coefficients kij are called stiffness influence coefficients and defined as the force corresponding to coordinate i due to a unit displacement of co-ordinate j. In matrix form the complete set of elastic force relationships may be written as

$$\begin{bmatrix} F_{S1} \\ F_{S2} \\ \cdot \\ F_{Si} \end{bmatrix} = \begin{bmatrix} K_{11} & K_{12} & K_{1j} & K_{1N} \\ K_{21} & K_{22} & K_{2j} & K_{2N} \\ \cdot & \cdot & \cdot & \cdot \\ K_{i1} & K_{i2} & K_{ij} & K_{iN} \end{bmatrix} \begin{bmatrix} V_1 \\ V_2 \\ \cdot \\ V_i \end{bmatrix} \qquad (2.4)$$

or symbolically $\{F_s\} = [K]\ (v)$ (2.5)

in which the matrix of stiffness coefficients K is called the elastic stiffness matrix of the structure and v is the displacement vector representing the deflected shape of the structure.

If it is assumed that the damping forces depends on the velocity, that is viscous type, the damping forces corresponding to the selected degrees of freedom may be expressed by means of damping influence co-efficients in similar fashion. By analogy, the complete set of damping forces is given by

$$\begin{bmatrix} F_{D1} \\ F_{D2} \\ \cdot \\ F_{Di} \end{bmatrix} = \begin{bmatrix} C_{11} & C_{12} & C_{1j} & C_{1N} \\ C_{21} & C_{22} & C_{2j} & C_{2N} \\ \cdot & \cdot & \cdot & \cdot \\ C_{i1} & C_{i2} & C_{ij} & C_{iN} \end{bmatrix} \begin{bmatrix} \dot{V}_1 \\ \dot{V}_2 \\ \cdot \\ \dot{V}_i \end{bmatrix} \qquad (2.6)$$

in which $\dot{v}_i$ represents the time rate of change of the ith displacement coordinate and the co-efficients c_{ij} are called damping

influence coefficients. These co-efficients may be defined in an analogous fashion as that for stiffness influence coefficients k_{ij}. Hence, C_{ij} is the force corresponding to coordinate i due to unit velocity of coordinate j. Symbolically, Eq. 2.6 may be written as

$$\{F_D\} = [C](\dot{V}) \tag{2.7}$$

in which the matrix of damping coefficients c is called the damping matrix of the structure and v is called the velocity vector.

The inertia forces may also be expressed by a set of influence coefficients called the mass co-efficients. These represent the relationship between the acceleration of the degrees of freedom and the resulting inertia forces. By analogy, the inertia forces may be expressed as

$$\begin{bmatrix} F_{I1} \\ F_{I2} \\ \cdot \\ F_{Ii} \end{bmatrix} = \begin{bmatrix} m_{111} & m_{12} & m_{1j} & m_{1N} \\ m_{21} & m_{22} & m_{2j} & m_{2N} \\ \cdot & \cdot & \cdot & \cdot \\ m_{i1} & m_{i2} & m_{ij} & m_{iN} \end{bmatrix} \begin{bmatrix} \ddot{v}_1 \\ \ddot{v}_2 \\ \cdot \\ \ddot{v}_i \end{bmatrix} \tag{2.8}$$

where $\ddot{V}_i$ is the acceleration of the degree of freedom corresponding to the coordinate i and the coefficients m_{ij} are the mass influence coefficients defined as the force corresponding to coordinate i due to unit acceleration of the coordinate j. Simbolically, Eq. 2.8 may be written as

$$\{F_I\}=[m](\ddot{V}) \qquad (2.9)$$

in which the matrix of mass coefficients m is called the mass matrix of the structure, $\ddot{v}$ is the acceleration vector and F_I is the force of inertia vector.

Now substituting Eqs. 2.5, 2.7, and 2.9 into Eq. 2.2, the complete dynamic equilibrium of the structure, considering all degrees of freedom becomes

$$m\ddot{v} + C\,\dot{v} + K\,v = P(t) \qquad (2.10)$$

The foregoing equation is the equation of motion for MDOF system and is equivalent to the corresponding equation for a SDOF system. The order of the matrices in Eq. 2.10 corresponds to the number of degrees of freedom used in describing the displacements

of the structure. Thus, Eq. 2.10 express the N equations of motion which serve to define the response of a multiple degrees of freedom system.

2.2.2 Axial Force Effects

From the review of literature, it was observed that axial forces or any load which may tend to cause buckling of a structure may have significant effect on the stiffness of the structure. This phenomena is valid for both SDOF and MDOF systems. The load components acting parallel to the axis of the members lead to additional load components corresponding to the nodal degrees of freedom denoted by F_G. When these forces are included, the dynamic equilibrium equation modifies to

$$\bar{F}_I + \bar{F}_D + \bar{F}_S - \bar{F}_G = \bar{P}(t) \qquad (2.11)$$

in which the negative sign results from the fact that the forces F_G are assumed to contribute to the deflection rather than to oppose it.

These forces resulting from axial loads or any load which tends to cause buckling depends on the displacement of the structure and may be expressed by influence co-efficients, called geometric

stiffness coefficients, as follows:

$$\begin{bmatrix} F_{G1} \\ F_{G2} \\ \cdot \\ F_{Gi} \end{bmatrix} = \begin{bmatrix} F_{G11} & F_{G12} & F_{G1j} & F_{G1N} \\ F_{G21} & F_{G22} & F_{G2j} & F_{G2N} \\ \cdot & \cdot & \cdot & \cdot \\ F_{Gi1} & F_{Gi2} & F_{Gij} & F_{GiN} \end{bmatrix} \begin{bmatrix} v_1 \\ v_2 \\ \cdot \\ v_2 \end{bmatrix} \qquad (2.12)$$

in which the geometric stiffness influences coefficients K_{Gij} is defined as the force corresponding to coordinate i due to unit displacement of coordinate j and resulting from axial force components in the structure. Symbolically, Eq. 2.12 may be written as

$$\{F_G\} = [K_G]\ (v) \qquad (2.13)$$

where $[K_G]$ is called the geometric stiffness matrix of the structure. When this expression is introduced, the equation of dynamic equilibrium of the structure becomes

$$m\ddot{v} + c\dot{v} + Kv - K_G v = P(t) \qquad (2.14)$$

or when it is noted that both the elastic stiffness and the geometric stiffness are multiplied by the displacement vector, the combined stiffness matrix can be expressed by a single symbol and Eq. 2.14 may be written as

$$m\ddot{v} + c\dot{v} + Kv = P(t) \qquad (2.15)$$

in which $\bar{K} = K - K_G$ (2.16)

$\bar{K}$ is called the combined stiffness matrix, which includes both elastic and geometric effects. The dynamic properties of the structure are expressed completely by the four influence coefficient matrices while the dynamic loading is fully defined by the load vector.

2.3 EVALUATION OF STRUCTURAL PROPERTY MATRICES

From the equation of motion that has been developed in the foregoing article, it is clear that the structural properties, which are generally considered in the dynamic analysis, are mass

matrix, elastic stiffness matrix, damping matrix and geometric stiffness matrix. In principle, these properties associated with any prescribed set of nodal displacements can be obtained by direct application of their definition. In practice, however, the finite element procedure, frequently provides the most convenient means for evaluating the structural properties. By this approach, the structure is assumed to be divided into a system of discrete elements which are interconnected only at a finite number of nodal points. The properties of the complete structure are then found by evaluating the properties of the individual finite elements and assembling them appropriately.

2.3.1 Analytical Model of Thin-walled Space Frame Element

In the conventional theory of bending of bars, longitudinal deformations are obtained from Navier's hypothesis which states that, during bending, plane cross sections will remain plane. This hypothesis is, however, abandoned in this analysis as the cross section will warp if a bar of thin-walled open section is twisted. But it is assumed that Navier's hypothesis remains valid for each of the flat plates of which the bar is composed. This appears to be justified as the thickness of the plate is very small and the centre line of the cross-section of a thin plate remains in a plane during torsion. The other assumption adopted for this analysis presume that during buckling applied loads

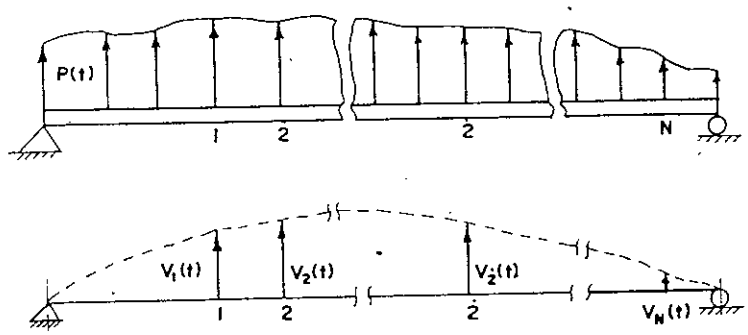

FIG. 2.1 DISCRETIZATION OF A GENERAL BEAM TYPE STRUCTURE.

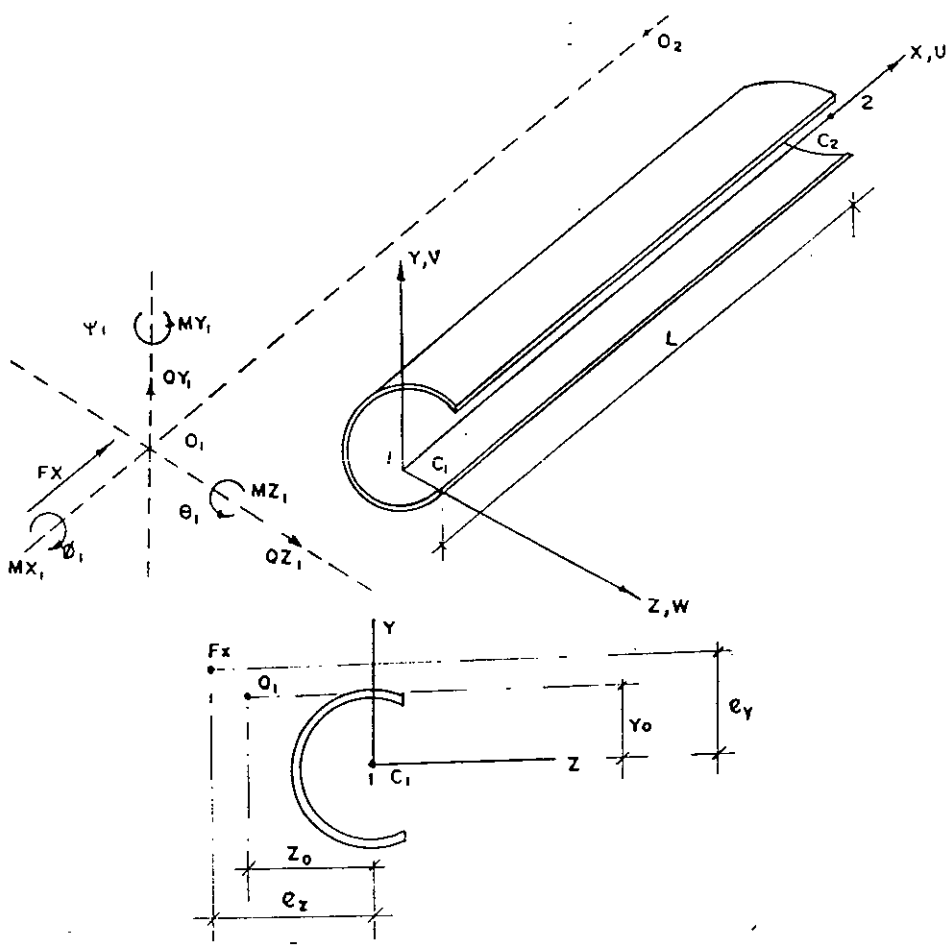

FIG. 2.2 TYPICAL THINWALLED ELEMENT

remain constant in magnitude and direction but move perpendicular to the original structure.

An element of thin-walled member between the nodes 1 and 2 of the body is shown in Fig. 2.2. The rectangular coordinate system x,y,z is so chosen that y and z axes coincide with the principle axes of the cross section of the element and x axis coincides with the centroidal axis C_1-C_2 before buckling. The shear centres of the cross sections at nodes 1 and 2 are denoted by O_1 and O_2 and the dotted line through these points represents the shear centre axis. The element is acted upon by an axial force F_x with ecentricities e_y and e_z with respect to the centroid. End forces and end moments corresponding to y and z axes are Q_{y1}, Q_{y2}, Q_{z1}, Q_{z2}, M_{y1}, M_{y2}, M_{z1}, M_{z2} respectively. Here the number 1 and 2 refer to the node where the force or moment is acting. There is also a torque M_x which acts about shear centre axis. All these forces together form load vector. The displacement vector is composed of the axial displacement u, displacements v and w of the shear centre axes in y and z directions respectively, the angle of twist ϕ, about the shear centre axis and also θ, Ψ and χ which are defined as

$$\theta = dv/dx, \qquad \Psi = dw/dx, \qquad \chi = d\ /dx \qquad (2.17)$$

Thus from the above discussion it is clear that the degrees of

freedom developed at any end of a thin-walled space frame element is seven. So a thin-walled space frame element is a fourteen degrees of freedom system.

The displacement functions are so chosen that the appropriate nodal displacements are obtained when the coordinates of the appropirate nodes are inserted. In general, the displacements are assumed as

$$a = N_i a_i \tag{2.18}$$

where N_i are the prescribed functions, called shape functions and a_i represent a listing of nodal displacements for a particular element. As a matter of fact, the N_i's describe the displacement field for a unit value of the joint displacement a_i when all other joint displacements are suppressed. These parameters are functions of co-ordinate x. For a beam element, the shape functions are derived by Zeinkiewicz (44) for flexural analysis and he assumed a cubic expression for the deflected shape of the element. Accordingly, the independent displacements u,v,w and for the present analysis will be adopted as

$$U = \begin{bmatrix} 1 - x/L & x/L \end{bmatrix} \begin{bmatrix} u1 \\ u2 \end{bmatrix} = \begin{bmatrix} Nu \end{bmatrix} \begin{bmatrix} u1 & u2 \end{bmatrix}^T \tag{2.19}$$

$$V = \begin{bmatrix} 1+2(x/L)^3 - 3(x/L)^2 & 3(x/L)^2 - 2(x/L)^3 & -x(x/L-1)^2 & -x(x/L)^2 - x/L \end{bmatrix} \begin{bmatrix} V_1 \\ V_2 \\ \theta_1 \\ \theta_2 \end{bmatrix} \tag{2.20}$$

$$= [Nv] \; [V_1 \quad V_2 \quad \theta_1 \quad \theta_2]^T$$

$$W = \begin{bmatrix} 1+2(x/L)^3 - 3(x/L)^2 & 3(x/L)^2 - 2(x/L)^3 & -x(x/L-1)^2 & -x(x/L)^2 - x/L \end{bmatrix} \begin{bmatrix} W_1 \\ W_2 \\ \psi_1 \\ \psi_2 \end{bmatrix} \tag{2.21}$$

$$= [Nw] \; [W_1 \quad W_2 \quad \psi_1 \quad \psi_2]^T$$

$$\phi = \begin{bmatrix} 1+2(x/L)^3 - 3(x/L)^2 & 3(x/L)^2 - 2(x/L)^3 & -x(x/L-1)^2 & -x(x/L)^2 - (x/L) \end{bmatrix} \begin{bmatrix} \phi_1 \\ \phi_2 \\ \chi_1 \\ \chi_2 \end{bmatrix} \tag{2.22}$$

$$= [N\phi] \; [\phi_1 \quad \phi_2 \quad \chi_1 \quad \chi_2]^T$$

In the above expression it is assumed

$$\theta_1 = \left(\frac{dv}{dx}\right)_1 \qquad \theta_2 = \left(\frac{dv}{dx}\right)_2$$

$$\psi_1 = \left(\frac{dw}{dx}\right)_1 \qquad \psi_2 = \left(\frac{dw}{dx}\right)_2$$

$$\chi_1 = \left(\frac{d}{dx}\right)_1 \qquad \chi_2 = \left(\frac{d}{dx}\right)_2$$

Now by using these shape functions, the structural properties of a thin-walled space frame element are formulated in the following articles.

2.3.2 Elastic Stiffness Matrix

The physical meaning of the stiffness influence co-efficients of the element represent the nodal forces due to nodal displacements. This is illustrated for a few degrees of freedom in Fig. 2.3. They represent the forces developed in the structure when a unit displacement corresponding to a particular degree of freedom is introduced and no other nodal displacement is permitted. It should be noted that the stiffness influence coefficients in Fig. 2.3 are numerically equal to the applied forces required to maintain the specified displacement condition. They are positive when the sense of the applied force corresponds to a positive displacement, and negative otherwise.

There are several methods available in the literature by which the stiffness matrix of a thin-walled space frame element can be formulated. The procedure used here is strainenergy method. The strain energy stored in any structure may be expressed con-

veniently in terms of either flexibility or the stiffness matrix. The strain energy U for a prismatic member from the nonlinear strain displacement relatiionship is shown by Gallagher. The general expression of the strain energy for the analytical model in Fig. 2.2 was obtained by Bleich (9), which is

$$U = \frac{1}{2} \int (EI_z v''^2 + EI_y w^2 + EC_w \phi''^2 + GJ \phi'^2 + EAu'^2) \, dx \quad (2.23)$$

here U = strain energy

u,v,w = displacements in the x, y and z direction respectively

= twisting angle

I_z, I_y = moments of inertia about principle axes.

Now, substitution of the displacement functions given by Eq. 2.19 to Eq. 2.22 into Eq. 2.23 gives the following transformed expression for strain energy U. Thus,

$$U = \frac{[u_1 \; u_2]}{2} \left\{ \int [N'_u]^T [N'_u] \, EA \, dx \right\} [u_1 \; u_2]^T$$

$$+ \frac{[v_1 \; v_2 \; \theta_1 \; \theta_2]}{2} \left\{ \int [N''_v]^T [N''_v] \, EI_z dx \right\} [v_1 \; v_2 \; \theta_1 \; \theta_2]^T$$

$$+ \frac{[w_1 \; w_2 \; \Psi_1 \; \Psi_2]}{2} \left\{ \int [N''_w]^T [N''_w] \, EI_y dx \right\} [w_1 \; w_2 \; \Psi_1 \; \Psi_2]^T$$

$$+ \frac{[\phi_1 \quad \phi_2 \quad \chi_1 \quad \chi_2]}{2} \{ \int [N''_\phi]^T [N''_\phi] \quad EC_w dx$$

$$+ \int [N'_\phi]^T [N'_\phi] \quad GJ\, dx \} [\phi_1 \quad \phi_2 \quad \chi_1 \quad \chi_2]^T$$

$$= \frac{1}{2} [a] \begin{bmatrix} K_{E1} & 0 & 0 & 0 \\ 0 & K_{E2} & 0 & 0 \\ 0 & 0 & K_{E3} & 0 \\ 0 & 0 & 0 & K_{E4} \end{bmatrix} [a]^T \qquad (2.24)$$

where [a] represents the displacement matrix and is given by

$$[a] = [u_1 \quad u_2 \quad v_1 \quad v_2 \quad \theta_1 \quad \theta_2 \quad w_1 \quad w_2 \quad \psi_1 \quad \psi_2 \quad \phi_1 \quad \phi_2 \quad \chi_1 \quad \chi_2]$$

and

$$K_{E1} = \int \left[N_u'\right]^T \left[N_u'\right] EA \; dx$$

$$K_{E2} = \int \left[N_v''\right]^T \left[N_v''\right] EI_x \, dx$$

$$K_{E3} = \int \left[N_w''\right]^T \left[N_w''\right] EI_y \, dx$$

$$K_{E4} = \int \left\{ \left[N_\phi''\right]^T \left[N_\phi''\right] EC_w + \left[N_\phi'\right]^T \left[N_\phi'\right] GJ \right\} dx$$

The second matrix of Eq. 2.24 consisting of K_{E1}, K_{E2} K_{E3}, K_{E4} is the element stiffness matrix and is represented by K_E

2.3.3 Mass Properties

The mass matrix formulation presented first by Archer (3) can be expressed as

$$\left[m\right]^e = \iiint_V \rho \left[N\right]^T \left[N\right] dv \qquad (2.25)$$

in which, ρ = density

N = shape functions

This is called the consistent mass matrix of an element because the same displacement model which is used for deriving the element stiffness is used for the derivation of mass matrix. It is of interest to note that several dynamic problems have been and are being solved with simpler forms of mass matrices. The simplest form of mass matrix that can be used is that obtained by placing point mass m_i at node points i in the direction of assumed displacement degrees of freedom. This is called the lumped mass matrix. In this article both the consistent and lumped mass procedures are described.

2.3.3.1 Consistent Mass Matrix

Making use of the finite element concept, it is possible to evaluate mass influence coefficients for each element of a structure by a procedure of virtual work method. For this purpose, the nonuniform beam segment shown in Fig. 2.4. is considered. The degrees of freedom of the segment are the translation and rotation at each end and it will be assumed that the displacements within the span are defined by the same interpolation functions $N_i(x)$ used in deriving the element stiffness. If the beam were

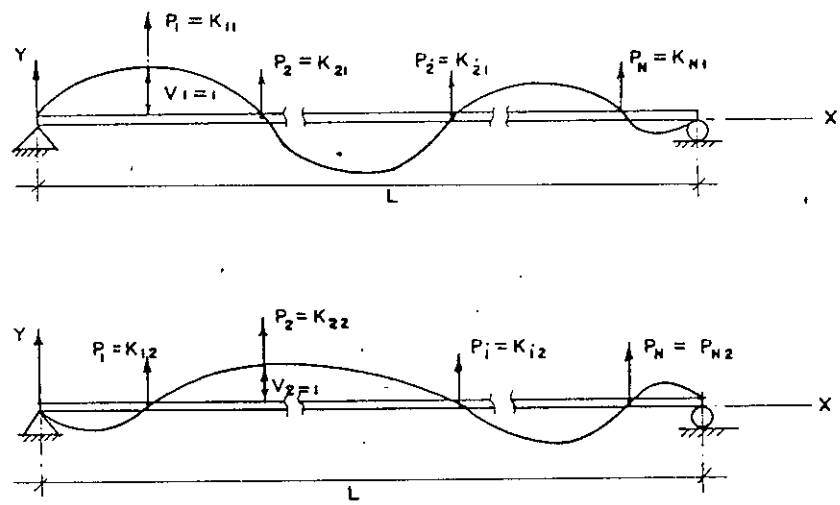

FIG. 2.3 DEFINITION OF STIFFNESS INFLUENCE CO EFFICIENTS

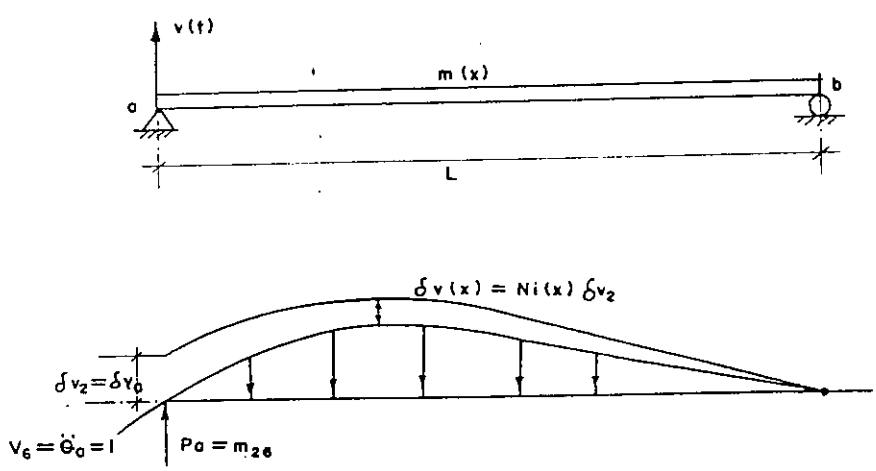

FIG. 2.4 BEAM SUBJECTED TO REAL ACTUAL ACCELERATION & VIRTUAL TRANSLATION

subjected to a unit angular acceleration at the left end, $V_6 = \theta_a = 1$, acceleration would be developed along its length as follows

$$\ddot{V}(x) = N_6(x)\ \ddot{V}_6 \qquad (2.26)$$

Now by d'Alembert's principle, the inertia force resisting this acceleration is

$$f_i(x) = m(x)\ N_6(x)\ \ddot{V}_6 \qquad (2.27)$$

The mass influence coefficients associated with this acceleration are defined as the nodal inertia forces which it produces. These can be evaluated from the distributed inertia forces of Eq. 2.27 by the principle of virtual displacements. For example, the vertical force of the left end can be evaluated by introducing a vertical virtual displacement and equating the work done by external nodal force Pa to the work done by the distributed inertia forces $f_I(x)$. Thus,

$$Pa\ \delta va = \int f_I(x)\ v(x) \qquad (2.28)$$

Expressing virtual displacement interms of the interpolation function and substituting Eq. 2.27 leads finally to

$$m_{26} = \int m(x)\, N_2(x)\, N_6(x)\, dx \qquad (2.29)$$

It should be noted that the mass influence coefficient represents the inertia force opposing the acceleration but that is numerically equal to the external force producing acceleration. From equation 2.30 it is evident that any mass influence co-efficient m_{ij} of an arbitrary beam segment can be evaluated by the equivalent expression

$$m_{ij} = \int m(x)\, N_i(x)\, N_j(x)\, dx \qquad (2.30)$$

The symmetric form of this equation shows that the mass matrix is symmetric, that is $m_{ij} = m_{ji}$. When the mass coefficients are computed in this way using the same interpolation functions which are used for calculating the stiffness coefficients, the consistent mass matrix is derived.

The consistent mass matrix of thin-walled space frame element can easily be computed by using the mass influence coefficients given by Eq. 2.30 which has been derived by virtual work method. A thin-walled space frame element will have fourteen degrees of freedoms, six displacements, six rotations and two additional

warping displacements at the two ends which have been shown in Fig. 2.2. The shape functions for all these generalized displacements have been given previously. Now for an element of uniform cross sectional area A, the mass per unit length is uniform and if the density of the element is denoted by ρ, then the quantity can be expressed by $m(x) = \bar{m} = \rho A$. From Eq. 2.30 the mass influence coefficient becomes

$$m_{ij} = \rho A \int N_i (x) N_j (x) dx$$

Substituting the expressions of shape functions for different displacements into the above equation and then integrating, the mass influence co-efficients for mass matrix of thin-walled space frame element are obtained. Thus

$$\begin{aligned} m_{11} &= \rho A \int N_1 (x) N_1 (x) dx \\ &= \rho A \int (1 - x/L)^2 dx \\ &= \rho AL/3 \end{aligned}$$

The consistent mass matrix of thin-walled member obtained in this way will be 14x14 matrix with respect to local axes system and it

can be transformed into global co-ordinate system by using transformation matrix.

The consistent mass matrix of thin-walled element can also be found by using the Archer derivation which is

$$m_E = \iiint_V [N]^T [N] \, dv$$

As before, if A is the uniform cross sectional area of element, dv can be replaced by Adx and the above equation can be written in the form

$$m_E = \rho A \int [N]^T [N] \, dx \qquad (2.31)$$

Here $[m_E]$ = the consistent mass matrix

$[N]$ = shape function matrix

The displacement model of thin-walled space frame element can be expressed as

$$a = \begin{bmatrix} u(x) \\ v(x \\ w(x) \\ \emptyset(x) \end{bmatrix} = [N(x)] \, [a]^T$$

Where [a] denotes the listing of nodal displacements

i.e $[a]^T = [u_1\ u_2\ v_2\ \theta_1\ \theta_2\ w_1\ w_2\ \Psi_1\ \Psi_2\ \Phi_1\ \Phi_2\ x_1\ x_2]^T$

And the motation

$$u(x) = [N_u]\ [u_1\ u_2]^T$$

$$v(x) = [N_v]\ [v_1\ v_2\ \ \theta_1\ \ \theta_2]^T$$

$$w(x) = [N_w]\ [w_1\ w_2\ \ \Psi_1\ \ \Psi_2]^T$$

$$\Phi(x) = [N_\Phi]\ [\Phi_1\ \Phi_2\ \ x_1\ \ x_2]^T$$

The shape functions [Nu], [Nv],[Nw], [N] have already been expressed previously.

So from these relations, the shape fucntion matrix can be expressed as

$$[N] = \begin{bmatrix} N_u \\ N_v \\ N_w \\ N_\Phi \end{bmatrix}$$

[N] will be 4x14 order matrix and $[N]^T$ will be 14x4 order matrix. Hence using these two matrices [N] and $[N]^T$ in the derivation of Eq. 2.31 and by integrating for all the elements, it is seen that the consistent mass matrix of thin-walled space frame element will be of order 14x14 and can be expressed as follows

$$m_E = \begin{bmatrix} m_{E1} & 0 & 0 & 0 \\ 0 & m_{E2} & 0 & 0 \\ 0 & 0 & m_{E3} & 0 \\ 0 & 0 & 0 & m_{E4} \end{bmatrix}$$

In this matrix

$$m_{E1} = \rho A \int [N_u]^T [N_u] \, dx$$

$$m_{E2} = \rho A \int [N_v]^T [N_v] \, dx$$

$$m_{E3} = \rho A \int [N_w]^T [N_w] \, dx$$

$$m_{E4} = \rho A \int [N_\phi]^T [N_\phi] \, dx$$

The submatrices m_{E1}, m_{E2}, m_{E3} and m_{E4} can be evaluated by substituting the shape functions in their expression and subsequently integrating. Thus,

$$m_{E1} = \rho A \int [N_u]^T [N_u] \, dx$$

$$= \rho A \int \begin{bmatrix} 1 - x/L \\ x/L \end{bmatrix} \begin{bmatrix} 1 - x/L & x/L \end{bmatrix} dx$$

$$= \rho AL \begin{bmatrix} 1/3 & 1/6 \\ 1/6 & 1/3 \end{bmatrix}$$

$$mE2 = \rho A \int [Nv]^T [Nv] \, dx$$

$$= \rho A \int \begin{bmatrix} 1 + 2x^3/L^3 - 3x^2/L^2 \\ 3x^2/L^2 - 2x^3/L^3 \\ -x(x/L - 1)^2 \\ -\frac{x^3}{L^2} + x^2/L \end{bmatrix} \begin{bmatrix} 1+\frac{2x^3}{L^3} - \frac{3x^2}{L^2}, & \frac{3x^2}{L^2} - \frac{2x^3}{L^3}, & -x(x/L-1)^2, & -\frac{x^3}{L^2} + \frac{x^2}{L} \end{bmatrix}$$

$$= \rho AL \begin{bmatrix} 13/35 & 9/70 & -11L/210 & 13L/420 \\ 9/70 & 13/35 & 13L/420 & 11L/210 \\ -11L/210 & 13L/420 & L^2/105 & -L^2/140 \\ 13L/420 & 11L/210 & -L^2/140 & L^2/105 \end{bmatrix}$$

$$m_{E3} = \rho A \int [N_w]^T [N_w] \, dx$$

$$= \rho AL \begin{bmatrix} 13/35 & 9/70 & -11L/210 & 13L/420 \\ 9/70 & 13/35 & 13L/420 & 11L/210 \\ -11L/210 & 13L/420 & L^2/105 & -L^2/140 \\ 13L/420 & 11L/210 & -L^2/140 & L^2/105 \end{bmatrix}$$

$$m_{E4} = \rho A \int [N\phi]^T [N\phi] \, dx$$

$$= \rho AL \begin{bmatrix} 13/35 & 9/70 & -11L/210 & 13L/420 \\ 9/70 & 13/35 & 13L/420 & 11L/210 \\ -11L/210 & 13L/420 & L^2/105 & -L^2/140 \\ 13L/420 & 11L/210 & -L^2/140 & L^2/105 \end{bmatrix}$$

The element mass matrix can be found by using these submatrics.

Hence the elements of the mass matrix are

$m_{11} = \rho AL/3 = m_{8,8}$

$m_{8,1} = m_{1,8} = \rho AL/6$

$m_{2,2} = m_{9,9} = 13\rho AL/35$

$m_{6,6} = m_{13,13} = \rho AL^3/105$

$m_{2,9} = m_{9,2} = 9\rho AL/70$

$m_{2,6} = m_{6,2} = -11\rho AL^2/210$

$m_{2,13} = m_{13,2} = 13\rho AL^2/420$

$m_{6,9} = m_{9,6} = 13\rho AL^2/420$

$m_{13,9} = m_{9,13} = 11\rho AL^2/210$

$m_{13,6} = m_{6,13} = \rho AL^3/140$

$m_{3,3} = m_{10,10} = 13\rho AL/35$

$m_{5,5} = m_{12,12} = \rho AL^3/105$

$m_{3,10} = m_{10,3} = 9\rho AL/70$

$m_{3,5} = m_{5,3} = 21\rho AL^2/210$

$m_{3,12} = m_{12,3} = 13\rho AL^2/420$

$m_{5,10} = m_{10,5} = 13\rho AL^2/420$

$m_{5,10} = m_{10,5} = 13\rho AL^2/420$

$m_{12,10} = m_{10,12} = 11\rho AL^3/210$

$m_{12,5} = m_{5,12} = \rho AL^3/140$

$m_{4,4} = m_{11,11} = 13\rho AL/35$

$m_{7,7} = m_{14,14} = \rho AL^3/105$

$m_{4,11} = m_{11,4} = 9\rho AL/70$

$m_{4,7} = m_{7,4} = 11\rho AL^3/210$

$m_{4,14} = m_{14,4} = 13\rho AL^2/420$

$m_{7,11} = m_{11,7} = 13\rho AL^2/420$

$m_{14,7} = m_{7,14} = -\rho AL^3/140$

$m_{14,11} = m_{11,14} = 11\rho AL^3/210$

2.3.3.2 Lumped Mass Matrix

The simplest proceedure for defining the mass properties of any structure is to assume that the entire mass is concentrated at the points at which the translational displacements are defined. The usual procedure for defining the point mass to be located at each node is to assume that the structure is divided into segments, the nodes serving as connection points. Fig. 2.5 illustrates the procedure for a beam type structure. The mass of each segment is assumed to be concentrated as point masses at each of its nodes, the distribution of the segment mass to these points being determined by statics. The total mass concentrated at any nodes of the complete structure is the sum of the nodal contributions from all the segments attached to that node. In the beam system of Fig. 2.5, there are two segment contributing to each node; for example

$$m_1 = m_{1a} + m_{1b}$$

For a system in which only translational degrees of freedom are defined the lumped mass matrix has a diagonal form; for the sys-

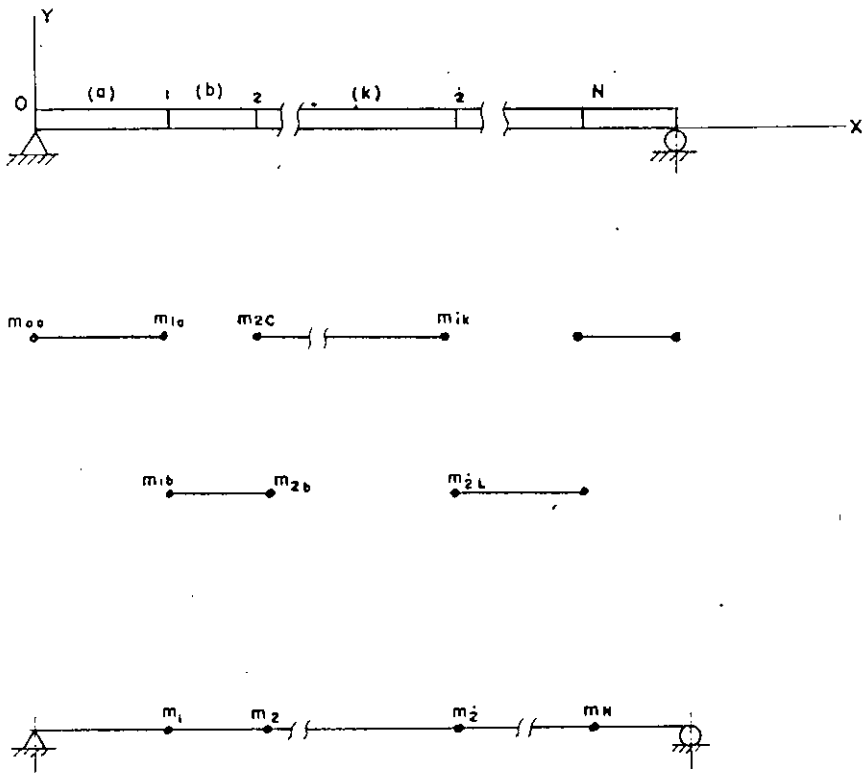

FIG. 2.5 LUMPING OF MASS AT BEAM NODES

tem of Fig. 2.5 it would be

$$m = \begin{bmatrix} m_1 & 0 & \cdot & 0 \\ 0 & m_2 & \cdot & 0 \\ \cdot & \cdot & m_1 & \cdot \\ 0 & 0 & \cdot & m_N \end{bmatrix} \qquad (2.32)$$

in which there are as many terms as there are degrees of freedom. The off-diagonal terms m_{ij} of this matrix vanish because an acceleration of any mass point produces an inertia force at that point only. The inertia force at node i due to a unit acceleration of point i is obviously equal to the mass concentrated at that point, thus the mass coefficient $m_{ii} = m_i$.

2.3.4 Damping Properties

Various methods have been formulated for the construction of damping matrix. If the various damping forces acting on a structure could be determined quantitatively, the finite element con-

cept could be used again to define the damping coefficient of the system. For example, the coefficient for any element might be of the form

$$C_{ij} = \int C(x)\ N_i(x)\ N_j(x)\ dx \qquad (2.33)$$

in which $C(x)$ represents a distributed viscous damping property; N_i and N_j are the shape functions at nodes i and j respectively. After the element damping influence coefficients have been determined, the damping matrix of the complete structure could be obtained by a superposition process equivalent to the direct stiffness method.

If it is assumed that the viscous damping properties $C(x)$ is constant then the damping influence coefficient

$$C_{ij} = C \int N_i(x)\ N_j(x)\ dx \qquad (2.34)$$

where C = constant viscous damping property.

This expression is identical to mass matrix given by Eq. 2.30. For this reason, sometimes damping matrix can be evaluated as the percentage of mass matrix. So the damping matrix can be expressed

in the matrix form similar to mass matrix.

$$[C] = C \begin{bmatrix} C_{E1} & 0 & 0 & 0 \\ 0 & C_{E2} & 0 & 0 \\ 0 & 0 & C_{E3} & 0 \\ 0 & 0 & 0 & C_{E4} \end{bmatrix} \qquad (2.35)$$

Where the submatrices C_{E1}, C_{E2}, C_{E3}, and C_{E4} have the following expressions.

$$C_{E1} = \int [N_u]^T \quad [N_u] \quad dx$$

$$C_{E2} = \int [N_v]^T \quad [N_v] \quad dx$$

$$C_{E3} = \int [N_w]^T \quad [N_w] \quad dx$$

$$C_{E4} = \int [N_\phi]^T \quad [N_\phi] \quad dx$$

The submatrix C_{E1} is a 2x2 matrix and other submatrices are of 4x4 order. Hence the damping matrix of a thin-walled space frame element is a 14x14 matrix. These submatrices can be evaluated by substituting the shape functions in their expression and subsequently integrating. Thus.

$$C_{E1} = \int \left[N_u\right]^T \left[N_u\right] dx$$

$$= \begin{bmatrix} L/3 & L/6 \\ L/6 & L/3 \end{bmatrix}$$

$$C_{E2} = \int \left[N_v\right]^T \left[N_v\right] dx$$

$$= L \begin{bmatrix} 13/35 & 9/70 & -11L/210 & 13L/420 \\ 9/70 & 13/35 & 13L/420 & 11L/210 \\ -11L/210 & 13L/420 & L^2/105 & -L^2/140 \\ 13L/420 & 11L/210 & -L^2/140 & L^2/105 \end{bmatrix}$$

The above submatrices can now be arranged as shown in Eq. 2.35 to obtain the element damping matrix. As it is seen, that the mass influence coefficients coincide with the damping influence coef-

ficients except the damping property C and the mass property ρ, the damping matrix can be related to the mass matrix as

$$[C] = \mu [m]$$

where μ can be expressed as a percentage.

After evaluation of damping matrix of thin-walled space frame element, the overall structure damping matrix can be found by assembling the element damping matrices.

In practice, however, evaluation of damping constant C(x) (or any other specific damping property) is impracticable. For thsi reason, the damping is generally expressed in terms of damping ratio established from experiments on similar structures rather than by means of an explicit expression of damping matrix C. If an explicit expression of the damping matrix is needed, it generally is computed from the specified damping ratios. Here the damping matrix, derived from the given damping ratios is used. In principle, the procedure can be explained by considering the complete diagonal matrix of generalised damping coefficients, which may be obtained by pre and post multiplying the damping matrix by the mode shape matrix. The generalized damping co-efficients are given by

$$C' = \Phi^{T} C \Phi = \begin{bmatrix} \varepsilon_1 w_1 M_1 & 0 & 0 \\ 0 & \varepsilon_2 w_2 M_2 & 0 \\ 0 & 0 & \varepsilon_3 w_3 M_3 \end{bmatrix} \quad (2.36)$$

where C is the damping matrix and Φ is mode shape matrix which can be derived from free vibration analysis.

ε_1 ε_2 = given damping ratios.

W_1', W_2' = Natural vibration frequencies

M = Generalized mass

It is evident from this equation that the damping matrix can be obtained by pre and post multiplying C' by the inverse of the mode shape matrix or its transpose.

$$[\Phi]^{-1} C' [\Phi]^{-1} = C \quad (2.37)$$

Thus, it is observed that for any specified set of nodal damping ratios ε, the generalized damping coefficients C' can be

evaluated, as indicated in Eq. 3.36, and then the damping matrix C is evaluated as in Eq. 2.37.

In this thesis the damping matrix has been developed by using this latter procedure. The damping ratio is assumed and the mode shape matrix is used from the free vibration analysis.

2.3.5 Geometric Stiffness

The geometric stiffness property represents the tendency toward buckling induced in a structure by axially directed load components. It depends both on the configuration of the structure and the condition of loading. The geometric stiffness can be developed from the potential of the applied loads. The potential of the applied loads V consists of two parts. The first part V_1 is formed by the product of the applied loads and their displacements and gives the potential of the applied loads in the prebuckling deformations. Thus, for the element shown in Fig. 2.2

$$V_1 = F_x(u_1 - u_2) + Q_{y1}\, v_1 + Q_{y2}\, v_2 + Q_{z1}\, w_1 + Q_{z2}\, w_2 + M_{y1}\, \Psi_1$$

$$+ M_{y2}\, \Psi_2 + M_{z1}\, \theta_1 + M_{z2}\, \theta_2 + M_x(\phi_1 - \phi_2) \qquad (2.38)$$

The second part V_2 takes into account the instability criteria and is formed from the potential of the aplied loads in the adjacent equilibrium position. Formation of V_2 is, however, quite extensive and it is due to the studies of Barsoum and Gallagher (5) that the formation of V_2 was possible. As this part of the potential of the applied loads relates to the instability criteria, the geometric stiffness matrix is therefore derived from this part. Barsoum and gallagher first recognized this part of the applied loads and showed that V_2 is given as a summation of the seperate contributions of different forces. Thus

$$V_2 = \Sigma_j \quad v_j \tag{2.39}$$

Where $V_i = \frac{1}{2}\int F_x \left[(v'^2 + w'^2) + S_0 \phi^2\right] dx$

$$S_0 = I_0/A + e_y K_7 + e_z K_8$$

$$K_7 = 1/I_y \left[\int Z^3 dA + \int y^2 z \, dA\right] - 2z_o$$

$$K_8 = 1/I_z \left[\int y^3 dA + \int Z^2 y \, dA\right] - 2y_o$$

$$V_{ii} = -\tfrac{1}{2}Q_{y1}\int w'' \phi \; x \, dx - \tfrac{1}{2}Q_{y2}\int w'' \phi \; (L-x) \, dx$$

$$V_{iii} = -\tfrac{1}{2}Q_{z1} \int v''\phi \, x \, dx - \tfrac{1}{2}Q_{z2} \int v''\phi \, (L - x) \, dx$$

$$V_{iv} = -\tfrac{1}{2}M_{y1} \int v''\phi \, dx + \tfrac{1}{2}M_{y2} \int v''\phi \, dx$$

$$V_{v} = -\tfrac{1}{2}M_{z1} \int w''\phi \, dx + \tfrac{1}{2}M_{z2} \int w''\phi \, dx$$

$$V = -\tfrac{1}{2}M_{x} \int (v'w'' - w'v'') \, dx$$

The above expression v_{vi} was, however, drived by H. Ziegler and it was shown by him that this expression is valid for the buckling analysis of circular shaft only. Now substituting the above expressions into Eq. 2.39, the potential of the applied load V_2 is easily formulated.

Substituting the displacement functions from Eq. 2.19 to 2.22 into Eq. 2.39, the transformed expression for the potential of the applied loads in the adjacent equilibrium position V_2 is obtained. Thus,

$$V_2 = \frac{[v_1 \; v_2 \; \theta_1 \; \theta_2]}{2} \; F_x \left\{ \int [N_v']^T \, [N_v'] \, dx \right\} [v_1 v_2 \; \theta_1 \; \theta_2]^T$$

$$+ \frac{[W_1 \quad W_2 \quad \psi_1 \quad \psi_2]}{2} \; F_x \{ \int [N_w']^T [N_w'] dx \} \; [W_1 \quad W_2 \; \psi_1 \; \psi_2]^T$$

$$+ \frac{[\phi_1 \quad \phi_2 \quad \chi_1 \quad \chi_2]}{2} \; F_x \{ \int S_o [N_\phi']^T [N_\phi'] dx \} [\phi_1 \; \phi_2 \; \chi_1 \; \chi_2]^T$$

$$+ \quad Q_{z2} \int [N_v'']^T \quad [N\phi] \quad (L-x) \; dx \} [\phi_1 \quad \phi_2 \; \chi_1 \; \chi_2]^T$$

$$- \frac{[V_1 \; V_2 \; \theta_1 \; \theta_2]}{2} \{ \quad Q_{z1} \int [N_v'']^T \quad [N\phi] \quad x \quad dx$$

$$- \frac{[W_1 \quad W_2 \; \psi_1 \; \psi_2]}{2} \{ \quad Q_{y1} \int [N_w'']^T \quad [N\phi] \quad x \quad dx$$

$$+ \quad Q_{y2} \int [N_w'']^T \quad [N\phi] \quad (L-x) \; dx \} [\phi_1 \quad \phi_2 \; \chi_1 \; \chi_2]^T$$

$$- \frac{[V_1 \quad V_2 \; \theta_1 \; \theta_2]}{2} \{ \quad (M_{y1} - M_{y2}) \int [N_v'']^T \quad [N\phi] dx \} [\phi_1 \quad \phi_2 \; \chi_1 \; \chi_2]^T$$

$$- \frac{[W_1 \; W_2 \; \psi_1 \; \psi_2]}{2} \{ \quad (M_{z1} - M_{z2}) \quad \int [N_w^*]^T \; [N\phi] \; dx \} [\phi_1 \quad \phi_2 \; \chi_1 \; \chi_2]^T$$

$$- \frac{[V_1 \quad V_2 \; \theta_1 \; \theta_2]}{2} M_x \{ \int [N_v']^T \; [N_w''] \; dx \; - \; [N'_w]^T \; [N_v''] \; dx \}$$

$$[W_1 \quad W_2 \; \theta_1 \; \theta_2]^T$$

$$\text{or } V_2 = -\frac{[a]}{2}\begin{bmatrix} 0 & 0 & 0 & 0 \\ 0 & K_{G1} & K_{G8} & K_{G4}+K_{G6} \\ 0 & K_{G8} & K_2 & K_{G5}+K_{G7} \\ 0 & K_{G4}+K_{G6} & K_{G5}+K_{G7} & K_{G3} \end{bmatrix}\{a\}^T$$

Where

$$K_{G1} = -F_x \int [N_v']^T [N_v'] \, dx$$

$$K_{G2} = -F_x \int [N_w']^T [N_w'] \, dx$$

$$K_{G3} = -F_x \int S_o [N\phi']^T [N\phi'] \, dx$$

$$K_{G4} = Q_{z1} \int [N_v'']^T [N\phi] \, x \, dx + Q_{z2} \int [N_v'']^T [N\phi] \, (L-x) \, dx$$

$$K_{G5} = Q_{y1} \int [N_w'']^T [N\phi] \, x \, dx + Q_{y2} \int [N_w'']^T [N\phi] \, (L-x) \, dx$$

$$K_{G6} = (M_{y1} - M_{y2}) \int [N_v'']^T [N\phi] \, dx$$

$$K_{G7} = (M_{z1} - M_{z2}) \int [N_w'']^T [N\phi] \, dx$$

$$K_{G8} = -M_x \int \{ [N_v']^T [N_w''] - [N_w']^T [N_v''] \} dx$$

Here the second matrix of the equation 3.40 consisting of K_{G1}, K_{G2}, K_{G3}, K_{G4}, K_{G5}, K_{G6}, K_{G7} and K_{G8} is the element geometric matrix and is denoted by $[K_G]$

2.4 PREBUCKLING ELASTIC ANALYSIS

For any load acting on a structure, the end forces of an element are not known at the beginning and the element geometric matrix can not be determined directly. For this reason an elastic analysis must first be carried out to determine the internal forces at each node of the member. The elastic analysis is performed by finite element procedure. First of all, the element stiffness matrixes $[K_{Ei}]$'s are determined by Eq. 2.24 and then assembled to form the overall stiffness matrix $[K_E]$. The displacements are obtained from the following equation after introduction of proper boundary conditions.

$$[P] = [K_E]\ [a] \qquad (2.41)$$

Where P is the total joint or nodal load vector including equivalent joint loads resulting from loaded members. From the displacement vector a, the appropriate nodal displacements are utilized for calculating the element nodal forces from

$$[P_i] = [K_{Ei}]\,[a_i] \qquad (2.42)$$

These forces are then used to derive the element geometric matrices K_{Gi}'s, which are assembled subsequently to form the overall geometric matrix.

2.5 ANALYSIS OF VIBRATION FREQUENCIES

The equation of motion for multiple degreeof freedom system as derived in article 2.2.1 is

$$m\,\ddot{v} + c\,\dot{v} + Kv = p \qquad (2.43)$$

where P is the load vector. For undamped free vibration system the equation of motion can be obtained by dropping the damping matrix and applied load vector i.e c = 0 and p = 0. In this case the equation of motion becomes

$$m\,\ddot{v} + Kv = 0 \qquad (2.44)$$

This is the equation of motion for undamped free vibration in which 0 is a zero vector. For a simple harmonic free vibration motion of a MDOF system,

$$v(t) = \hat{v} \sin(\acute{w}t + \theta) \tag{2.45}$$

In this expression v represents the shape of the system or mode shape and θ is a phase angle. When the second time derivation of v(t) is taken, the accelerations in free vibration are

$$\ddot{v} = -\acute{w}^2 v \sin(\acute{w}t + \theta)$$

$$\ddot{v} = -\acute{w}^2 v \tag{2.46}$$

Substituing for v and $\ddot{v}$ from Eq. 2.45 and 2.46 in Eq. 2.44 the equation of motion becomes

$$-\acute{w}^2 m\hat{v} \sin(\acute{w}t + \theta) + k\hat{v} \sin(\acute{w}t + \theta) \tag{2.47}$$

which may be written as

$$\left[K - \acute{w}^2 m\right]\hat{v} = 0 \tag{2.48}$$

Now it can be shown that finite amplitude free vibrations are possible only when

$$\left\| K - w'^2 m \right\| = 0 \qquad (2.49)$$

This equation is called the frequency equation of the system. For a system having N degrees of freedom, expanding the corresponding determinantal equation as derived from Eq. 2.49, an algebraic equation of the Nth degree in the frequency parameter w^2 will be obtained. The N roots of this equation ($w_1'^2$, $w_2'^2$ . . . . . $w_n'^2$) represent the frequencies of the N modes of vibration which are possible in the system. Again, these frequencies may also be evaluated by solving Eq. 2.49, considering it as an eigen value problem. The mode having the lowest frequency is called the first mode, the next higher frequency the second mode and so on. The vector made up of the entire set of modal frequencies, arranged in sequence, is called the frequency vector w'.

$$w' = \begin{bmatrix} w_1' \\ w_2' \\ w_n' \end{bmatrix} \quad . \; . \; . \; . \; . \qquad (2.50)$$

The values (w_1', w_2', ...w_N') are known as frequencies of vibration or natural frequencies. By using these frequency vectors, the mode shape $\hat{v}$ for any nth mode can be determined from Eq. 2.48. The mode shape matrix Φ and vibration frequencies are ob-

tained from the solution of eigen value problem as in Eq. 2.48 where the frequdncy square terms are the eigen values and the mode shapes are the eigen vectors.

2.6 INFLUENCE OF AXIAL FORCES

It has been shown previously that when a structure is subjected to a constant axial force, torque, or any lateral load which may buckle the structure the effective stiffness of the structure reduces. In this case the geometric stiffness must be included in the equation of motion and the equation for free vibration becomes

$$m\ddot{v} + kv - k_G v = 0 \qquad (2.51)$$

$$m\ddot{v} + \bar{k}\, v = 0 \qquad (2.52)$$

Here $\bar{k}$ is the combined stiffness matrix. And the frequency equation becomes

$$\left\| \bar{k} - w^2 m \right\| = 0 \qquad (2.53)$$

So in the mode shape and frequency analysis, it is necessary to substitute the combined stiffness $\bar{k}$ for the elastic stiffness k

otherwise the analysis is exactly the same as for a system without considering axial force effect.

2.7 BUCKLING LOAD

From the frequency equation 2.53 including axial force effect, it is seen that the gradual increase of geometric stiffness k_G reduces the effective stiffness of the structure. It also reduces the frequences of vibration w. At a certain value of k_G when the frequency of vibration is zero, the inertia forces vanish and the dynamic equation of equilibrium reduces to

$$k_v - k_G v = 0 \qquad (2.54)$$

This equation represents the condition of elastic instability. So this condition, under which a nonzero displacement is possible constitutes the static buckling condition; in other words the definition of buckling is the state in which the vibration frequency becomes zero. In order to evaluate the critical buckling load of the structure, it is convenient to express the geometric stiffness in terms of a reference loading multiplied by an arbitrary choosen load factor, so that it can be solved as a general eigen value problem. Now introducing the scale factor λ .

$$[K_G] = \lambda\,[K_G']$$

where $[k_G']$ is defined as the value of $[k_G]$ when the load vector $[P]$ corresponds to unit scale factor. Thus the equation becomes the eigen value equation

$$[K - \lambda\, k_G]\ \hat{V} = 0 \qquad (2.55)$$

A nontrival solution of this set of equations can be obtained under the condition.

$$\left\| K - \lambda\, K_G \right\| = 0 \qquad (2.56)$$

which represents the buckling condition of the structure.

The roots of this equation represent the values of the load factor λ at which buckling will occur. The mode shapes can be evaluated exactly the same way as vibration mode shapes. In practice, only the first buckling load and mode shape have any real significance, buckling in the higher modes generally is of little practical importance because the system will have failed when the load exceeds the lowest critical load. A more efficient technique to evaluate the lowest eigen value is to transform the equation 2.55 into the following form

$$[K]\ \hat{v} = \lambda\ [K_G]\ \hat{v}$$

$$\frac{1}{\lambda}\ \hat{v} = [K^{-1}][K_G]\ \hat{v} \qquad (2.57)$$

Eq. 2.57 can be solved for lowest eigen value λ i.e the highest value of $1/\lambda$ will give the lowest of λ and corresponding mode shape will be the backling mode shape.

2.8 ANALYSIS OF DYNAMIC RESPONSE

In article 2.5, the computation of free vibration frequency and corresponding mode shapes are shown. The dynamic response of a structure constitutes the displacement, acceleration, and velocity as a function of time due to any dynamic loading. Hence the dynamic response is evaluated by the solution of equation of motion

$$m\ddot{v}(t) + c\dot{v}(t) + kv(t) = p(t) \qquad (2.58)$$

where p(t) = dynamic load vector

Several methods are in practice for the evaluation of dynamic response. The methods used in this work for the analysis of

dynamic response of thin-walled space framed system are

i) Mode super position method

and ii) Step-by-step integration method.

The solution procedure of dynamic response by these two methods are described in the following article.

2.8.1 MODE SUPERPOSITION METHOD

For dynamic response analysis of linear systems, a much more useful representation of the displacements is provided by the free vibration mode shapes. These shapes constitute N independent displacements patterns, the amplitude of which may serve as generalized coordinates to express any form of displacement. Any displacement vector v for a structure can be developed by superimposing suitable amplitudes of the N degrees of freedom. For any modal component v_n, the displacements are given by the mode shape n multiplied by the amplitude Y_n thus

$$v_n = \phi_n Y_n \qquad (2.59)$$

The total displacement is then obtained as the sum of modal components,

$$v = \phi_1 Y_1 + \phi_2 Y_2 + \cdot \cdot \cdot \cdot \cdot + \phi_n Y_n = \sum \phi_n Y_n \qquad (2.60)$$

or in matrix notation, $\bar{v} = \Phi \bar{Y}$ (2.61)

In this equation it is apparent that the mode shape matrix serves to transform the generalized coordinates Y to the geometric co-ordinates v. These mode amplitude generalized coordinates are called the normal coordinates of the structure. Because the mode shape matrix Φ for a system with N degrees of freedom consists of N independent modal vectors, it is nonsingular and can be inverted. Thus it is always possible to solve Eq. 2.61 directly for the normal coordinate Y associated with any displacement vector v. Now the equation of motion for damped condition is

$$m \ddot{v} + c \dot{v} + k v = p(t) \qquad (2.62)$$

Introducting the normal coordinate expression as in Eq. 2.61 and its time derivatives and premultiplying by the transpose of the nth mode shape vector ϕ^T_n leads to

$$\phi^T_n m \phi \ddot{Y} + \phi^T_n C \phi \dot{Y} + \phi^T_n K \phi Y = \phi^T_n P(t) \qquad (2.63)$$

the orthogonality conditions show that

$$\phi_m^T \, m \, \phi_n = o$$
$$\phi_m^T K \, \phi_n = o \qquad \text{when } m \neq n \tag{2.64}$$
$$\phi_m^T C \, \phi_n = o$$

Now introducing the relation as in Eq. 2.60 and also using the orthogonality conditions, Eq. 2.63 reduces to

$$\phi_n^T m \, \phi_n \ddot{Y}_n + \phi_n^T C \dot{Y}_n + \phi_n^T K \, \phi_n = \phi_n^T P(t) \tag{2.65}$$

Using new symbols known as normal coordinate properties, the Eq. 2.65 can be modified to

$$M_n \ddot{Y}_n + C_n \dot{Y}_n + K_n Y_n = P_n(t) \tag{2.66}$$

which is a SDOF equation of motion for mode n. The normal coordinate properties are

$$M_n = \phi_n^T \, m \, \phi_n$$
$$C_n = \phi_n^T \, C \, \phi_n$$
$$K_n = \phi_n^T \, K \, \phi_n \tag{2.67}$$
$$P_n(t) = \phi_n^T \, P(t)$$

These are also known as generalized mass, damping,stiffness, and load respectively.

The procedure described abvoe can be used to obtain an independent SDOF equation of motion for each mode of vibration of the structure. Thus, the use of normal coordinates serves to transform the equations of motion from a set of N simultaneous differential equations, which are coupled by the off-diagonal terms in the mass and stiffness matrices, to a set of N indpendent normal coordinate equations. The dynamic response can be obtained by solving seperately for the response of each normal coordinate and then superposing these by Eq. 2.61. This procedure is called the mode superposition method.

Now to solve the displacement response in normal coordinate, Eq. 2.66 can be written as

$$\ddot{Y}_n + 2\,\varepsilon_n w'_n \dot{Y} + w_n^2\, Y_n = \frac{P_n(t)}{M_n} \qquad (2.68)$$

where $C_n/M_n = 2\,\varepsilon_n w'_n$

and $K_n/M_n = w'^2_n$

The SDOF system in Eq. 2.68 for n modes can be solved by using the Duhamel Integral for each mode.

2.8.1.1 Duhamel Integral

The derivation of Duhamel Integral formula can be developed on the basis of response of a structure due to a short duration impulse. For any arbitrary general dynamic loading p(t), with intensity of loading $p(\tau)$ acting at time $t = \tau$, a short duration impulse $p(\tau)\, d\tau$ is produced by the load $p(\tau)$ acting during the short interval of time $d\tau$. It is assumed that for damped system the response will be subjected to exponential decay. Thus for the differential time interval $d\tau$, the response produced by the loading $p(\tau)$ is exactly

$$dv(t) = e^{-\varepsilon w'(t-T)} \quad \frac{P(T)\, dT}{m\, w'_D} \sin w'_D(t-T) \tag{2.69}$$

in which the exponential decay begins as soon as the load is applied at time $t = \tau$.

Summing up the differential response terms over the entire loading interval, it follows

$$V(t) = \frac{1}{m w'_D} \int P(T)\ e^{-\varepsilon w'(t-T)} \sin w'_D(t-T)\ dT \qquad (2.70)$$

This is known as the Duhamel Integral for a damped system. Now by using Duhamel Integral, the general response expression from Eq. 2.68 for each mode is obtained as

$$Y_n = \frac{1}{M_n\ w'_{Dn}} \int P_n(t)\ e^{-\varepsilon_n w'_n(t-T)} \operatorname{Sin} w'_{Dn}(t-T)\ dT \qquad (2.71)$$

The right hand side integration can be performed easily by using e.q. Simpoon's rule.

2.8.2 STEP BY STEP INTEGRATION METHOD

It follows from preceding discussion that the normal coordinate transformation, which serves to change the set of N coupled equations of motion of a MDOF system into a set of N uncoupled equations, is the basis of the mode superposition method of dynamic analysis. This method can be used to evaluate the dynamic response of any linear structure for which the dynamic resisting forces are related to the acceleration, velocity, or displacement vectors by means of linear influence coefficients. This method is

therefore applicable only for linear structures, where the physical properties are constant during the dynamic response.

However, in many instances, the physical properties do not remain constant during the response period. The stiffness influence coefficients may be altered by yielding of the structural materials or by significant changes of axial forces in the members of the structure which causes changes in the geometric stiffness coefficients. It is also possible that mass or damping coefficients will undergo changes during the dynamic response. Any such changes will alter the vibration characteristics of the system and therefore, the normal co-ordinate uncoupling of the equations of motion is not possible.

The only genrally applicable method for the analysis of arbitrary nonlinear systems is the step by step integration of the coupled equations of motion.This procedure is also applicable to linear structures, in which case the computation procedure is greatly simplified because it is not necessary to modify the structural properties at each step. In some cases it may be advantageous to use this direct integration approach rather than mode superposition because it does not require the evaluation of the vibration mode shapes and frequencies, which is a very large computational task in systems with many degrees of freedom. In general, direct step by step integration tends to be most useful in evaluating

the response of large complex structures to short duration impulsive loads which usually excite many modes of vibration but require only a short response history to be evaluated.

In this approach, the response is evaluated for a series of short time increments t, generally taken of equal length for computational convenience. The condition of dynamic equilibrium is established at the beginning and end of each interval, and the motion of the system during the time increment is evaluated approximately on the basis of an assumed mechanism. The nonlinear nature of the system is accounted for by calculating new properties appropriate to the current deformed state at the beginning of each time increment. The complete response is obtained by using the velocity and displacement computed at the end of one computational interval as the initial conditions for the next interval; thus the process may be continued step by step from the initial of loading to any desired time, approximating the nonlinear behaviour as a sequence of successively changing linear systems.

2.8.2.1 Incremental Equations of Equilibrium

The general nonlinear characteristics of a MDOF system, for stiffness and damping, are shown in Fig. 2.6, where it is assumed that the mass m does not change with time but stiffness and damp-

ing forces do change. An arbitrarily applied loading is also sketched. At any instant of time t, the equilibrium of forces is given by

$$f_I(t) + f_D(t) + f_S(t) = P(t) \tag{2.72}$$

While a short time Δt later, the equation would be

$$f_I(t+\Delta t) + f_D(t+\Delta t) + f_S(t+\Delta t) = P(t+\Delta t) \tag{2.73}$$

Thus taking the difference between the equilibrium relationships defined for times t and t + Δt gives the incremental equilibrium equation

$$\Delta f_I(t) + \Delta f_D(t) + \Delta f_S(t) = \Delta P(t) \tag{2.74}$$

The incremental forces in this equation may be expressed as

$$\begin{aligned} f_I(t) &= f_I(t+\Delta t) - f_I(t) = m\,\ddot{v}(t) \\ f_D(t) &= f_D(t+\Delta t) - f_D(t) = C(t)\,\Delta\dot{v}(t) \\ f_S(t) &= f_S(t+\Delta t) - f_S(t) = K(t)\,\Delta v(t) \\ P(t) &= P(t+\Delta t) - P(t) \end{aligned} \tag{2.75}$$

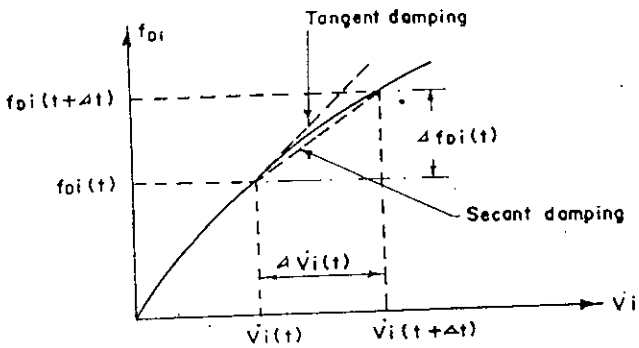

(a)

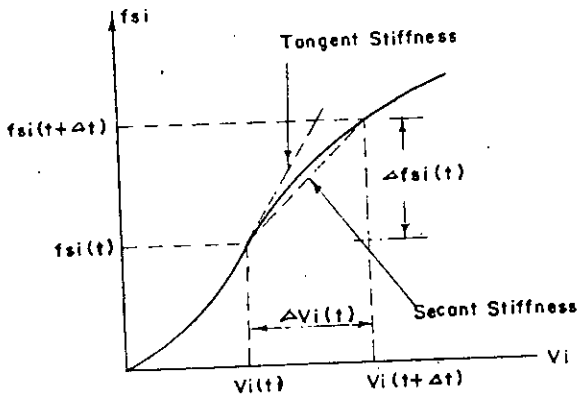

(b)

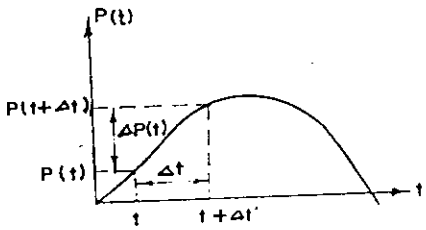

(c)

FIG. 2.6 (a) NONLINEAR VISCOUS DAMPING
(b) NONLINEAR STIFFNESS
(c) APPLIED LOAD

The elements of the incremental damping and stiffness matrices c(t) and k(t) are influence coefficients $c_{ij}(t)$ and $k_{ij}(t)$. It is now convenient to use the initial tangent rather than the secant as a measure of the damping or stiffness property in order to avoid the need for iteration at each step of solution. Hence the influence coefficients are given by

$$C_{ij}(t) = \left(\frac{df_{Di}}{d\,v_j}\right)_t \quad \text{and} \quad K_{ij}(t) = \left(\frac{df_{si}}{df_{sj}}\right)_t \tag{2.76}$$

Now the incremental equation of motion becomes

$$m\,\Delta\ddot{v}(t) + c(t)\Delta\dot{v}(t) + k(t)\,\Delta v(t) = \Delta p(t). \tag{2.77}$$

The solution of this incremental equation gives the incremental dynamic response from which the total response at any time t can be obtained.

The basic operation in the step-by-step solution of simultaneous differential equations of motion is their conversion to a set of simultaneous algebric equations. This is accomplished by introducing a simple relationship between displacement, velocity, and

acceleration which may be valid for a short increment of time. And the basic assumption of solution process is that acceleration varies linearly while the variations of velocity and displacement are quadratic and cubic respectively. The relationship between displacement, velocity and acceleration can conveniently be established by assuming the manner of variation of the acceleration vector with time. These variations and relations are shown in Fig. 2.7. From Fig. 2.7, at the end of interval ($\tau = \Delta t$), the increments of velocity and displacement are

$$\Delta\dot{v}(t) = \ddot{v}(t)\,\Delta t + \Delta\ddot{v}(t)\,\frac{\Delta t}{2}$$
$$\Delta v(t) = \dot{v}(t)\,\Delta t + \ddot{v}(t)\,\frac{\Delta t^2}{2} + \Delta\ddot{v}(t)\,\frac{\Delta t^2}{6} \qquad (2.78)$$

It is convenient to use the incremental displacement as the basic variable in analysis and for this reason from Eq. 2.77 it follows

$$\Delta v(t) = \frac{6}{\Delta t^2}2\Delta v(t) - \frac{6}{t}\Delta\dot{v}(t) - 3\Delta\ddot{v}(t)$$
$$\Delta v(t) = \frac{3}{\Delta t}\Delta v(t) - 3\dot{v}(t) - \frac{\Delta t}{2}\ddot{v}(t) \qquad (2.79)$$

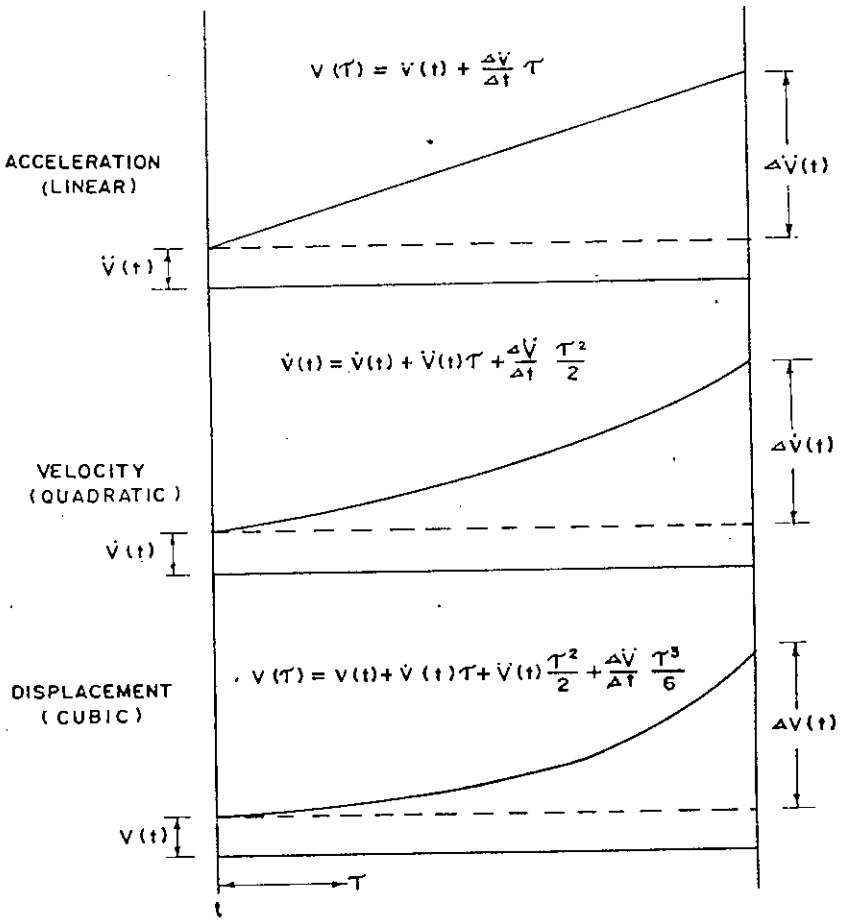

FIG. 2.7 MOTION OF SYSTEM DURING TIME INCREMENT

Substituting $\Delta v(t)$ and $\Delta v(t)$ into the incremental equation of motion (2.77).

$$m\left[\frac{6}{\Delta t^2}\Delta v(t) - \frac{6}{\Delta t}\dot{v}(t) - 3\ddot{v}(t)\right] + C(t)\left[\frac{3}{\Delta t}\Delta v(t) - 3\dot{v}(t) - \frac{\Delta t}{2}\ddot{v}(t)\right] \tag{3.80}$$

$$+ K(t)\,\Delta v(t) = \Delta P(t)$$

and finally

$$\tilde{K}(t)\Delta v(t) = \widetilde{\Delta P}(t) \tag{3.81}$$

in which

$$\tilde{K}(t) = K(t) + \frac{6}{\Delta t^2} m + \frac{3}{\Delta t} C(t)$$

and $$\widetilde{\Delta P}(t) = \Delta P(t) + m\left[\frac{6}{\Delta t}\dot{v}(t)\right] + C(t)\left[3\dot{v}(t) + \frac{\Delta t}{2}\ddot{v}(t)\right] \tag{3.82}$$

Eq. 2.82 has the form of a standard static stiffness equation for the incremental displacement vector $\Delta v(t)$ in which $\Delta k(t)$ and $\Delta p(t)$ may be interpreted as the effective dynamic stiffness matrix and the effective load increment respectively. The analysis is carried out by evaluating $k(t)$ from the mass, damping and stiffness properties defined for the conditions existing at the beginning of the time step and evaluating $\Delta p(t)$ from the velocity and

acceleration vectors at the beginning of the step and the load increment specified during the step. Then the displacement increment $\Delta v(t)$ is computed by solving Eq. 2.81 and using any standard equation solution procedure. When the displacement $\Delta v(t)$ has been determined, the velocity increment is found from

$$\Delta \dot{v}(t) = \frac{3}{\Delta t}\Delta v(t) - 3\dot{v}(t) - \frac{\Delta t}{2}\ddot{v}(t) \qquad (2.83)$$

The displacement and velocity vectors at the end of increment are given by

$$\begin{aligned} V(t+\Delta t) &= v(t) + \Delta v(t) \\ \dot{v}(t+\Delta t) &= \dot{v}(t) + \Delta v(t) \end{aligned} \qquad (2.84)$$

The vectors given by Eq. 2.84 represent the initial conditions for the next step. In addition, the acceleration vector is also needed as an initial condition for next step. This is calculated from the condition of dynamic equilibrium at the time $t+\Delta t$; Thus

$$\ddot{v}\ (t+\Delta t) = m^{-1}\left[P(t+\Delta t) - f_D(t+\Delta t) - f_S(t+\Delta t)\right] \qquad (2.85)$$

in wich $f_D(t+\Delta)$and $f_S(t+\Delta t)$ represent the damping and elastic force vectors respectively, and evaluated from the velocity and displacement conditions at time $(t+\Delta t)$.

CHAPTER - 3

THE COMPUTER PROGRAM

3.1 INTRODUCTION

In the previous chapter the theoretical procedure for the dynamic response analysis of thin walled space frame works using finite element approach has been presented. The purpose of this chapter is to develop a general computer program for the dynamic response analysis of thin walled space frame works in order to carry out the necessary investigations. The program is general in character and can be used to determine dynamic response for any type of thin-walled space frame-works. The scope of the program also covers the determination of critical buckling load. The prgoram described here has been written in FORTRAN language and run on the IBM 4331 computer of the BUET computer centre.

3.2 THE SOLUTION SCHEME

In this article the sequence of the solution procedure maintained during the computer analysis is described. The steps that are went through in the solution scheme, are as

follows:

Step 1: The number of elements, the total number of nodes and the degrees of freedom of each node are defined first.

Step 2: The next step is to define the geometric properties of member i,e the area of cross-section, the moments of inertia,the torsional and warping constants and the material properties including the modulus of elasticity, modulus of rigidity and torsional and warping rigidities.

Step 3: The co-ordinates of each node are then defined from which the length of each element is calculated.

Step 4: The applied joint loads and equivalent joint loads resulting from member loads are next defined. At the same time, the dynamic loading conditions at different time, and support conditions are described.

Step 5: The element stiffness matrices are then calculated and assembled to form the overall stiffness matrix.

Step 6: The boundary conditions are imposed and accordingly the stiffness matrix is modified.

Step 7: An elastic analysis is carried out to find the in-

ternal force distributions for static loading crresponding to unit scale factor.

Step 8: With known values of nodal forces, the element geometric matrices are calculated and assembled to form the overall geometric matrix.

Step 9: The element consistent mass matrices are, then calculated and assembled to form the overall consistent mass matrix.

Step 10: The combined stiffness matrix is formed by subtracting the overall geometric matrix from the overall stiffness matrix.

Step 11: The boundary conditions are imposed on combined stiffness matrix and consistent mass matrix for dynamic analysis.

Step 12: By an eigen value solution technique, the natural frequencies and corresponding mode shapes are calculated from free vibration analysis.

Step 13: Using the natural frequencies, given damping ratios

and dynamic loads, the damping matrix for the structure is calculated.

Step 14: The dynamic displacement response analysis is carried out separately following the step by step integration method and Duhamel integral solution.

3.3 NUMBERING SYSTEM FOR DISPLACEMENT

In case of a thin-walled space frame element, it is evident that the possible number of nodal degrees of freedom is seven. The generalized displacement corresponding to these degrees of freedom has been described in Art. 2.3.1. A space framework consists of several space frame elements, each of which is assigned a specific number i, as shown in Fig. 3.1. A particular element in a structure will have joint number j and k at its ends.

An orderly numbering system for the possible displacements at the ends of the elements may be derived from the corresponding numbers. Thus for a space frame element the seven possible displacements at each and can be described by the following index system.

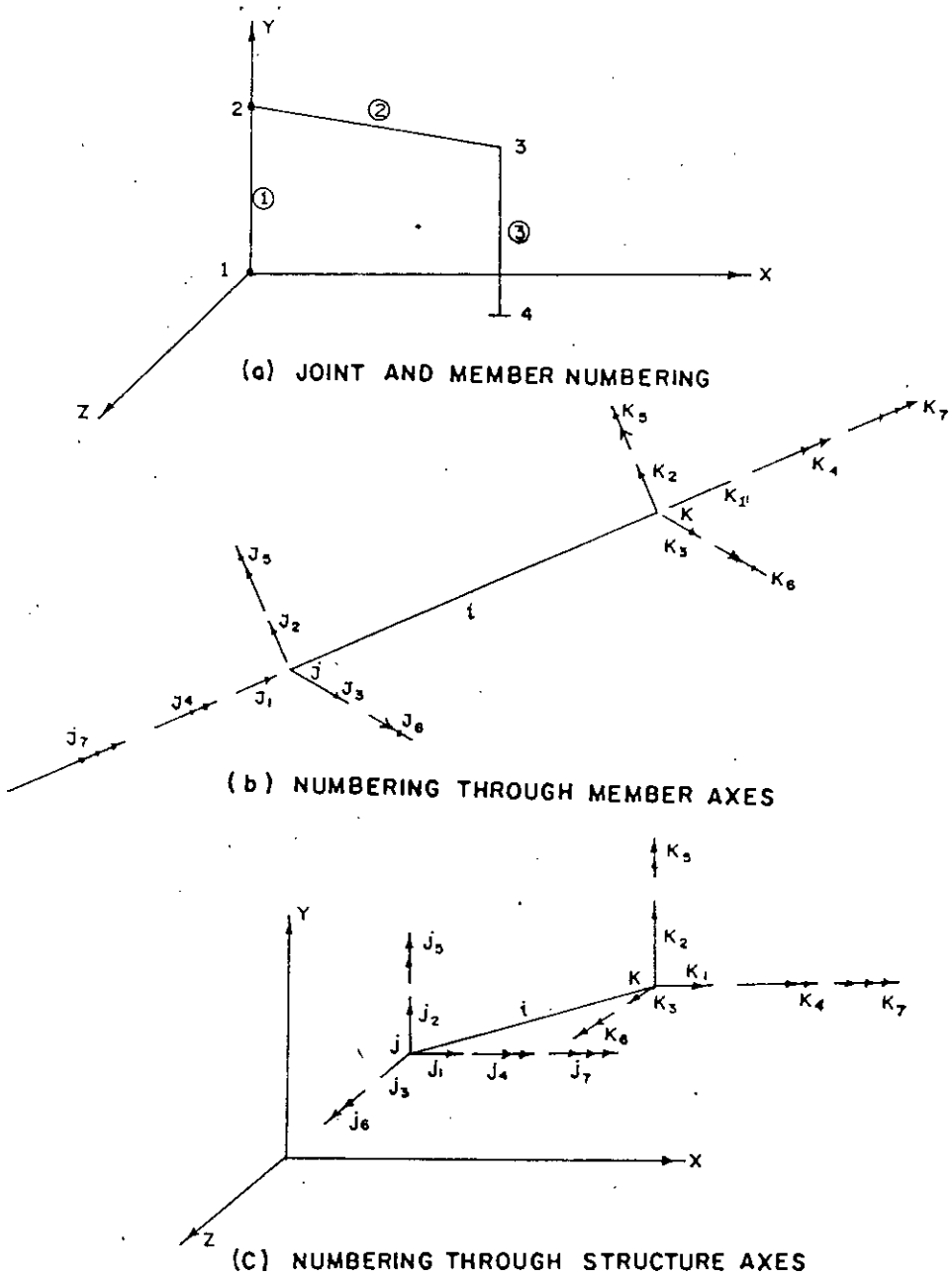

FIG.3.1 NUMBERING SYSTEM

ji = 7j-6, j2=7j-5, j3=7j-4, j4=7j-3, j5=7j-2, j6=7j-1, j7=7j

k1=7k-6, k2=7k-5, k3=7k-4, k4=7k-3, k5=7k-2, k6=7k-1, k7=7k

Here 1	stands	for	displacement	u	along	x	axis
2	,,	,,	,,	v	,,	y	,,
3	,,	,,	,,	w	,,	z	,,
4	,,	,,	rotation	0	about	x	,,
5	,,	,,	,,		,,	y	,,
6	,,	,,	,,	0	,,	z	,,
7	,,	,,	warping	x	i.e = $d\phi/dx$		

This numbering system is valid for both member and structure axes.

It has been shown that the derivation of the element stiffness matrix, mass matrix, geometric matrix presented in Art. 3.3 are of order 14x14 and the displacements are so ordered that each identical degree of freedom of the two nodes are placed together. This ordering of the displacement vectors, howeveer, has some disadvantages and to facilitate the assembling process the displacement vectors corresponding to each node should be seperated.The procedure of placing the displacements at one node together is quite simple and is

$[K_E] =$

	J_1	J_2	J_3	J_4	J_5	J_6	J_7	K_1	K_2	K_3	K_4	K_5	K_6	K_7
J_1	X							X						
J_2		X				X			X				X	
J_3			X		X					X		X		
J_4				X			X				X			X
J_5			X		X					X		X		
J_6		X				X			X				X	
J_7				X			X				X			X
K_1	X							X						
K_2		X				X			X				X	
K_3			X		X					X		X		
K_4				X			X				X			X
K_5			X		X					X		X		
K_6		X				X			X				X	
K_7				X			X				X			X

(a) ELEMENT STIFFNESS MATRIX

NOTE :

EACH 'X' INDICATES A NON ZERO ELEMENT.

FIG. 3.2 LAYOUT OF STIFFNESS AND MASS MATRICES

$[m] =$

	J_1	J_2	J_3	J_4	J_5	J_6	J_7	J_8	J_9	J_{10}	J_{11}	J_{12}	J_{13}	J_{14}
J_1	X							X						
J_2		X				X			X				X	
J_3			X		X					X		X		
J_4				X			X					X		X
J_5			X		X					X		X		
J_6		X				X			X				X	
J_7				X			X					X		X
J_8	X							X						
J_9		X				X			X				X	
J_{10}			X		X					X		X		
J_{11}				X			X				X			X
J_{12}			X		X					X		X		
J_{13}		X				X			X				X	
J_{14}				X			X				X			X

(b) ELEMENT MASS MATRIX

$[K_g] =$

	J_1	J_2	J_3	J_4	J_5	J_6	J_7	K_1	K_2	K_3	K_4	K_5	K_6	K_8
J_1		X		X	X	X	X		X		X	X	X	X
J_2			X	X	X	X	X			X	X	X	X	X
J_3		X	X	X	X	X	X		X	X	X	X	X	X
J_4		X	X	X	X	X	X		X	X	X	X	X	X
J_5		X	X	X		X	X		X	X	X	X	X	X
J_6		X	X	X	X	X	X		X	X	X	X	X	X
J_7														
K_1		X		X	X	X	X		X		X	X	X	X
K_2			X	X	X	X	X			X	X	X	X	X
K_3		X	X	X	X	X	X		X	X	X	X	X	X
K_4		X	X	X	X	X	X		X	X	X	X		X
K_5		X	X	X	X	X	X		X	X	X		X	X
K_6		X	X	X	X	X	X		X	X	X	X	X	X

NOTE:

EACH 'X' INDICATES A NON ZERO ELEMENT.

(C) ELEMENT GEOMETRIC MATRIX

FIG. 3.2 LAYOUT OF STIFFNESS AND MASS MATRICES (CONTD.)

illustrated in this article following the numbering system just introduced for nodal displacements. The location of non-zero elements of element stiffness, mass, and geometric matrices obtained from equation 2.24, 2.30 and 2.40 respectively are shown in Fig. 3.2 after rearrengment.

3.4 TRANSFORMATION OF AXES

The structural property matrices derived in chapter 2 are formulated for member axes. These property matrices corresponding to member axes must be transformed to property matrices for structure or global axes. A typical space frame element with local and global co-ordinate system of axes is shown in Fig. 3.3. To transform the element stiffness matrices from member to global axes, the proper transformation matrex is to be used. Actions and displacements can also be transformed from member axes to structure axes or vice versa by this transformation matrix Ti. Here i refers to the element number. When stiffness matrix for an element in local axes and corresponding matrix for transformation to global axes are known, stiffness martix in global co-ordinate system can easily be obtained by conventional procedures. Thus the element stiffness and element geometric matrices for an element i in the global co-ordinate system

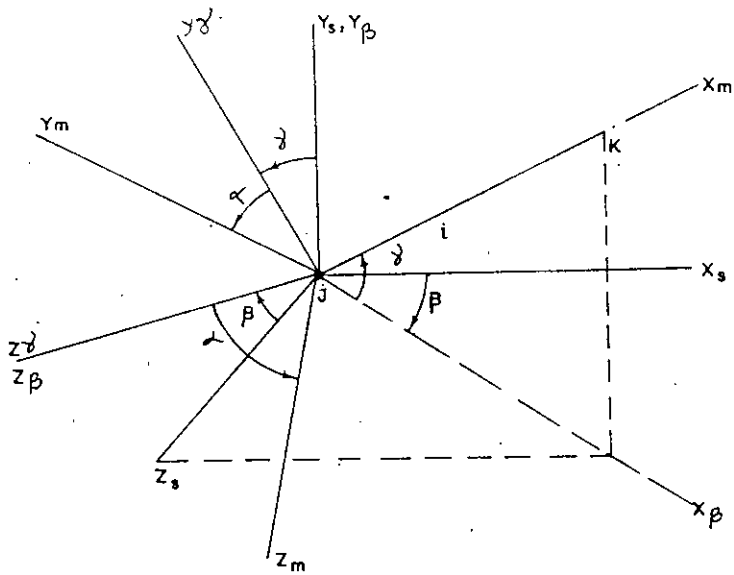

FIG. 3.3 a GLOBAL & MEMBER AXES OF A SPACE FRAME MEMBER

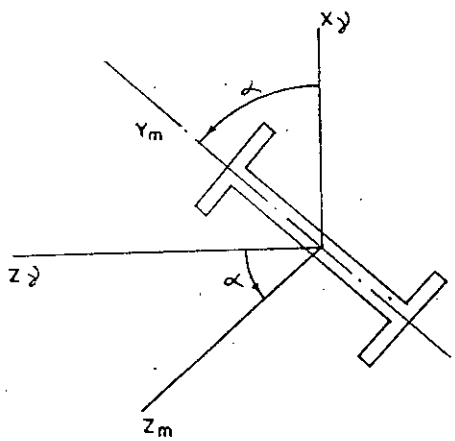

FIG. 3.3 b ROTATION OF SPACE FRAME MEMBER ABOUT Xm AXIS

may be obtained from

$$[K_{Ei}]^g = [T_i]^T [K_{Ei}] [T_i]$$

$$[K_{Gi}]^g = [T_i]^T [K_{Gi}] [T_i]$$

Now it is evident that the order of the transformation matrix [Ti] should be same as the order of $[K_{Ei}]$ or of $[K_{Gi}]$ i,e equal to 14. By partitioning the transformation matrix into its submatrices t_i, it can be written as;

$$[T_i] = \begin{bmatrix} ti & 0 \\ 0 & ti \end{bmatrix}$$

where [0] denotes the nullmatrix and the order of both t_i and [0] is seven.

The submatrix $[t_i]$ consists of rotational matrix R and $[t_i]$ can be expressed as

$$[ti] = \begin{bmatrix} R & 0 & 0 \\ 0 & R & 0 \\ 0 & 0 & 1 \end{bmatrix}$$

where the rotational matrix R arises due to orientation of axes and is given by

$$R = \begin{bmatrix} C_x & C_y & C_z \\ \dfrac{-C_xC_y \cos\alpha - C_z \sin\alpha}{C_x^2 + C_z^2} & C_x^2 + C_z^2 \cos\alpha & \dfrac{-C_yC_z\cos\alpha + C_x\sin\alpha}{CX^2 + C_z^2} \\ \dfrac{C_xC_y\sin\alpha - C_z\cos\alpha}{C_x^2 + C_z^2} & -C_x^2 + C_z^2\sin\alpha & \dfrac{C_yC_z\sin\alpha + C_x\cos\alpha}{C_x^2 + C_z^2} \end{bmatrix} \quad (3.1)$$

Here Cx, Cy, Cz are the direction cosines of the member axes as in Fig. 3.3a. And the angle α denotes the rotation about xm axis shown in Fig. 3.3b. The rotation matrix R expressed by Eq. 3.1 is valid for any member except vertical. The rotation matrix R for any vertical member is given by

$$R_{vert} = \begin{bmatrix} 0 & Cy & 0 \\ -Cy\cos\alpha & 0 & \sin\alpha \\ cy\sin\alpha & 0 & \cos\alpha \end{bmatrix}$$

3.5 COMPONENTS OF THE COMPUTER PROGRAM

The computer program consists of a number of subroutines combined together by a main program. Each of the subroutines carries out definite operations and is linked together by a series of simple statements contained in the main program. In fact the main program controls the overall analysis and maintains the sequence of solution scheme described in Art. 3.2. A flow chart is shown in Fig. 3.4 to show how the analysis is carried out and when the subroutines are called in the main program. The names of the subroutines that appear in the flow chart are used in this program and are described in the following article.

3.6 THE SUBROUTINE

In this article the functions of the subroutines how they are formed and some of their special features are described in brief.Flow charts are also enclosed for some of the subroutines. However, some subroutines have not been described because of their simplicity. These include TRANS, EEQLD, DIMP. MULT, TSTIF etc, For example TRANS evaluates the transformation matrix,while MULT is used for the multiplication of two matrices. The description of principal sub-

Read number of elements, number of nodes, properties of sectionns. co-ordinates of each node, element connectivity matrix, support conditions and loading corresponding to unit scale factor.

↓

Call subroutine ELSTIF to formulate the element stiffness matrix for each element. And by subroutine TRANS and TSTIF the element stiffness matrices are transfered from local to global ases.

↓

Call subroutine EELSTIE and subroutine ASSEM to assemble the element stiffness matrices to form the overall structure stiffness matrix.

↓

Call subroutine BOUND1 to modify the stiffness matrix in accordance with the boundary conditions for elastic analysis.

↓

Call subroutine SOLVE to find out the nodal displacements and then find the element end forces.

↓

(1)

1

Call subroutine GEOTM to obtain the element geometric matrices. And by subroutine TRANS and TSTIF, the element geometric matrices are transformed from local to global axes.

Call subroutine EELSTIF and subroutine ASSEM to assemble the element geometric matrices to form over all matrix.

Call subroutine BOUND2 to modify the overall stiffness and geometric matrices in accordance with the boundary conditions of the problem.

Convert Eq. 2.56 to a standard eigen value problem by inverting the overall stiffness matrix.

Call subroutine EIGEN to find out the critical load factor and corresponding mode shapes.

Call subroutine ECMAM to form the element mass matrices and transfer it from local axes to global axes by calling the subroutine TRNS and TSTIF just as for element stiffness matrix.

2

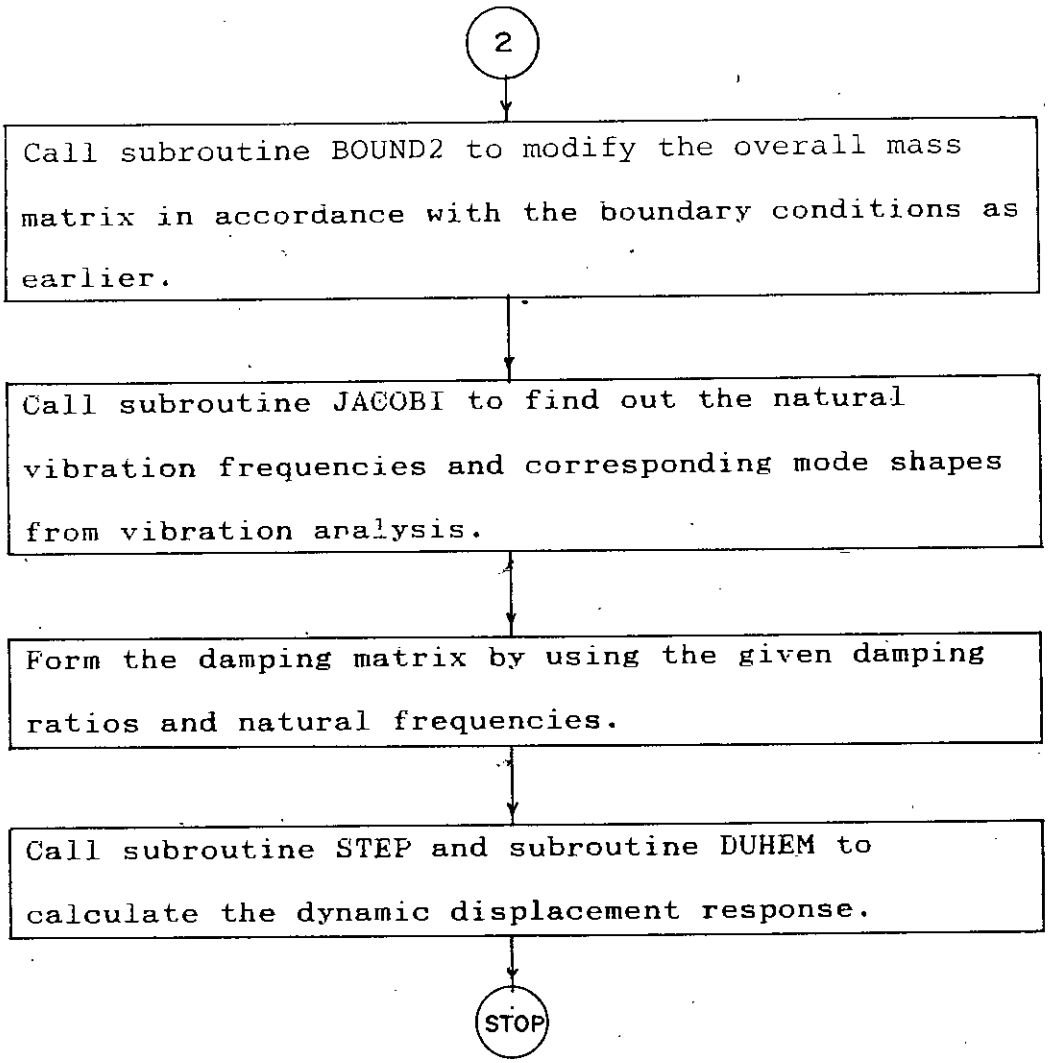

Fig. 3.4 FLOW CHART FOR MAIN PROGRAM

routines follows below.

Subroutine ELSTIF: The purpose of this subroutine is to form the element stiffness matrices by using Eq. 2.24. The integrations are performed by Simpson's Method. The stiffness matrix of thin walled space member is developed for member axes. By using proper transformation matrix, the stiffness matrix for local axes can be transformed to that for global axis.

Subroutine GEOTM: The purpose of this subroutine GEOTM is to form the element geometric stiffness matrices. The member nodal forces, necessary for the formation of element geometric matrix, are taken from prebuckling analysis. The formation of element geometric matrices is similar in principle to that for element stiffness matrices using Eq.2.40.

Subroutine ECMAM: The purpose of this subroutine ECMAM is to form the element consistent mass matrices by using Eq.2.30. The method of forming the consistent mass matrices for thin-walled space frame element has been described by Rao (32). However, he considered six degrees of freedom at each node. The procedure followed by him has been generalized in this

subprogram to form the consistent mass matrix in member axes.

Subroutines ASSEM and ESESTIF: Subroutine ASSEM is used to assemble the member stiffness and mass matrices into overall stiffness and mass matrices. The assembling procedure adodpted here is simple and similar to that presented by Rao (32). Another subroutine ESTIF is also called by main program to accomplish the purpose. By the subroutine EESTIF the elements of the member matrices are placed into their appropriate location in the overall matrices. Then by calling the subroutine ASSEM the overall matrices are formed. As the element stiffness matrix, geometric matrix, and mass matrix are of same oreder (14x14), the same subroutine is used to assemble them. Thus the subroutines EESTIF and ASSEM are called every time after each element elastic stiffsness, geometric stiffness and mass matrices are formed in the main program.

Subroutine BOUND1: The purpose of the subroutine BOUND1 is to introduce the boundary conditions into the overall stiffness matrix and load vector for the prebuckling analysis. The procedure of introducing the boundary conditions is quite simple and similar to that presented by Weaver (42). In this procedure, all the elements of rows and columns of the matrix corresponding to the zero displacements are

equated to zero except the main diagonal one which is equated to unity. The corresponding element of the load vector for zero displacement is taken to be zero. A flow chart of subroutine BOUND1 is shown in Fig. 3.5.

Subroutine SOLVE: With the help of this subroutine, the elastic prebuckling deformations of the structure are obtained. For the formation of element geometric matrix, the internal forces at the nodes of the structure should be determined first. For this purpose an initial elastic analysis has to be performed using known load vector and overall stiffness matrix. Hence, the nodal displacements are found first with the help of subroutine SOLVE. Gauss-Jordan method of solution of simultaneous equations has been utilized in this subroutine. The program was developed based on the mathematical logic presented by Wang (43).

Subroutine BOUND2: The purpose of subroutine BOUND2 is to introduce the boundary conditions into the assembled overall stiffness matrix, overall geometric matrix, and overall mass matrix. The procedure of imposing boundary conditions is quite simple. The rows and columns of the matrices corresponding to the zero displacements are suppressed. A flow chart of subroutine BOUND2 is shown in Fig. 3.6. Here, matrix AA is the given assembled overall matrix and CXC is

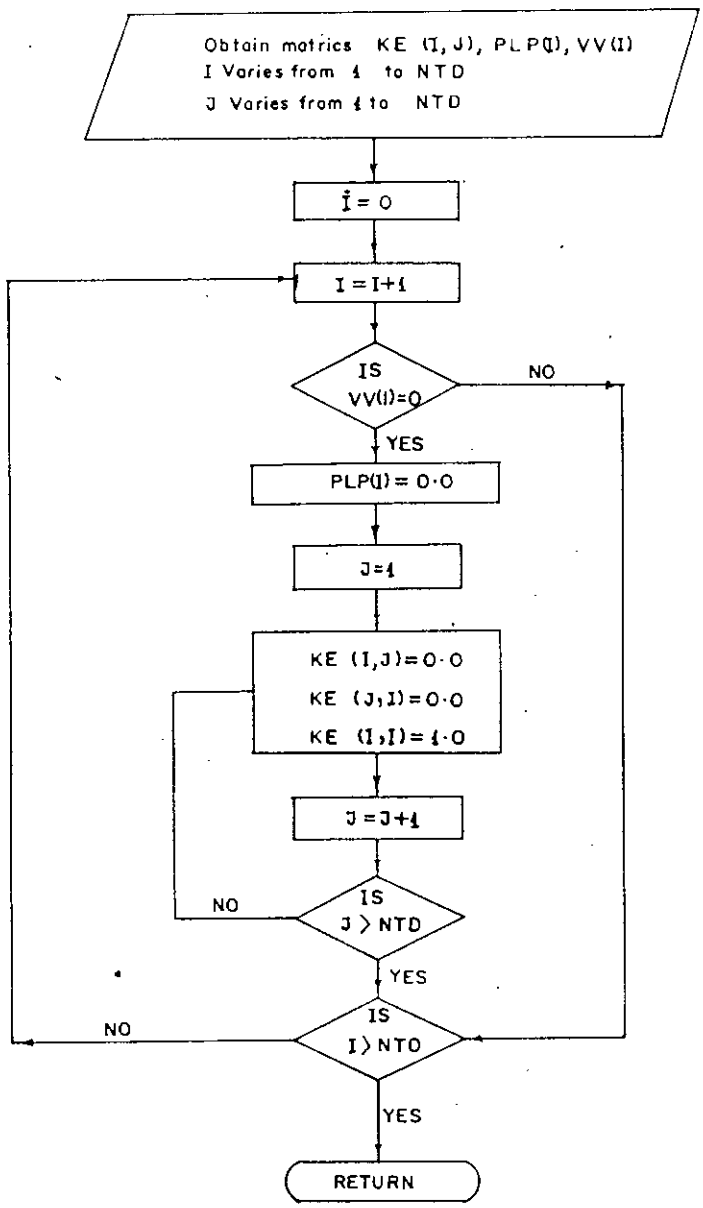

FIG. 3.5 FLOW CHART FOR SUBROUTINE BOUND 1

the matrix obtained after introducing the boundary conditions. The overall matrix AA is always a symmetric square matrix and it's order is equal to the total degrees of freedom NTD. Matrix VV is the predefined matrix that indicates the degrees of freedom corresponding to which the rows and columns of the matrix AA should be deleted. In fact matrix VV contains zero's at the zero displacements and one elsewhre.

Subroutine GAUSS: The function of this subroutine is to inverse any given matrix. The overall structure stiffness matrix is inversed for calculating the critical buckling load. Besides this, several other inversions are also required for dynamic analysis. Gauss-Jorden method of inversion of matrix has been used in this subroutine.

Subroutine EIGEN: The subroutine EIGEN is used to find the critical eigen value and the corresponding eigen vectors. For this purpose Eq. 2.54 is converted to a standard eigen value problem by inverting the stiffness matrix and then multiplying it by geometric stiffness matrix corresponding to unite scale factor. This is shown in Eq. 2.57. So the highest value of eigen value obtained from this equation will give the critical load factor. The order of matrices after introducing the boundary conditions is indicated in

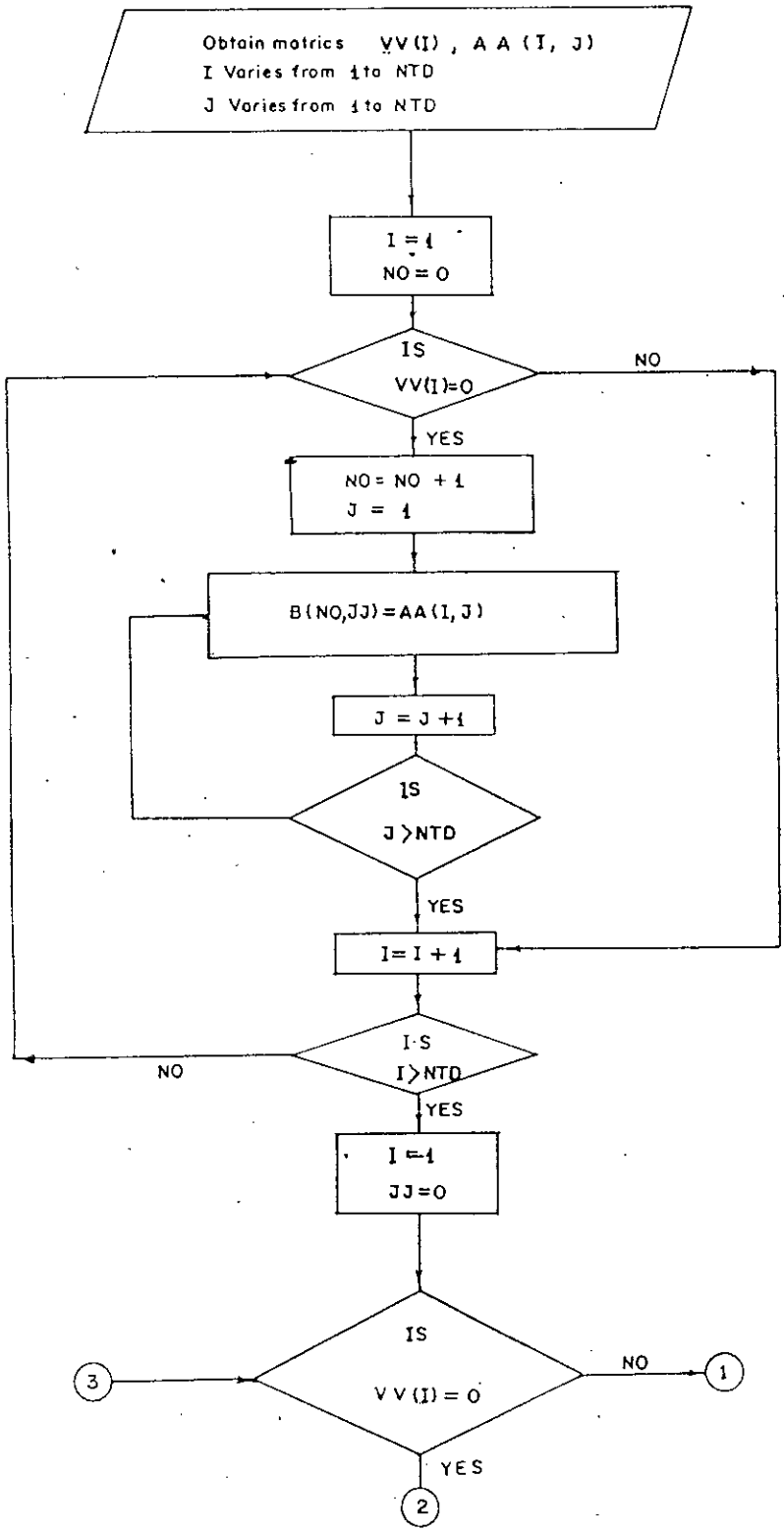
Obtain matrics VV(I) , A A (I, J)
I Varies from 1 to NTD
J Varies from 1 to NTD
I = 1
NO = 0
IS
VV(I)=0
NO
YES
NO = NO + 1
J = 1
B(NO,JJ) = AA(I, J)
J = J + 1
IS
J > NTD
YES
I = I + 1
I S
I > NTD
NO
YES
I = 1
JJ = 0
IS
VV(I) = 0
NO
1
3
YES
2

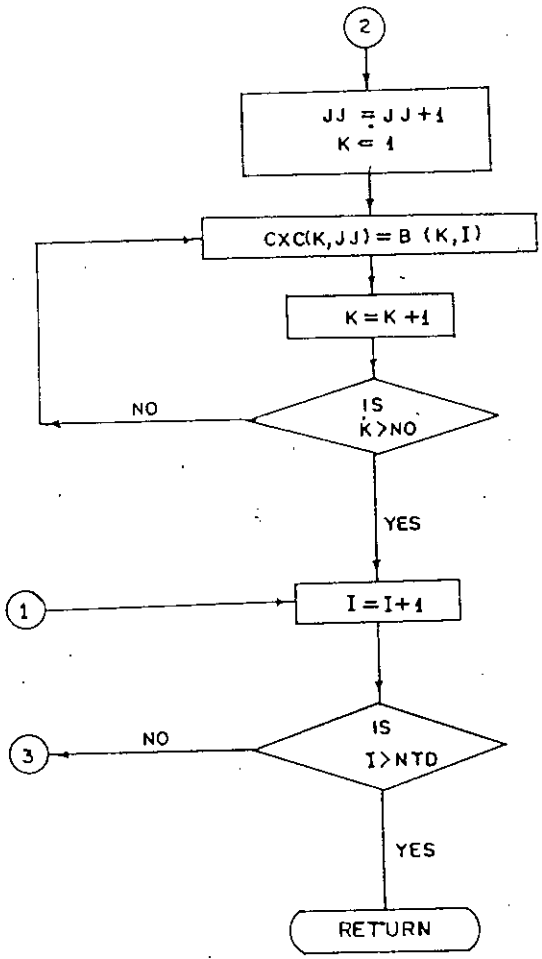

FIG. 3.6 FLOW CHART FOR SUBROUTINE BOUND 2

the subroutine by NO. The procedure for calculating the critical load and corresponding mode shapes are quite simple and is similar to that presented by Wang (43) with slight modification. The method presented by wang with Rayleigh Quotient has been used. A flow chart of subroutine EIGEN is shown in Fig. 3.7.

Subroutine JACOBI: The purpose of this subroutine is to calculate the natural frequencies and corresponding mode shapes by using Eq. 2.49. Combined stiffness matrix formed by subtracting the geometric stiffness matrix from the overall stifffness matrix is used for this purpose. The combined stiffness matrix and the consistant mass matrix used in this program are square, symmetric and of same order. The solution of the general eigen value problem gives the square of the frequencies and mode shapes. The general Jacobian method has been employed for solving the eigen value problem. This subroutine has been developed following the procedure described by Bathe (7).

Subroutine STEP: The subroutine STEP is used to determine the dynamic response such as, displacement, velocity and acceleration corresponding to different degress of freedom. The step-by-step integration method has been used in this subroutine to calculate the response. This procedure is ap-

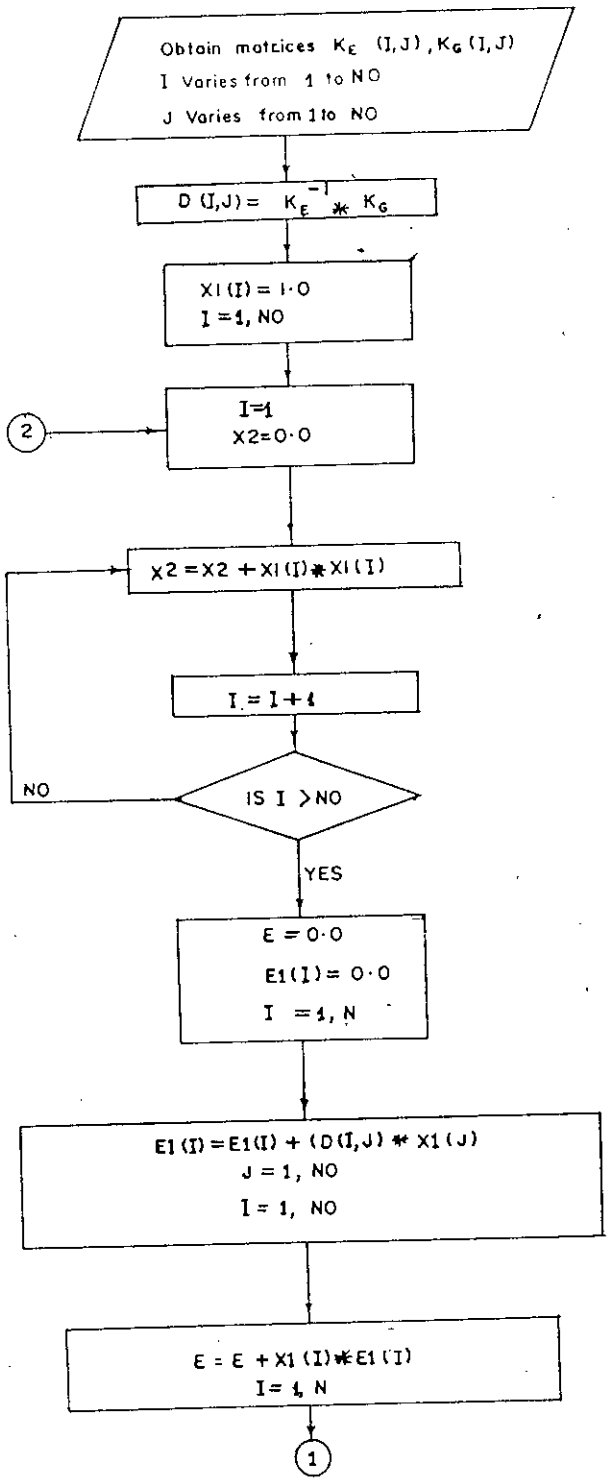
Obtain matrices K_E (I,J), K_G (I,J)
I Varies from 1 to NO
J Varies from 1 to NO
D (I,J) = K_E^{-1} * K_G
X1 (I) = 1·0
I = 1, NO
2
I=1
X2=0·0
X2 = X2 + X1 (I) * X1 (I)
I = I + 1
NO
IS I > NO
YES
E = 0·0
E1 (I) = 0·0
I = 1, N
E1 (I) = E1 (I) + (D (I,J) * X1 (J)
J = 1, NO
I = 1, NO
E = E + X1 (I) * E1 (I)
I = 1, N
1

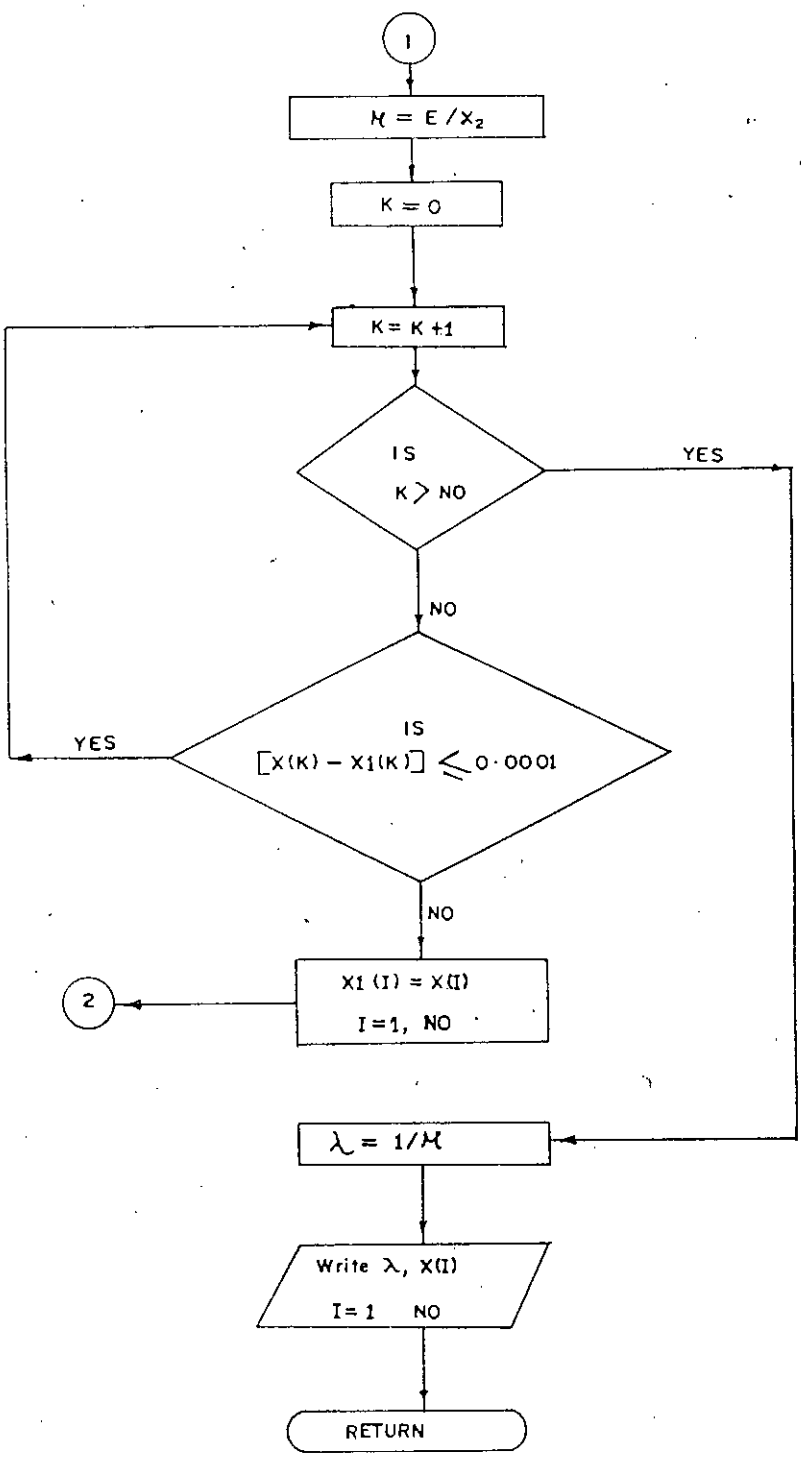

FIG. 3.7 FLOW CHART FOR SUBROUTINE EIGEN

plicable both to linear and nonlinear structures. The method that has been used here is simple and similar to that presented by Clough (12).

Subroutine DUHEM: The subroutine DUHEM calculates the dynamic response as an alternative method to step by step integration method. The Duhamel integral method, described by Clough (12), has been used in this subroutine. This method is applicable only for linear systems. The job is performed here by using Eq. 2.71. The integration has been done by Simpson's rule and incremental procedure has been employed for this purpose. By this procedure only the dis placement response can be determined. The normal co-ordinates are first found and then by Eq. 2.60 the displacement response is obtained.

CHAPTER 4

NUMERICAL ANALYSIS AND DISCUSSIONS

4.1 INTRODUCTION

The theoretical investigations and the computer program developed and described in the preceding chapters enable the solution of a wide variety of dynamic problems. In this chapter, several numerical examples are presented in order to assess the accuracy of the solution procedure and to arrive at definite conclusions regarding the effect of various important factors on dynamic response of thin-walled space and plane frame works. Since the dynamic response and critical load are both functions of sectional properties, a specific preselection of the sectional dimensions is needed at the beginning of each solution. The sectional properties chosen in each problem have been outlined in the description of their solution. The boundary conditions for static and dynamic analyses have also been elaborated at each description. The critical load is determined in the process of dynamic analysis by setting the condition that the frequency vanishes when the applied load approaches its critical value. The critical load thus obtained is then compared with that determined by using theoretical solutions if available in the existing

literature. The convergence of solution is also depicted. The effect of axial force, lateral buckling, structure geometry etc. on the dynamic response has been investigated and presented graphically.

4.2 CONVERGENCE OF THE SOLUTION

In the solution technique described in chapter 2; the structure is divided into a finite number of elements. The overall structural properties are formulated by assembling the individual element properties. The convergence of the solution procedure is first tested' for the determination of critical load in simple examples of beams and columns. For this purpose, these are divided into a number of elements. The number of elements has been varied to judge the convergence of the solution. The critical load computed in this way is compared with that obtained from available theoretical solutions for the problems treated in this article. It has been observed that finite element solution converges rapidly to the exact solution when number of element increases. The convergence of finite element solution for different problems is described in the following subarticles.

4.2.1 Concentrated Load at Middle of Simply Supported Beam

A simply supported doubly symmetric I section beam is considered here for lateral buckling. The beam is loaded by a concentrated load P at the center of its span. The selected coordinate system is shown in Fig. 4.1. The beam is of 2"x8"x1/4" cross section and of 100 inches length. The sectional properties of beam are shown in the figure. It is assumed that the load is applied at the centroid of the section. Lateral buckling will occur when the load reaches its critical value. It is assumed that during deformation the ends of the beam can rotate with respect to the principal axes parallel to the z and y axes, while rotation with respect to x axis is prevented by some constraint. The deviation of the solution for critical load, obtained from the present analysis, from its exact value given by analytical procedures of Timoshenko (37) is illustrated in Fig. 4.1. In this figure, the percentage of deviation is plotted against number of finite elements in which the member is divided. It is found that the critical load differs by about 4.76% from its exact value for a one element solution. For two element solution it varies by about 1.2%. It is observed that if the number of elements are increased, the percentage of deviation diminishes to a negligible

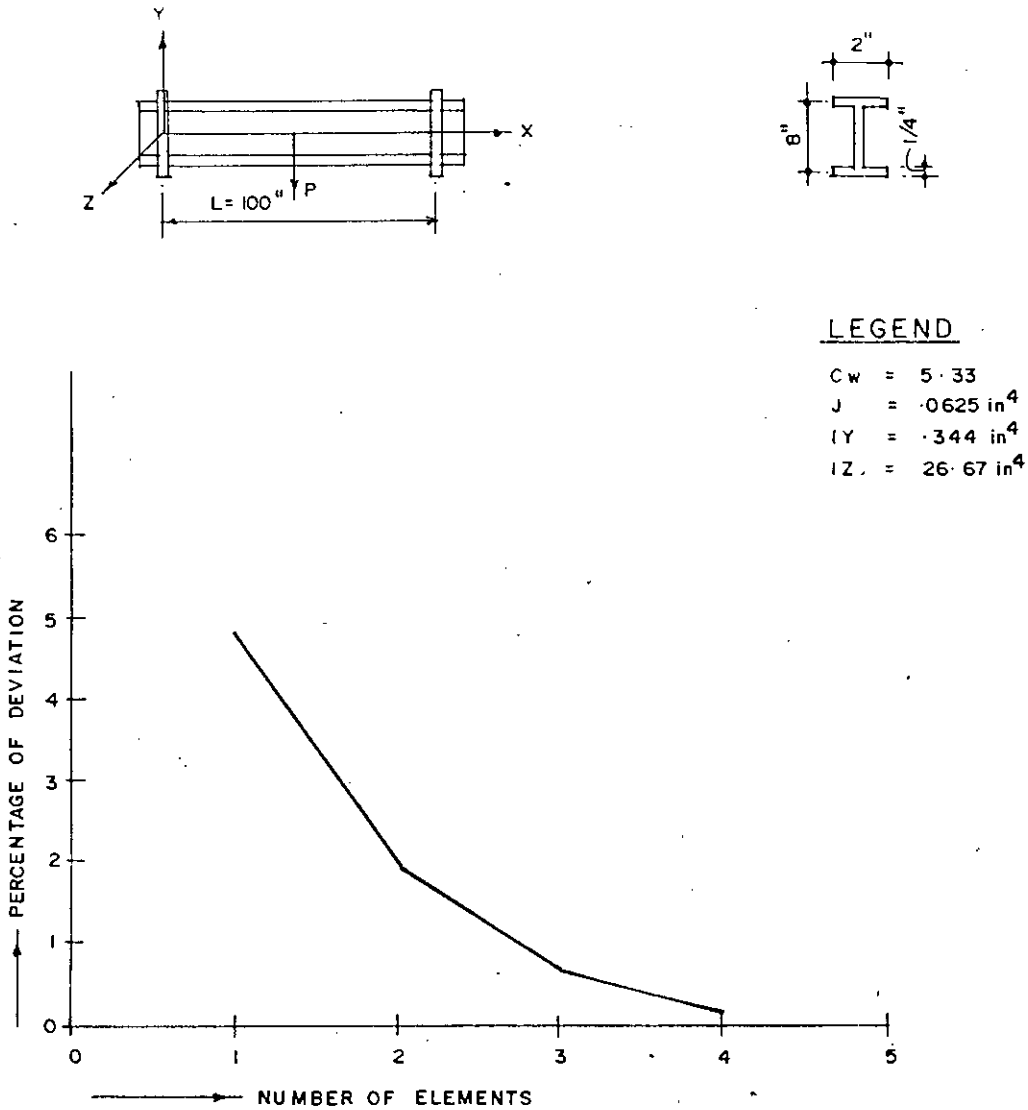

FIG. 4-1 CONVERGENCE OF FINITE ELEMENT SOLUTION FOR LATERAL BUCKLING

value and the solution from the present analysis closes to its exact value.

4.2.2 Lateral Buckling of a Cantilever Beam

Here lateral buckling is considered in an example of a cantilever beam acted upon by a force p applied at the centroid of the end cross section. A doubly symmetric I-section of 2"x8"x1/4" cross section and 100 inches in length has been selected for this purpose. The coordinate system and sectional properties are shown in Fig. 4.2. At the left end the bean is fixed and so all the degrees of freedom at this node are fully restrained. At the other end the beam section is free for all degrees of freedom. Now as the load p is increased gradually, the cantilever approaches to its critical condition when the deflected shape in the xy plane becomes unstable and lateral buckling occurs. The exact value of critical load for the cantilever beam has been calculated by solving the differential equations derived by Timoshenko (37) and can be expressed by

$$P_{cr} = \gamma \frac{\sqrt{EI_y C}}{L^2}$$

The deviation of critical load determined in the present solution

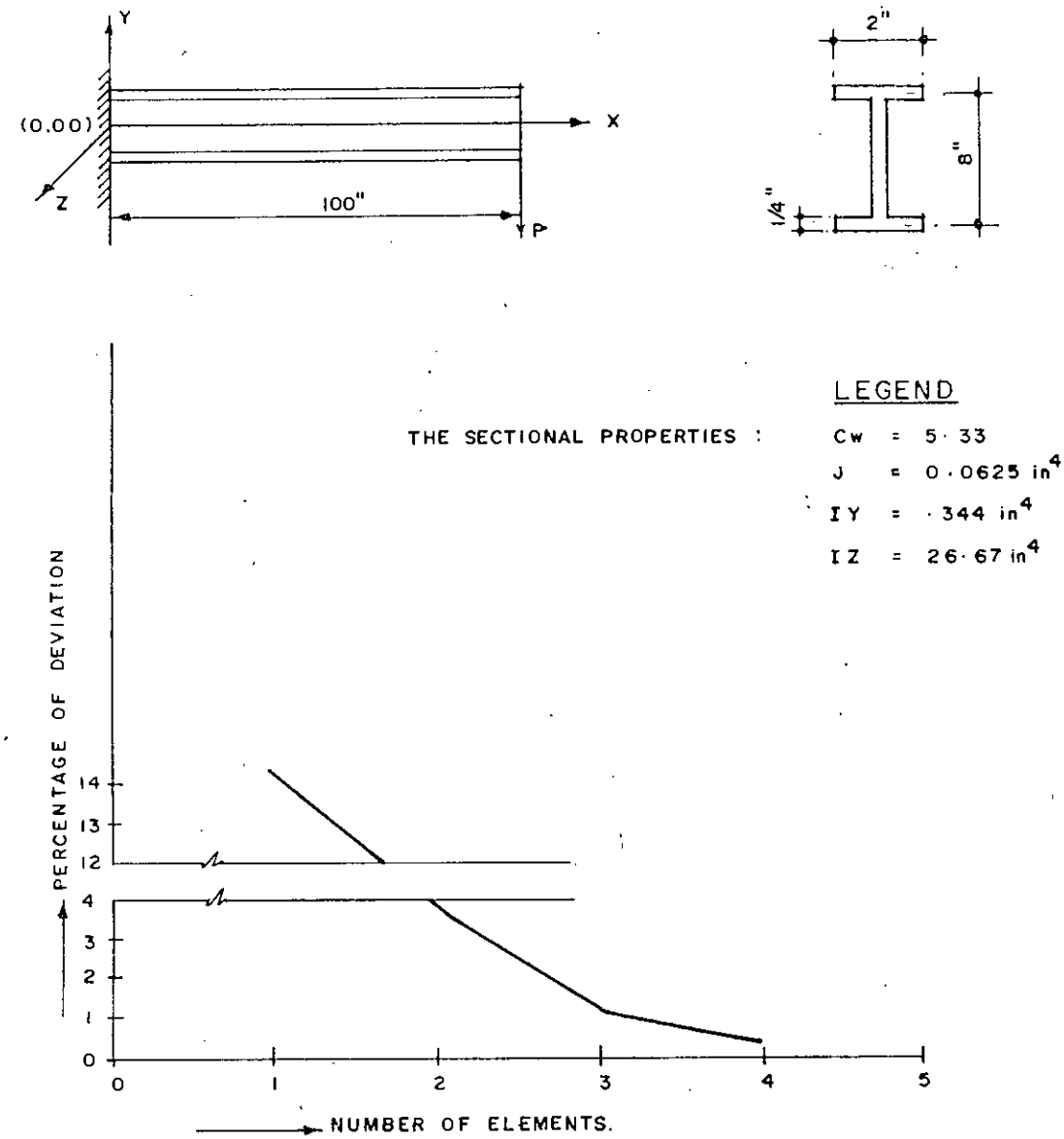

FIG.4-2 CONVERGENCE OF FINITE ELEMENT SOLUTION FOR LATERAL BUCKLING

from that of its exact value is shown in Fig. 4.2. Here also the percentage of deviation is plotted against the number of elements. It is found that the critical load differs significantly from its exact value for a one element solution, while for the two element solution the variation becomes negligible and close to its exact value. It is observed that taking three and four elements, the solution may be considered as exact for all practical purposes.

4.2.3 Buckling by Pure Torsion

As a last example for convergence test, pure torsional buckling of an axially loaded column of doubly symmetric I-section is considered. A pin ended column of 2"x8"x1/4" cross section and 100 inches in length has been selected for this purpose. The coordinate system for the member is shown in Fig. 4.3. The sectional properties are also shown in the figure. The load is assumed to be applied at the centroid of the section. As the shear center coincides with the centroid of the section, the torsional buckling is not coupled with the buckling by flexure. For the end supports of the column, it is assumed that they are free to warp and to rotate about the z and y axes but cannot rotate about x axis. The deflections in the y and z directions are also restrained at the ends. The deviation of the critical

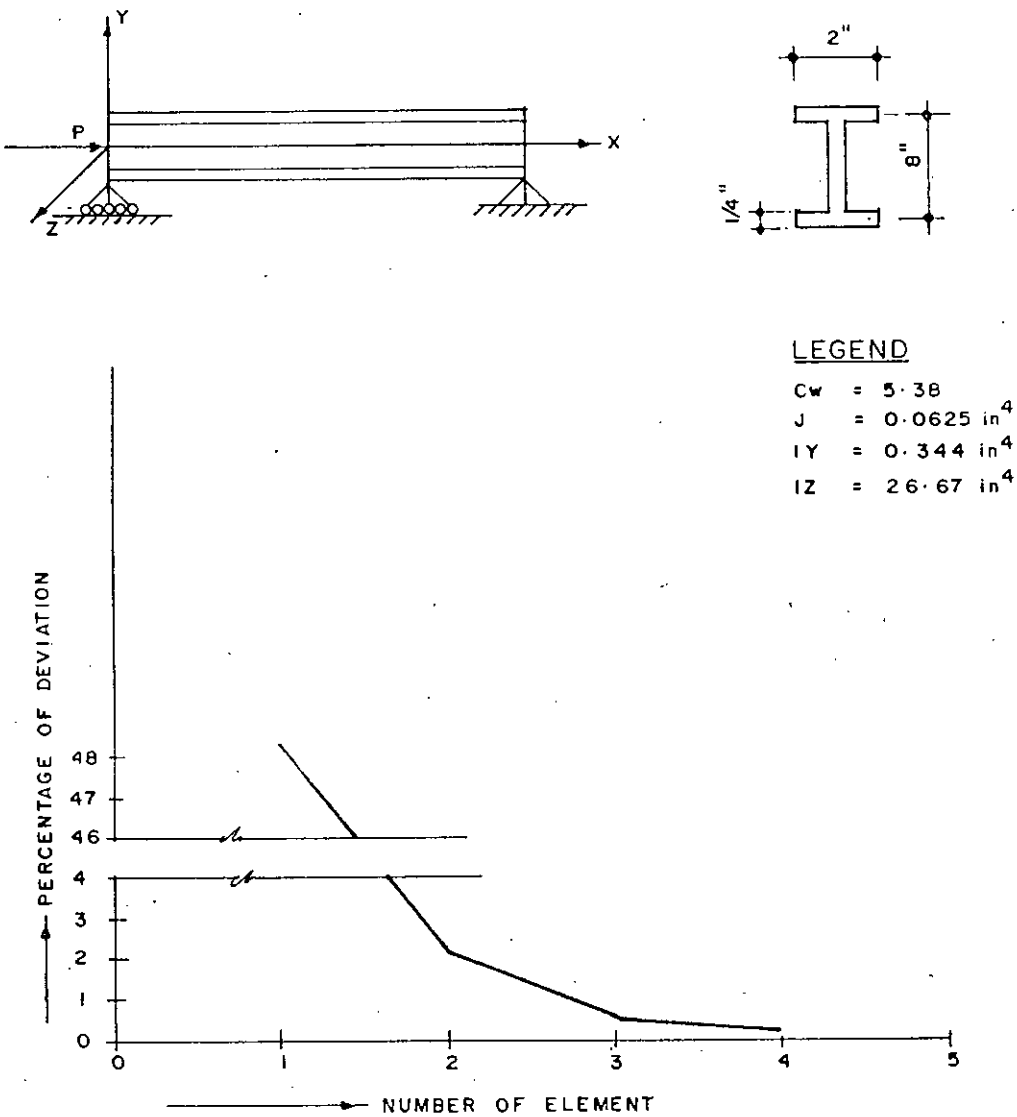

FIG. 4-3 CONVERGENCE OF FINITE ELEMENT SOLUTION FOR TORSIONAL BUCKLING

load obtained by using the present finite element approach from that of its exact value using analytical procedure of Timoshenko (37) is shown in Fig. 4.3. It is found that for one element solution, the deviation is very large. However, the solution converges rapidly to the exact value when the number of elements is increased. For four or five elements, the solution may be considered as exact.

4.3 COMPARISON OF SOLUTIONS BY STEP BY STEP INTEGRATION AND DUHAMEL INTEGRAL

In the theoretical investigation presented in chapter 2, it has been shown that the solution of dynamic analysis problem can be performed by step by step integration and Duhamel integral method. In this article, an attempt has been made to assess the variation of dynamic response solved by these two methods. To carry out this investigation, a simple portal frame of height h=100 inches and bay width b = 100 inches is selected. The sectional properties of all members are same and shown in Fig. 4.4. The static and dynamic loads are also shown in the figure. The structure is considered to be a plane frame. The load history for dynamic loads corresponding to different degrees of freedom are assumed to remain same and is shown in Fig. 4.4. The dynamic responses corresponding to degree of freedom 1 at different time has been calculated by both these methods and presented in

graphical forms. The curves in Fig. 4.4 have been drawn for displacement v_1 as a function of time t when the load factor λ 0.0. Fig. 4.5 represents similar curves for $\lambda = 1.0$. It is evident from Fig. 4.4 that the variation of dynamic response by these two methods is insignificant when the load factor $\lambda = 0.0$. However, Fig. 4.5 shows that the variation becomes significant when the load factor $\lambda = 1.00$. It is seen that the dynamic response v_1 by Duhamel integral method is higher than that by step by step integration method. Hence, it may be concluded from the two curves in Fig. 4.4 and Fig. 4.5, that the variation in dynamic response by two methods increases with the increasing value of λ . As the increase of load factor λ increases the nonlinearity of the structure, the difference in solution by two methods widens and for nonlinear structures the solution by two methods diverges significantly.

4.4 EFFECT OF AXIAL FORCE ON DYNAMIC RESPONSE

In the evaluation of structural properties presented in chapter 2, it has been shown that the geometric stiffness matrix k_G is the contribution of axial forces. It has also been shown that the combined stiffness matrix k is evaluated by subtracting the geometric stiffness matrix from elastic stiffness matrix. Hence, the stiffness of the structure will be reduced due to the effect of axial forces. It is therefore intended to assess the effect of

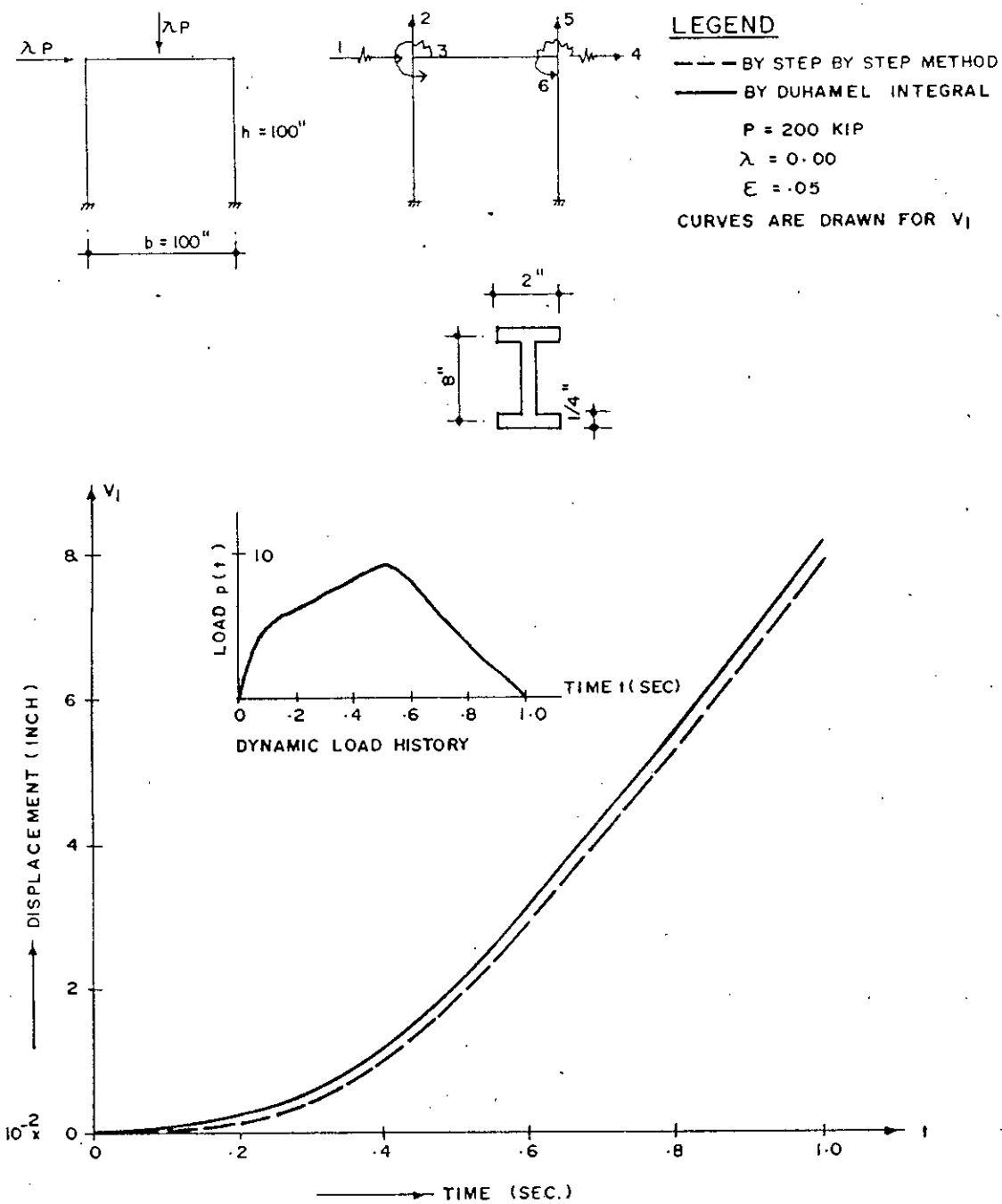

FIG. 4-4 COMPARISON OF STEP BY STEP AND DUHAMEL INTEGRAL

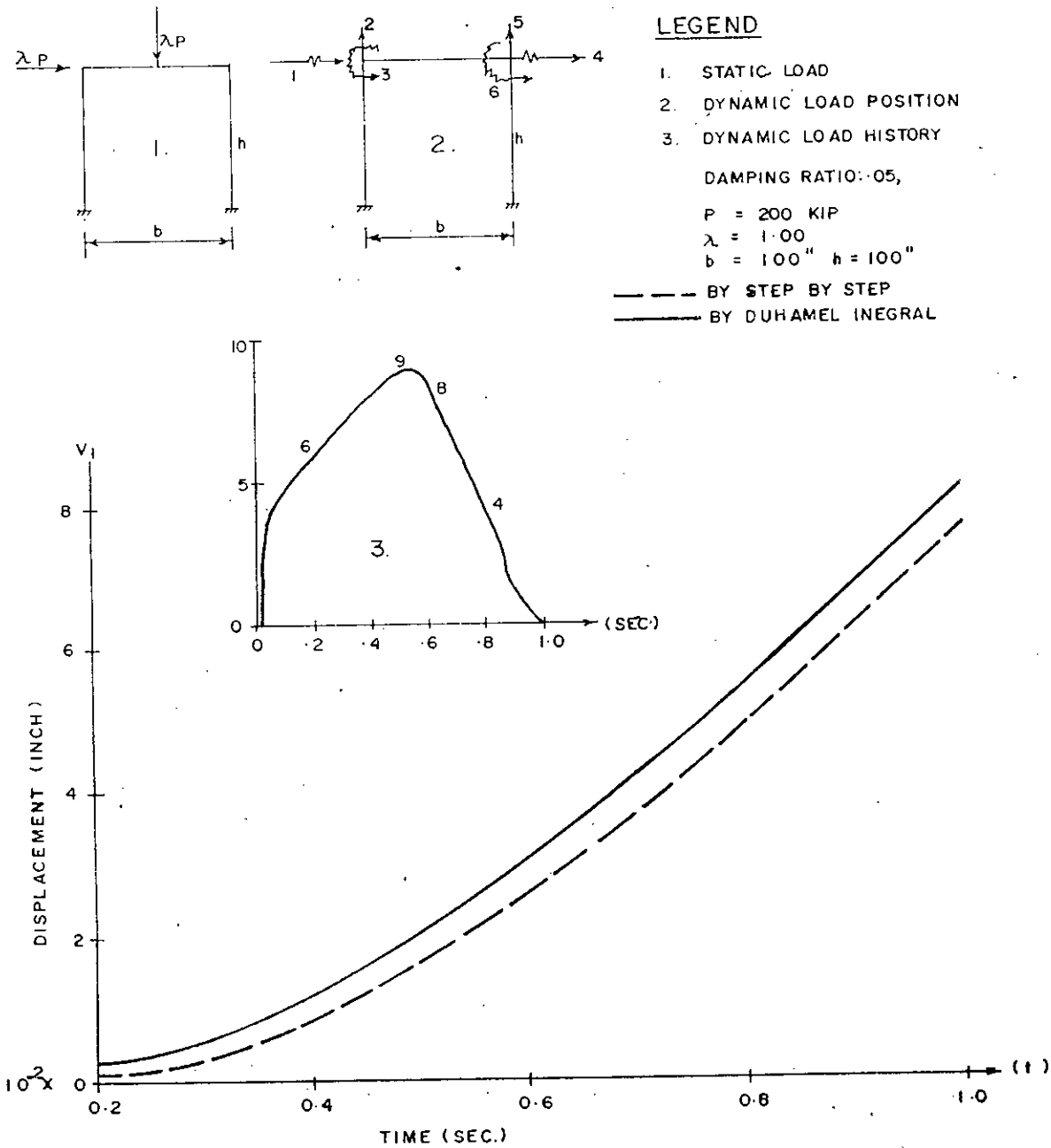
λP
λP
1.
h
b
2
5
1
3
6
4
2.
h
b
LEGEND
1. STATIC LOAD
2. DYNAMIC LOAD POSITION
3. DYNAMIC LOAD HISTORY
DAMPING RATIO: ·05,
P = 200 KIP
λ = 1·00
b = 100" h = 100"
BY STEP BY STEP
BY DUHAMEL INEGRAL
10
9
8
6
5
4
3.
0
0 ·2 ·4 ·6 ·8 1·0
(SEC)
V1
8
6
4
2
DISPLACEMENT (INCH)
10⁻²x 0
0·2 0·4 0·6 0·8 1·0
(t)
TIME (SEC.)

FIG. 4 - 5

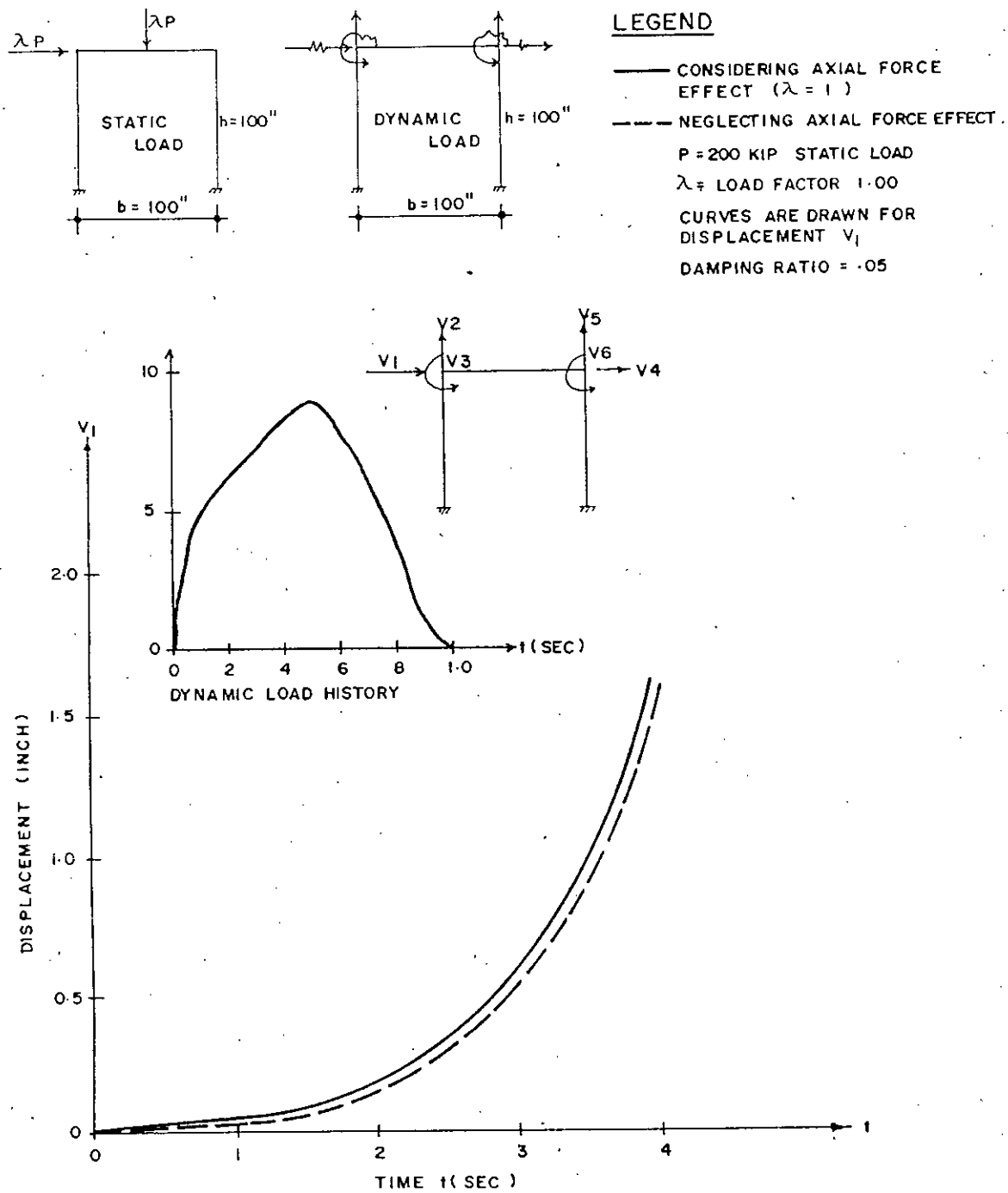

FIG.4-6 EFFECT OF AXIAL FORCE ON RESPONSE

axial force on the dynamic response of thin-walled space frame works. A portal frame is considered here with the same sectional properties as that for the one shown in Fig. 4.4. The height of the structure and the static loading conditions are shown in Fig. 4.6. The load history for dynamic loads corresponding to each degree of freedom is assumed to remain same and is shown in Fig. 4.6. The dynamic displacement response v_1 is computed first by including the axial force effect and then by neglecting the effect. The results v_1 verses time are plotted in Fig. 4.6. The solid curve represents response considering axial force effect and the broken curve that with out axial force effect. From these curves, it is evident that the displacement response increases due to the effect of axial force, and the response continues to increase with the increasing load factor λ as the combined stiffness of the structure reduces.

4.5 EFFECT OF DAMPING RATIO ON DYNAMIC RESPONSE

The evaluation of damping matrix has been performed by using different damping ratios corresponding to different degrees of freedom as described in chapter 2. The purpose of this article is to evaluate the influence of variation of damping ratio on dynamic response. A thin-walled portal frame having same structural properties and dimensions as that in Art. 4.3 is

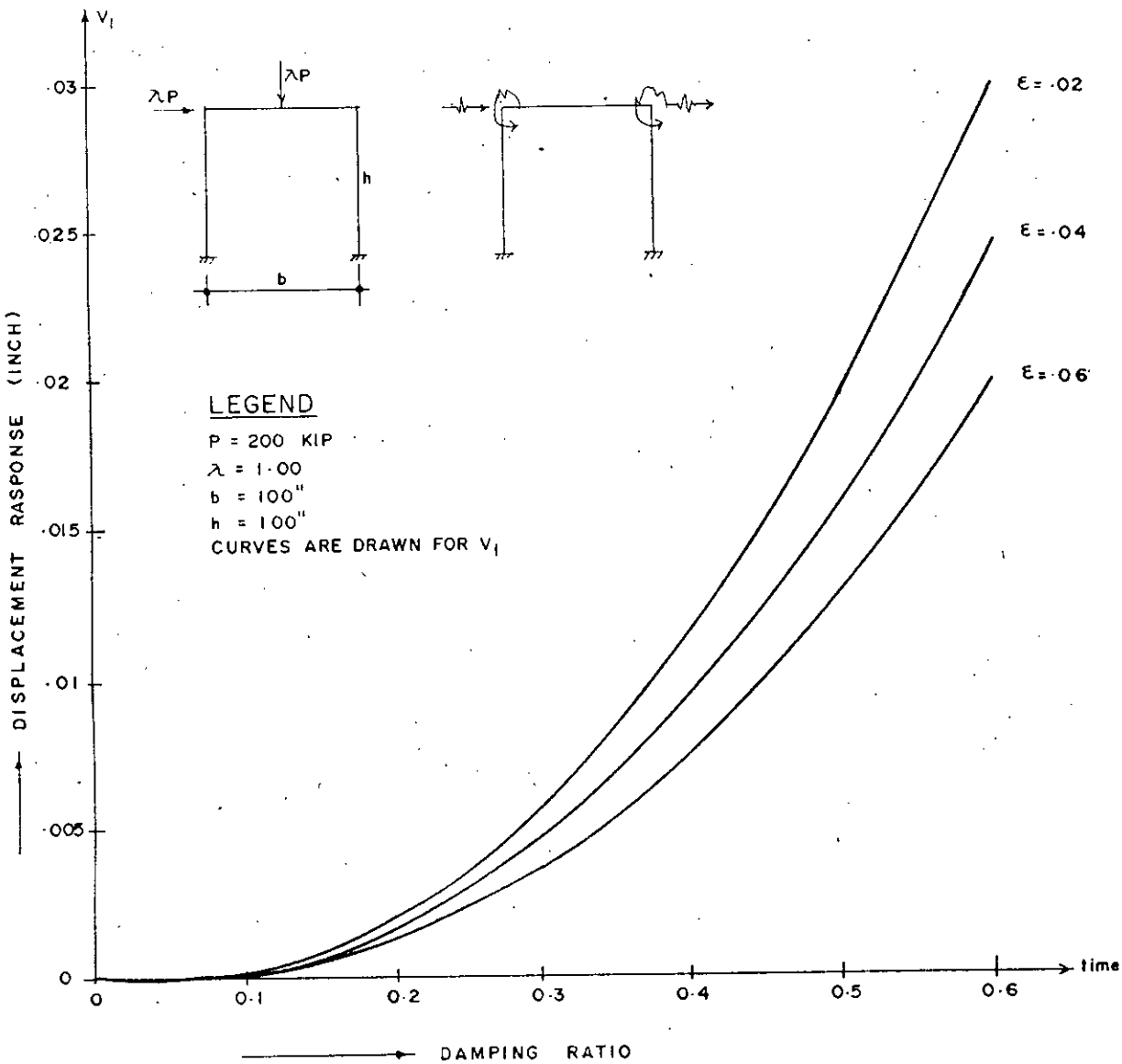

FIG. 4-7 EFFECT OF DAMPING RATIO

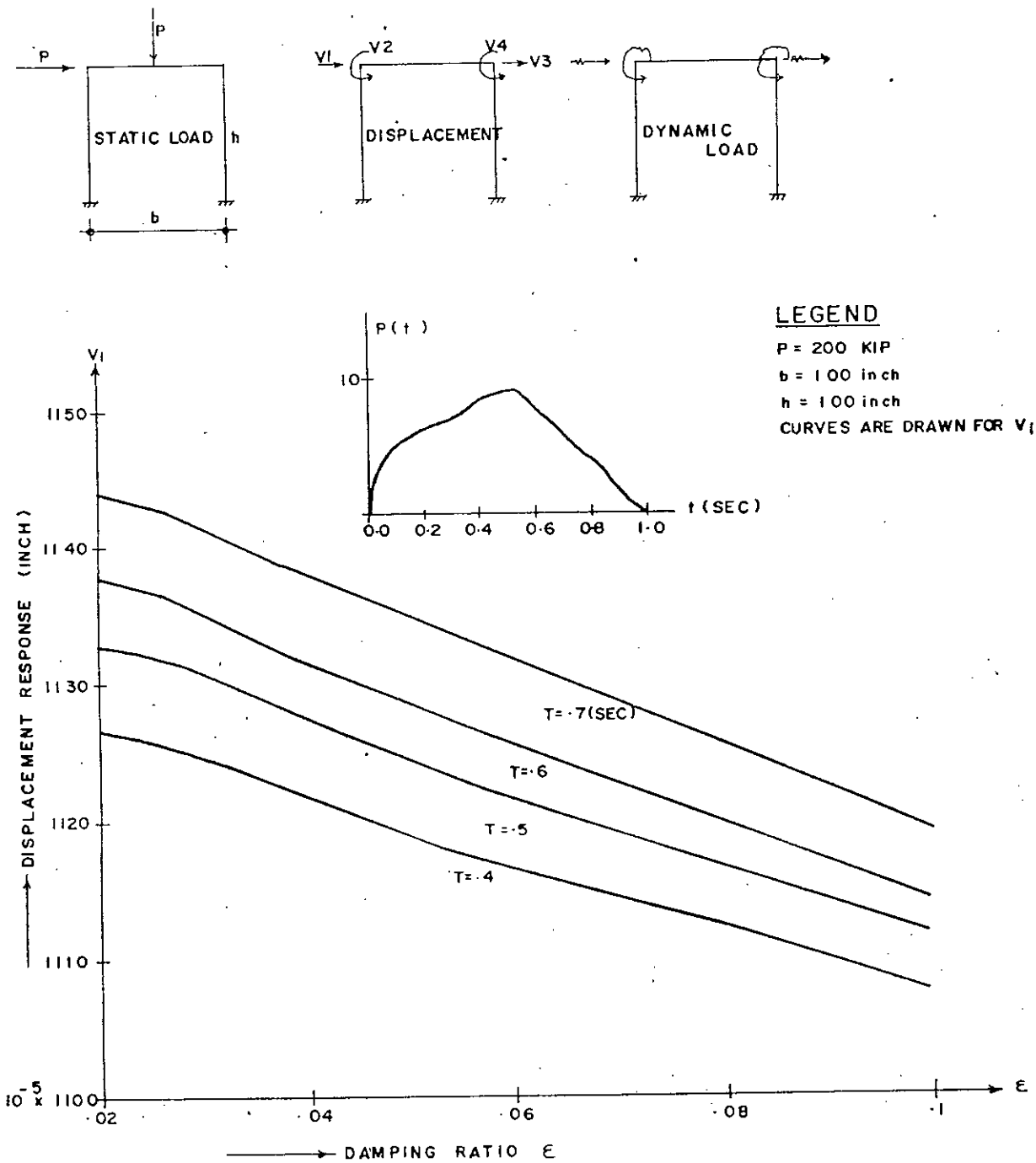

FIG.4 - 8 EFFECT OF DAMPING RATIO

selected for the investigation. The static load P and dynamic load history are shown in Fig. 4.7. The dynamic displacement response at different times corresponding to different damping ratios are computed. The variation of dynamic response with varying damping ratios illustrated by plotting displacement v_1 against time t in Fig. 4.7. and displacement v_1 against damping ratio ε in Fig. 4.8. Fig. 4.8 shows the variation of dynamic displacement response with damping ratio at different time. It is seen from this figure that at any particular time the dynamic displacement decreases gradually with increasing damping ratio. It is also evident that the corresponding response will be very low at a higher percentage of damping ratio. The same conclusion can be drawn from Fig. 4.7 as well. From this figure, it is evident that the response increases both with increasing time and decreasing damping ratio. However, the conclusion regarding the increase in displacement response with time may not be valid for times after the dynamic load ceases to act.

4.6 EFFECT OF STATIC LOAD FACTOR

It has been shown in chapter 2 that a prebuckling analysis is done corresponding to unit scale factor λ =1.00 for the evaluation of geometric stiffness matrix. It has also been shown that geometric stiffness matrix k_G is significantly influenced by static load factor λ i.e k_G will increase with a gradual

increase of load factor λ . So the combined stiffness matrix k will be affected by load factor. Here the influence of static load factor λ on frequencies , mode shapes and dynamic response are illustrated in the examples of different thin-walled structures. The following two subarticles describe in detail the influence of load factor λ on different factors in thin-walled planer and three dimensional frame works.

4.6.1 Effect of Load Factor on Frequency

The frequency of a structure can be computed from Eq.2.49. It can be seen from this equation that the frequency w, will be influenced by load factor λ . The variation of frequency with load factor is illustrated in Fig. 4.9 to 4.11 for three different structures. The dimensions and sectional properties of the structures are shown in the corresponding figures. The frequencies corresponding to each mode shape are computed by using the standard eigen value solution.

In Fig. 4.9 the frequencies w_1 , w_2 and w_3 corresponding to first three mode shapes are plotted against load factor λ for the space framework as shown. It is evident that all the frequencies decrease with the increase of static load factor and at a certain load factor, the minimum frequency w_1 vanishes. The higher frequencies also decrease and can vanish at higher load factor.

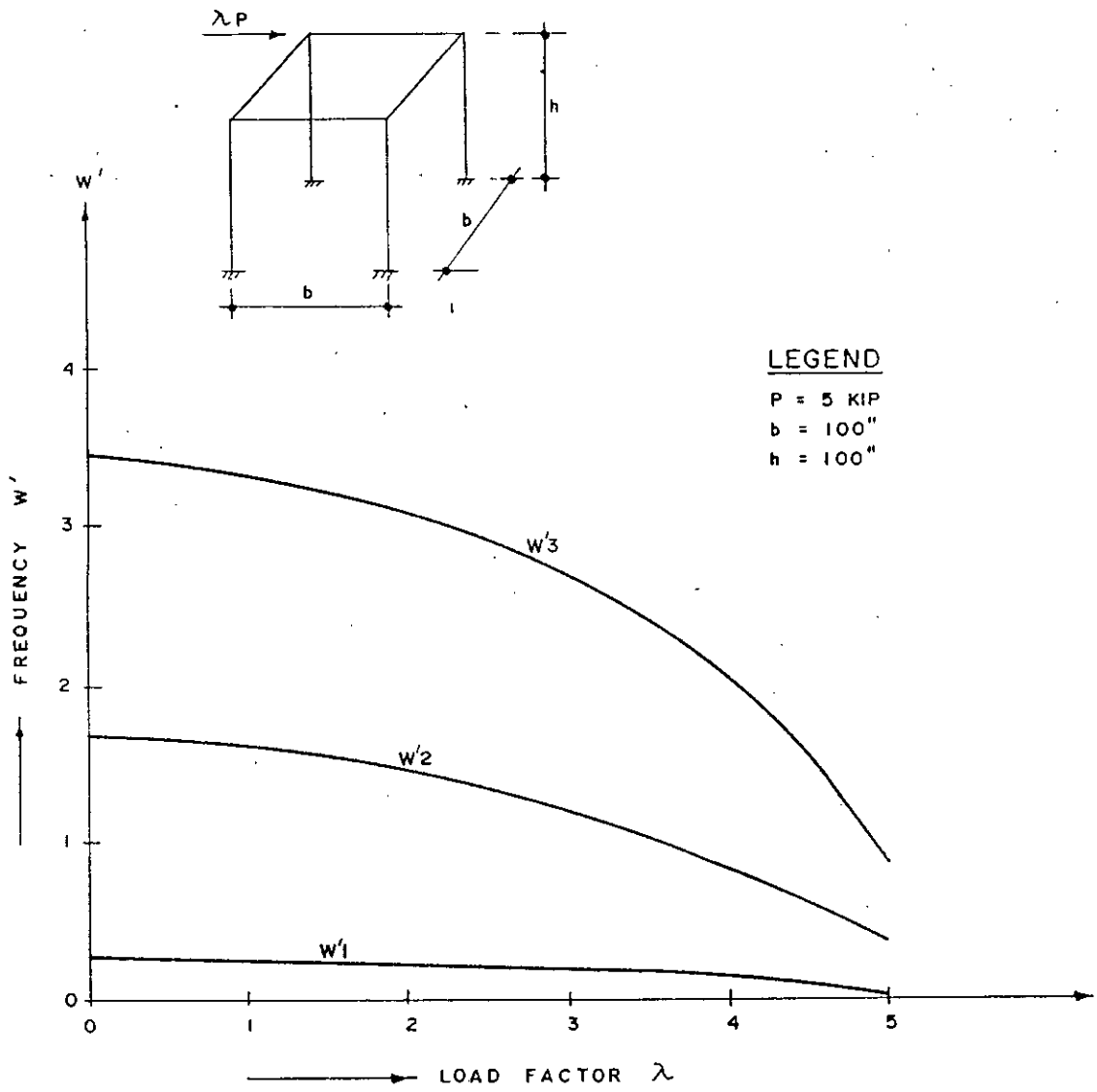

FIG. 4-9 EFFECT OF LOAD FACTOR ON FREQUENCY

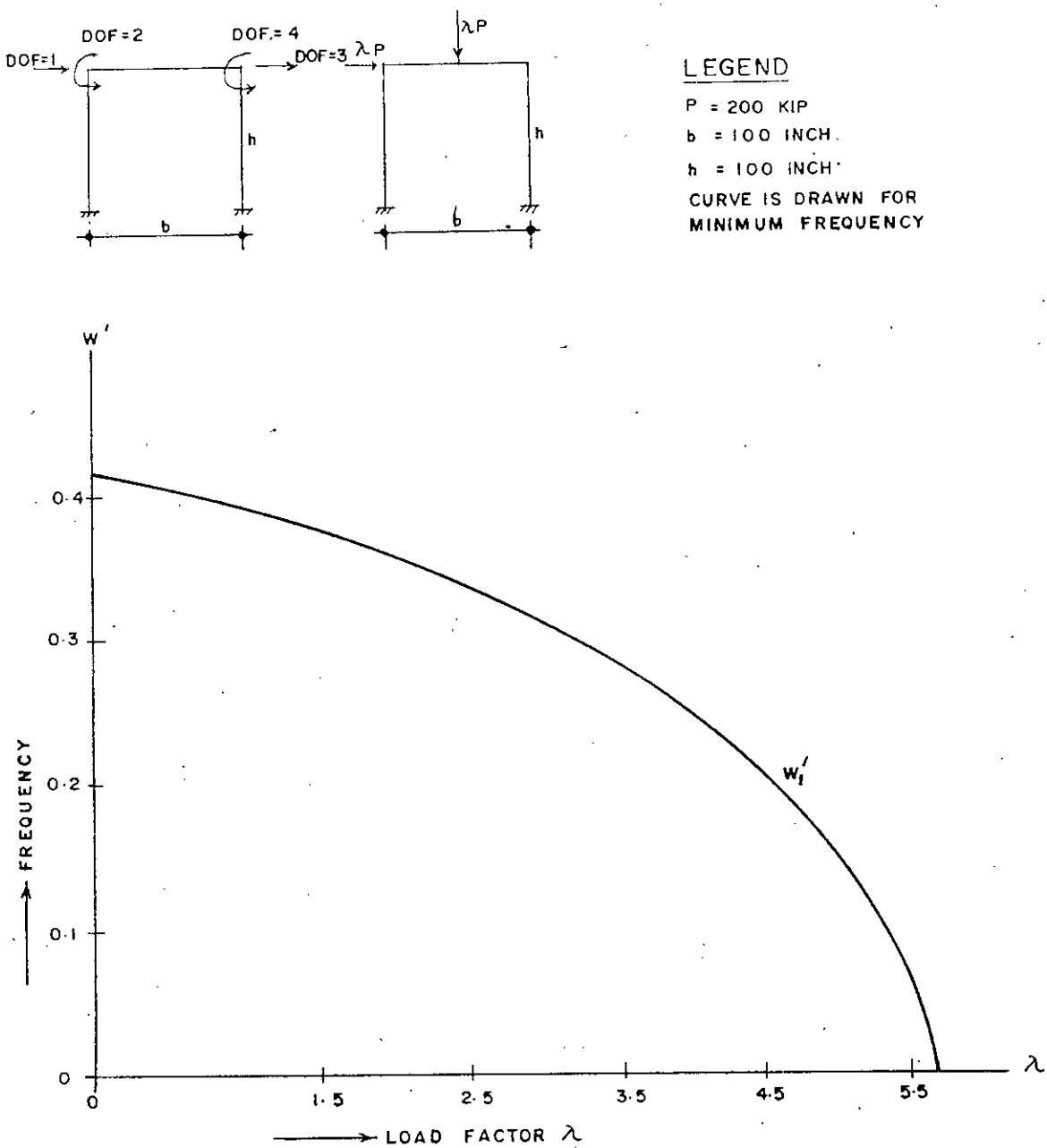

FIG. 4-10a : EFFECT OF LOAD FACTOR ON FREQUENCY

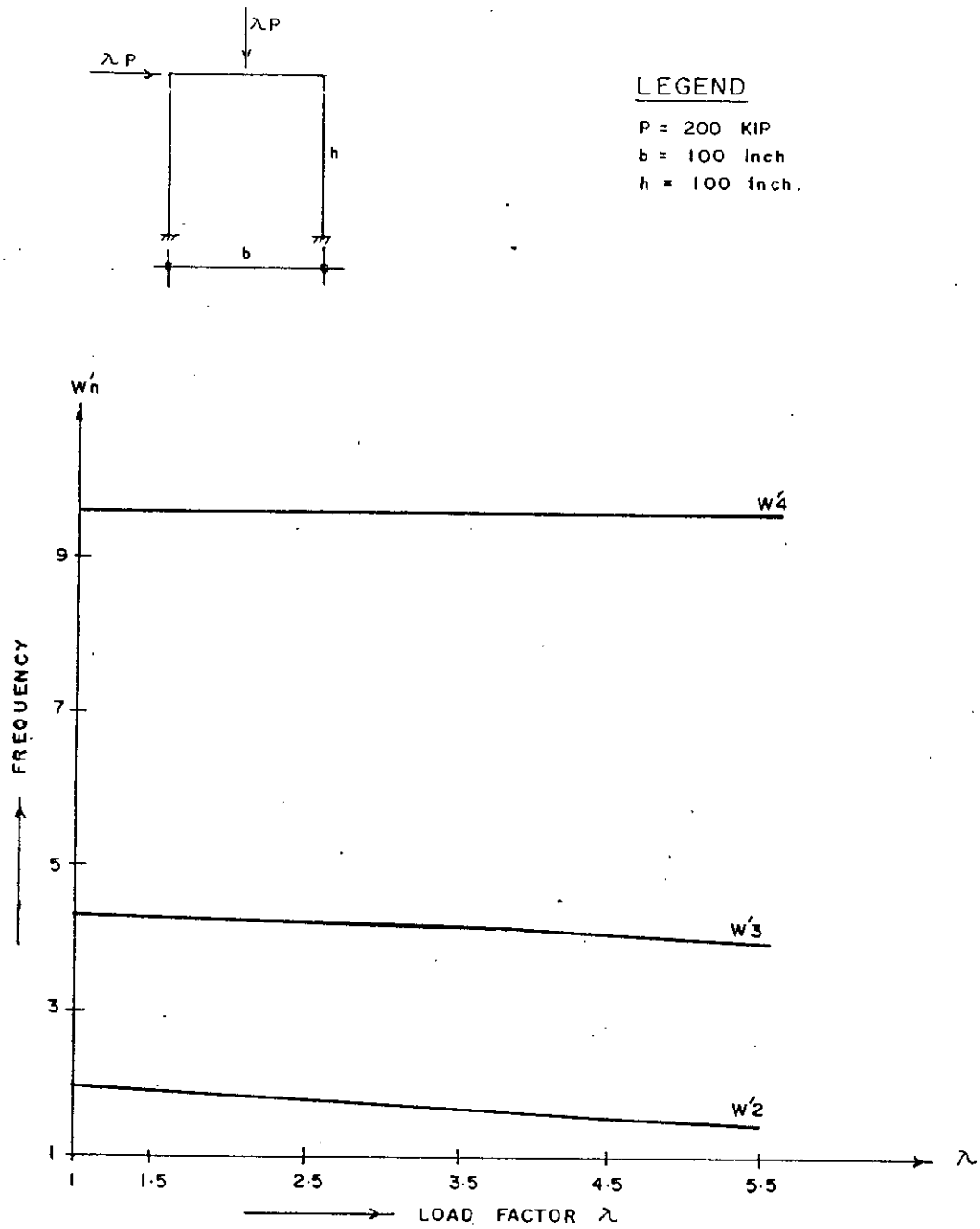

FIG.4 -10 b : EFFECT OF LOAD FACTOR ON FREQUENCY

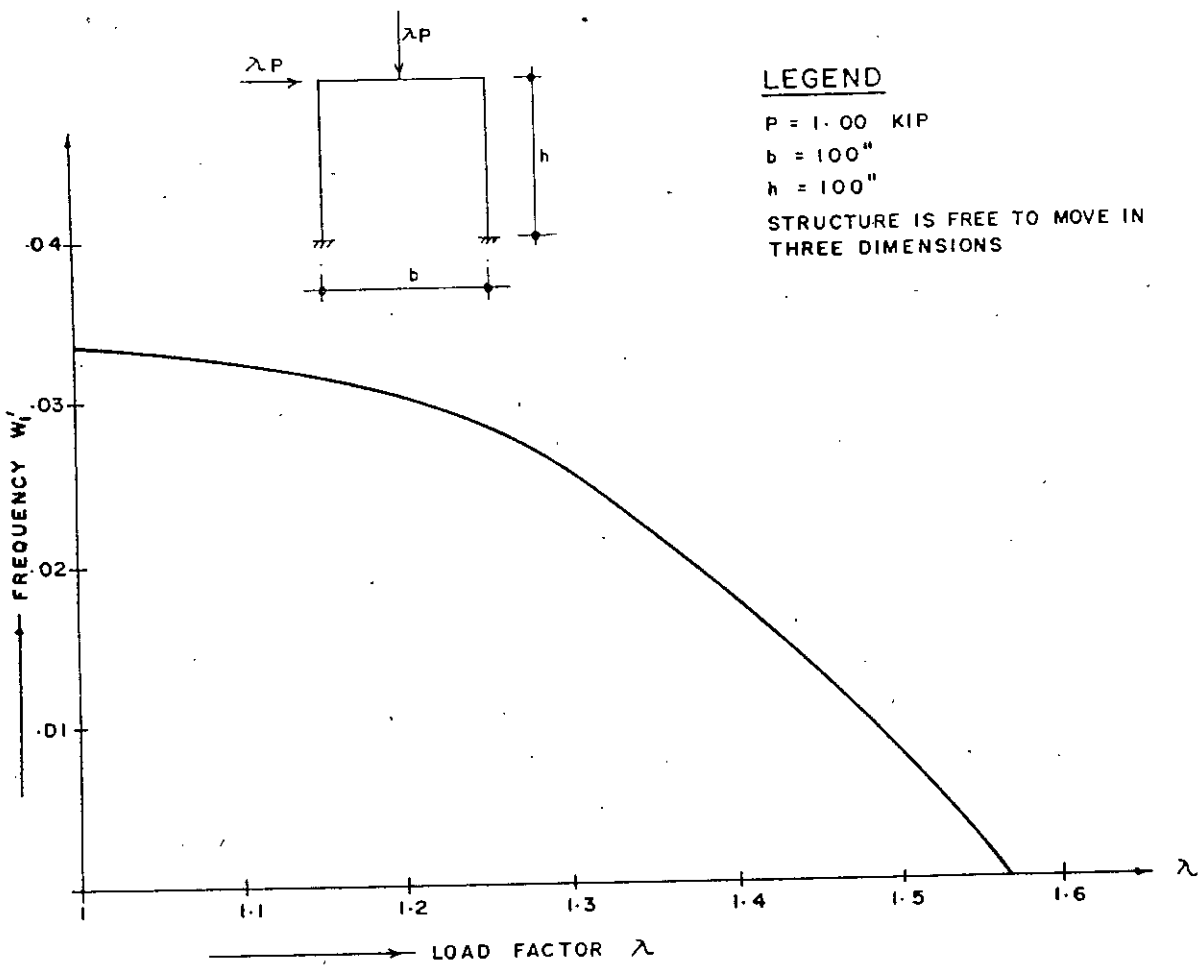

FIG. 4-11 : EFFECT OF LOAD FACTOR ON FREQUENCY

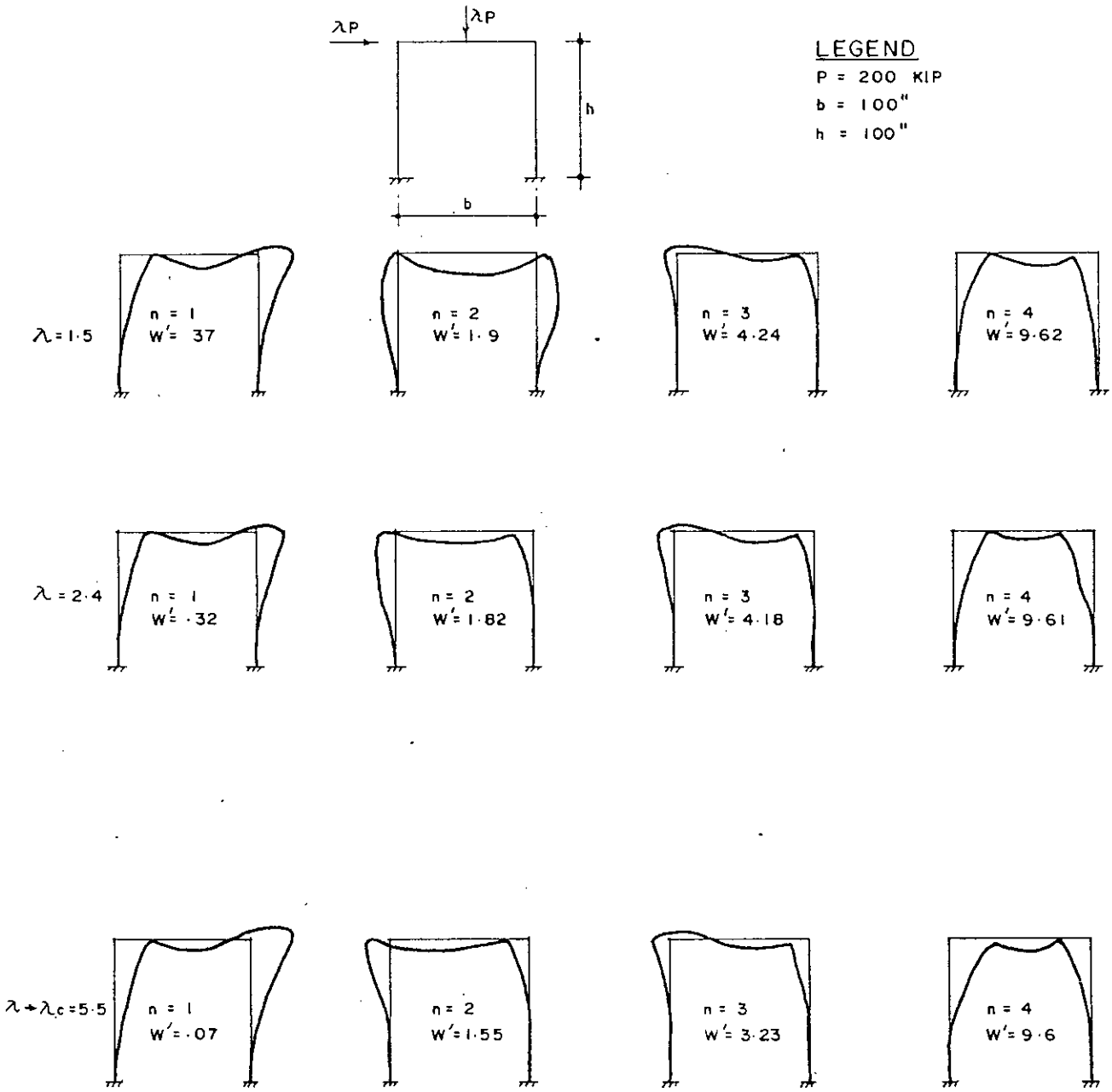

FIG. 4 -12 : MODE SHAPES AT DIFFERENT LOAD FACTOR

However, the corresponding load factors have no practical significance unless and otherwise the first mode of buckling is restrained in some way or other. The load factor at which the minimum frequency vanishes is the critical load factor λ for the structure. The critical load can be computed by multiplying the load on the structure by critical load factor λ .

Fig. 4.10 and Fig. 4.11 also represent the variation of frequency with load factor in the example of a portal frame. In Fig. 4.10, all the out of plane degrees of freedom of the frame are assumed to be restrained. Fig. 4.11 on the otherhand assumes that the motion of the frame can occur in three dimensions. From these figures, it becomes apparent that if the same structure is considered as plane framework, the critical load and frequency are much higher. However, comparing Fig. 4.9 with Fig. 4.11, it is seen that both frequency and critical load are increased when the portal frame free to move in three dimensions is transformed into a real space framework. This observation ascertains the need for bracing for a planar thin-walled system to be more stable and dynamically effective.

The different mode shapes corresponding to different frequencies have been investigated for the portal frame restrained for out of plane motion and is shown in Fig. 4.12. The mode shapes are given corresponding to three different factor λ . It is seen that at

the critical load factor λ the mode shape corresponding to minimum frequency is the actual failure mode of the structure.

4.6.2 Effect of Load Factor on Response

The static load factor λ must influence the dynamic response significantly as the combined stiffness changes due to a change in load factor. The extent of this influence is investigated in this article by studying the variation of dynamic response with load factor for two different structures. A portal frame of height h = 100 inches and span b = 100 inch is considered first. The static loading condition with load factor λ and dynamic loads are shown in Fig. 4.13. It is assumed that the dynamic load history is identical for all degrees of freedom as shown in figure. The damping ratios corresponding to each degree of freedom is assumed different. The dynamic response corresponding to each degree of freedom is computed by step by step integration method. The variation of displacement response v_1 with load factor is illustrated in Fig. 4.13 at four different times.
Fig. 4.14 illustrates the influence of time on the response v_1 for five different load factors. From Fig. 4.13 it is observed that dynamic response increases practically linearly with the increase of load factor. From Fig. 4.14 it is seen that v_1 increase both with increase in time and load factor.

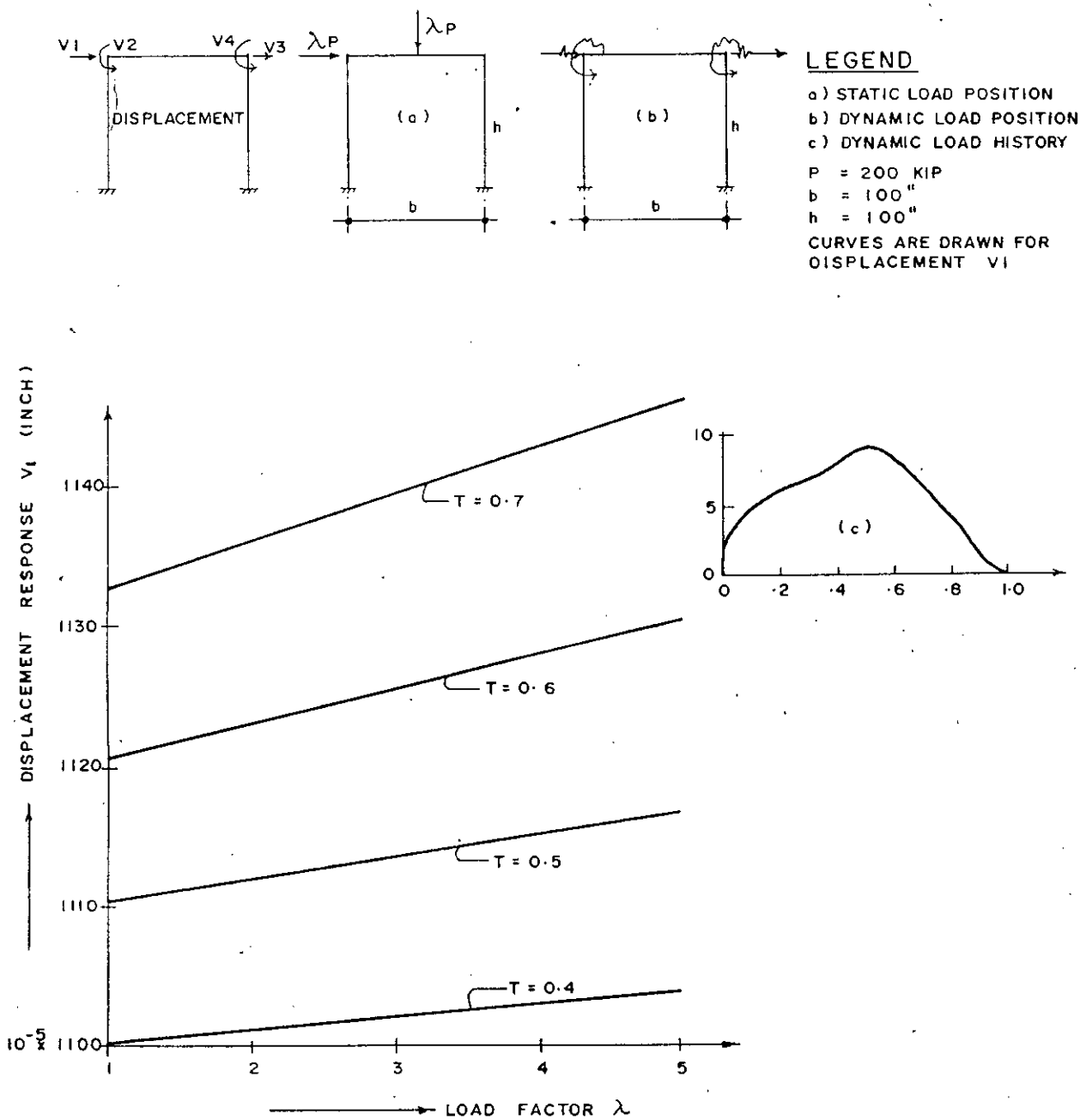

FIG.4-13 : EFFECT OF LOAD FACTOR ON RESPONSE

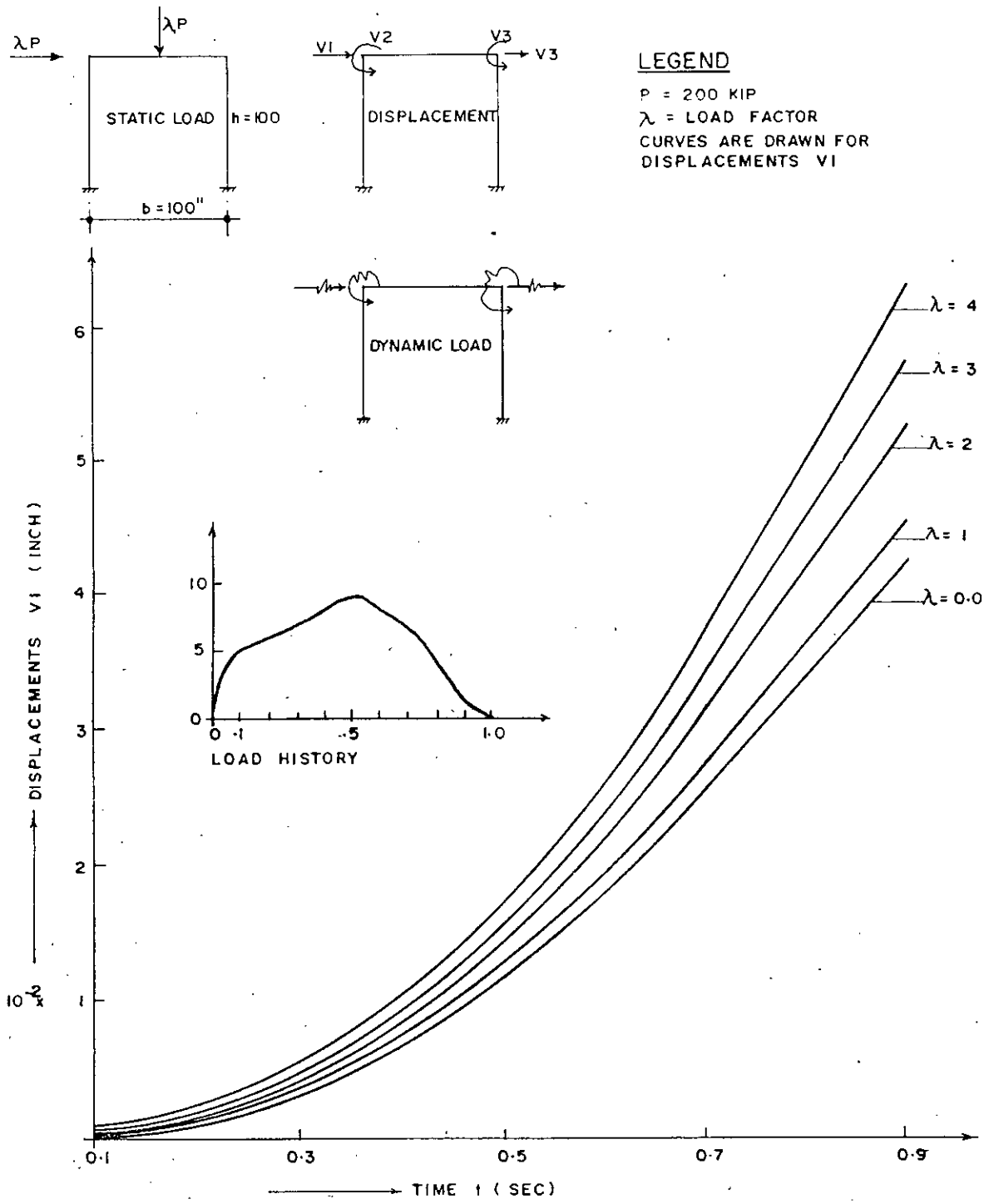

FIG. 4-14 : EFFECT OF LOAD FACTOR ON RESPONSE

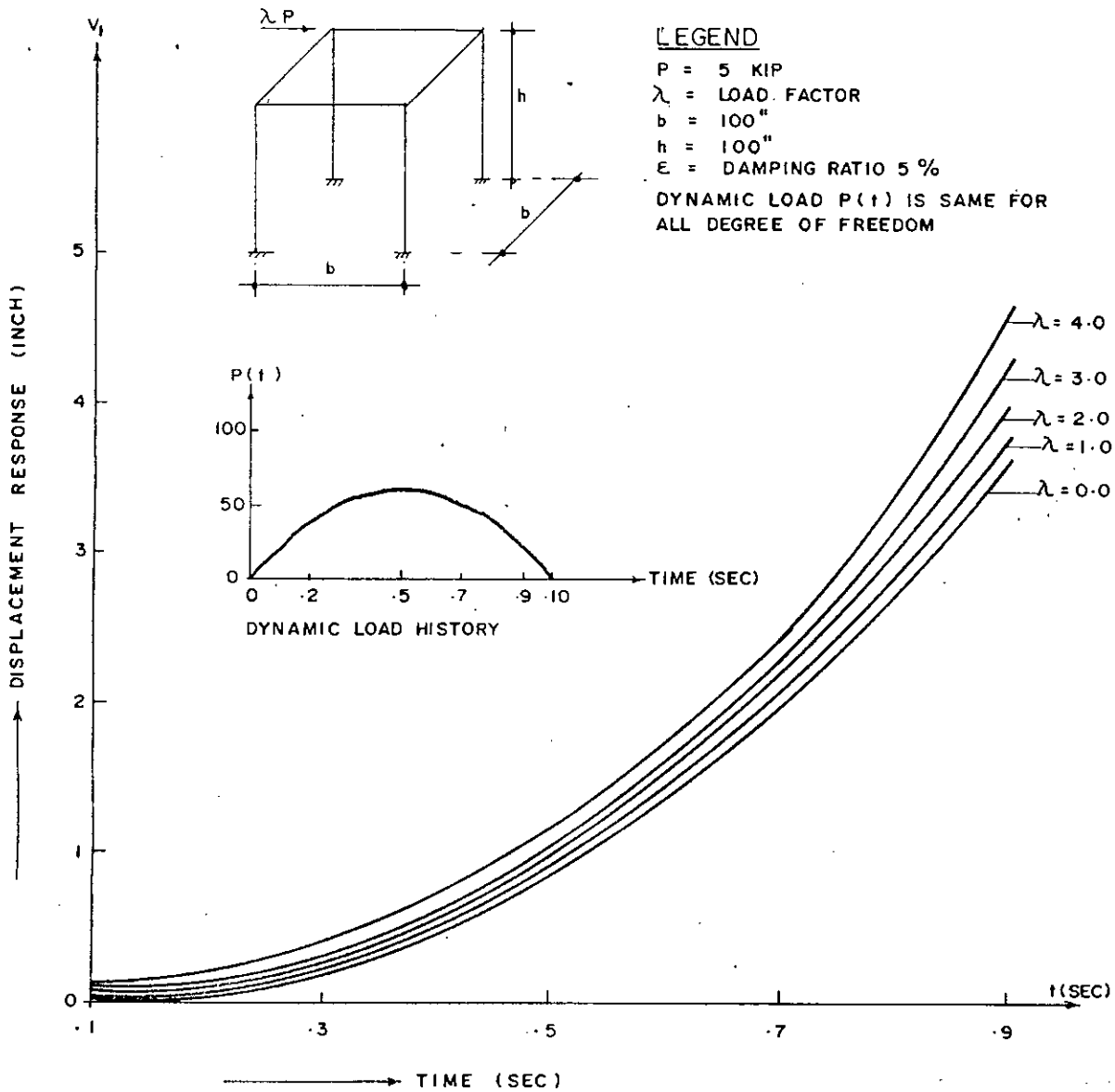

FIG. 4-15: EFFECT OF LOAD FACTOR ON RESPONSE

In Fig. 4.15, displacement response v_1 has been plotted against time for different load factors for a space framework. the dimensions of the three dimensional thin-walled system along with the dynamic load history and static loading conditions are shown in the figure. The dynamic response corresponding to different load factor is computed and plotted against time. It is observed that as in plane frame, the response increases both with time and load factor. From Figs. 4.14 and 4.15, it can be further concluded that in both cases of plane and space framed systems, the rate of increase in displacement is higher at higher time.

4.7 INFLUENCE OF STRUCTURE HEIGHT

The stiffness and mass matrices of a structure are functions of member lengths. If the height of a structure changes, the vertical member lengths will be changed and correspondingly the structural properties will change. The change in structure properties will bring about changes in frequency, critical load, and dynamic response of the structure. So these factors are supposed to be influence by the structure height. The purpose of this article is to study the influence of this geometric factor on different quantities such as frequency, critical load, dynamic response etc. The investigation has been carried out in the examples of a plane and a space framework. The analysis of the plane frame system has been conducted again for two different

conditions. First the out of plane degrees of freedom of it are assumed to be completely restrained and next it is assumed that the frame motion occurs with these degrees of freedom unrestrained.

4.7.1 Plane Frame-Work

A simple portal plane frame as shown in Fig. 4.16 is taken, the base of which is considered as fixed. Due to the plane frame action the displacement perpendicular to the plane of the frame is not possible and the axial deformation is also neglected. The sectional properties of all the members are assumed same. The bay width b of the structure is constant, and is equal to 100 inch. Two static concentrated loads P, one vertical and the other horizontal, are shown in the figure. The load factor λ is assumed to be unity. The height of the structure, h is varied and the influence of this geometric factor on different parameters are studied.

The frequency of this structure is computed by the standard eigen value solution. The square root of the eigen value gives the frequency. For this purpose, the height, h is first taken equal to 100 inch and the frequencies of the structure corresponding to all modes are computed. Again by changing the height h

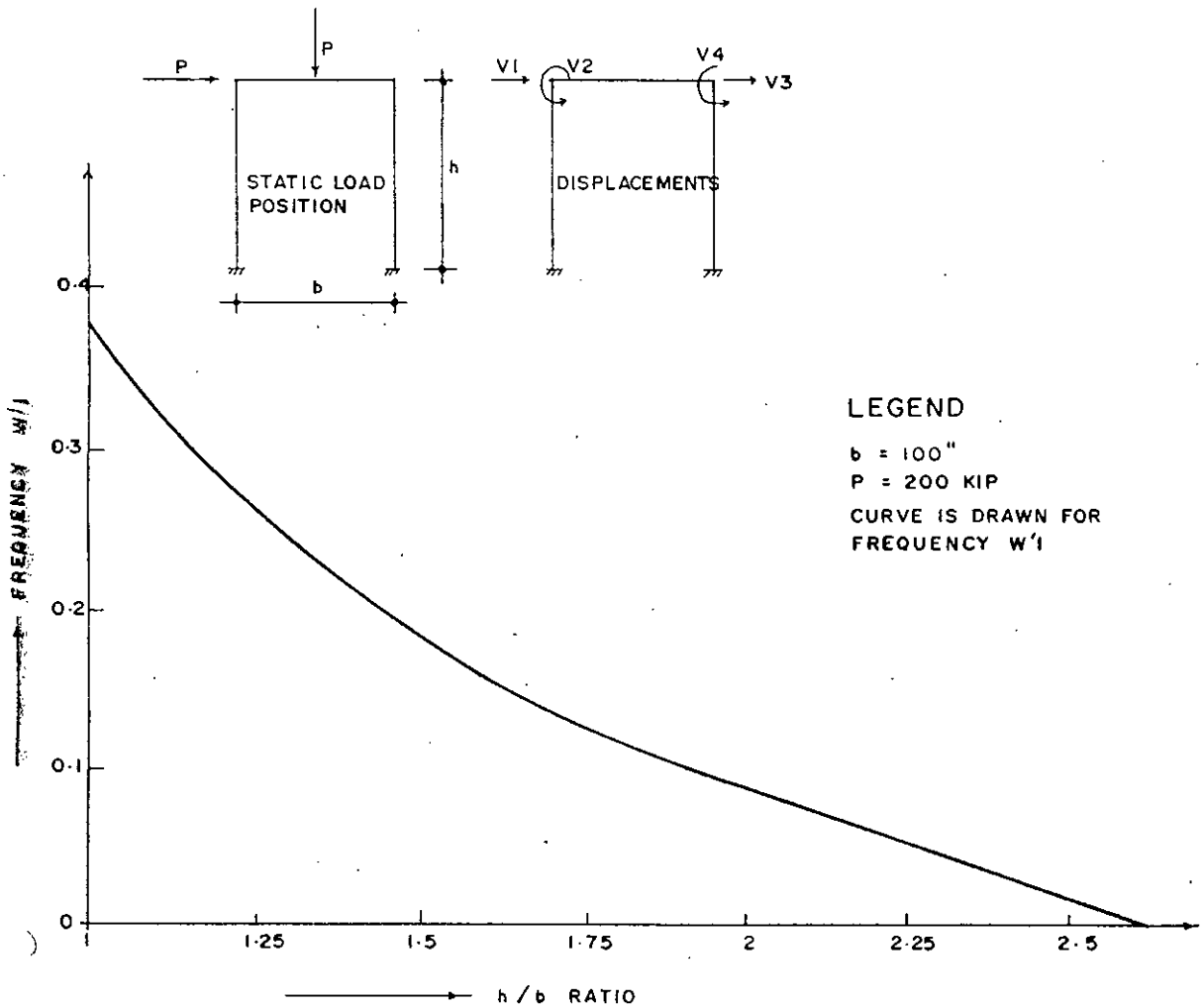

FIG. 4-16 : W′ VS. h/b CURVE FOR PLANE FRAME

successively, the frequencies are computed. The variation of frequency corresponding to first mode with the height is illustrated by plotting the curve w_1 verses h/b in Fig. 4.16. With b=constant, the variation of the ratio h/b implies variation in height. It is observed from this figure that the frequency decreases gradually with an increase in height. At a certain height the frequency vanishes and this height is the critical height for the structure with the applied loads. If the height h is further increased beyond this critical height, the system will no more be an oscillatory.

The critical load for a structure can be computed as the load at which its frequency vanishes. Again to investigate the influence of structure height h on the critical load, the width b is assumed to remain constant at b = 100 inch. The height h is gradually increased from h = 100 inch and the corresponding critical load factor λ is computed. The initial value of the load P was assumed to be P=200 kip. The variation of critical load factor $_{cr}$ with the height h is shown in Fig. 4.17. The critical load Pcr is then the product of P and λ_{cr}. It is evident from Fig. 4.17 that the critical load factor decreases with the increase in height h. At a certain height h, the crtical load factor λ is found to be equal to one. This means at this height of the structure, critical load is the same as the initial value of the load P. This height represents the critical height

of the structure subjected to initial loads. It also indicates that if the structure height is further increased, the structure will no more oscillate. From the figure 4.17 it appears that the curve becomes asymptotic to the horizontal axis after a certain h/b ratio. In other words, the rate of change of λ_{cr} becomes insignificant after a certain height to width ratio for a particular structure. It implies that for high structures, the critical loads will differ insignificantly which is practically understood.

To investigate the influence of h/b ratio on displacement response, the dynamic load history corresponding to all degrees of freedom is assumed same and is shown in Fig. 4.18. The damping ratios corresponding to different degrees of freedom also assumed different which are shown in the figure. The dynamic response analysis has been performed by step by step integration method. For a particular initial height h = 100 inch, the dynamic displacement response v_1 is computed at different times. Then gradually changing the height h, computation of the dynamic response v_1 is performed corresponding to different heights. The variation of dynamic response with height at different times is illustrated in Fig. 4.18. From the curves it appears that the influence of structure geometry on the dynamic response may be different at different times. It is understood that the nature of the dynamic load history will certainly have its own influence on the response. For the particular load history considered here, an

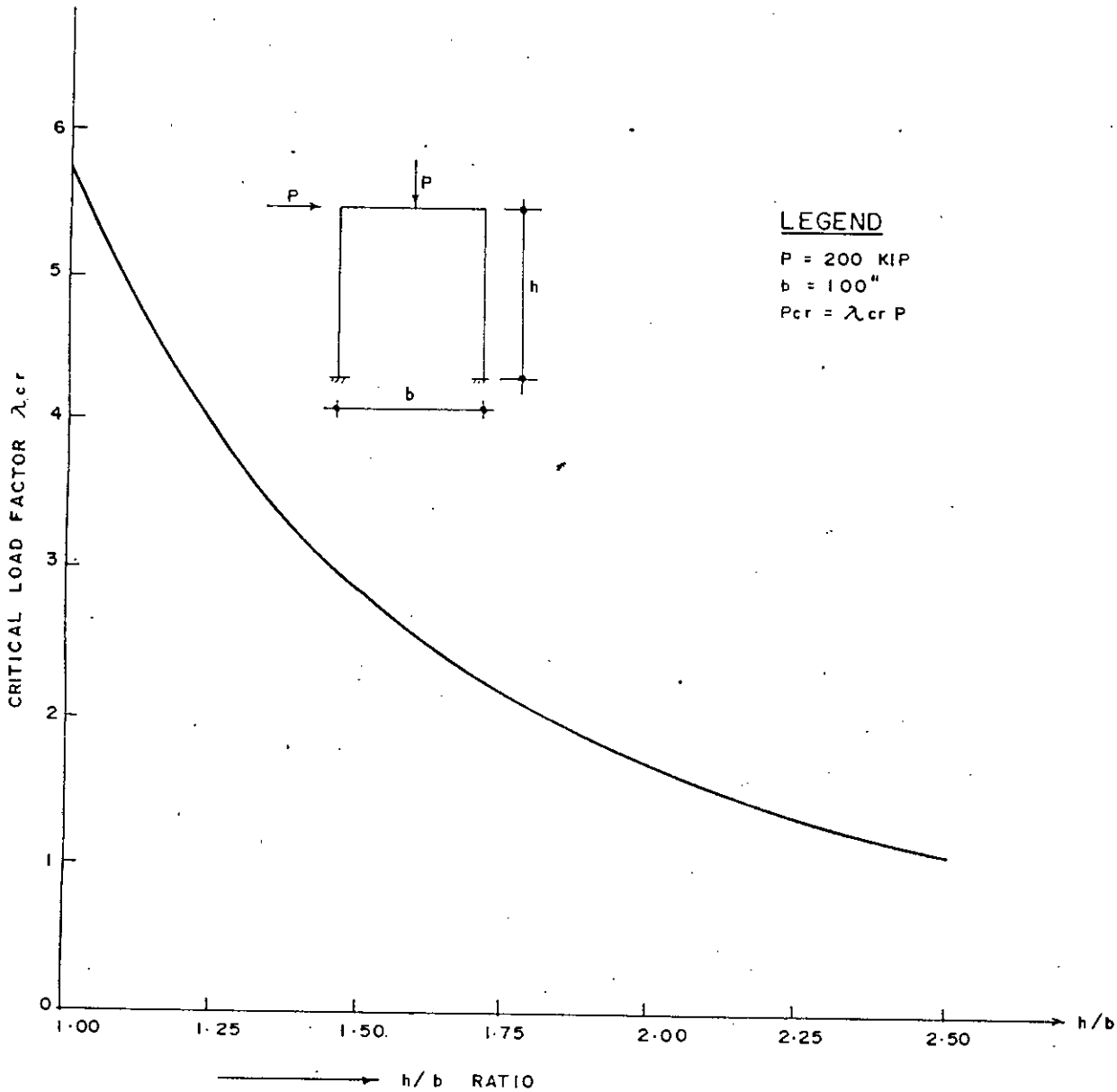

FIG. 4-17 : λcr VS h/b CURVE FOR PLANE FRAME

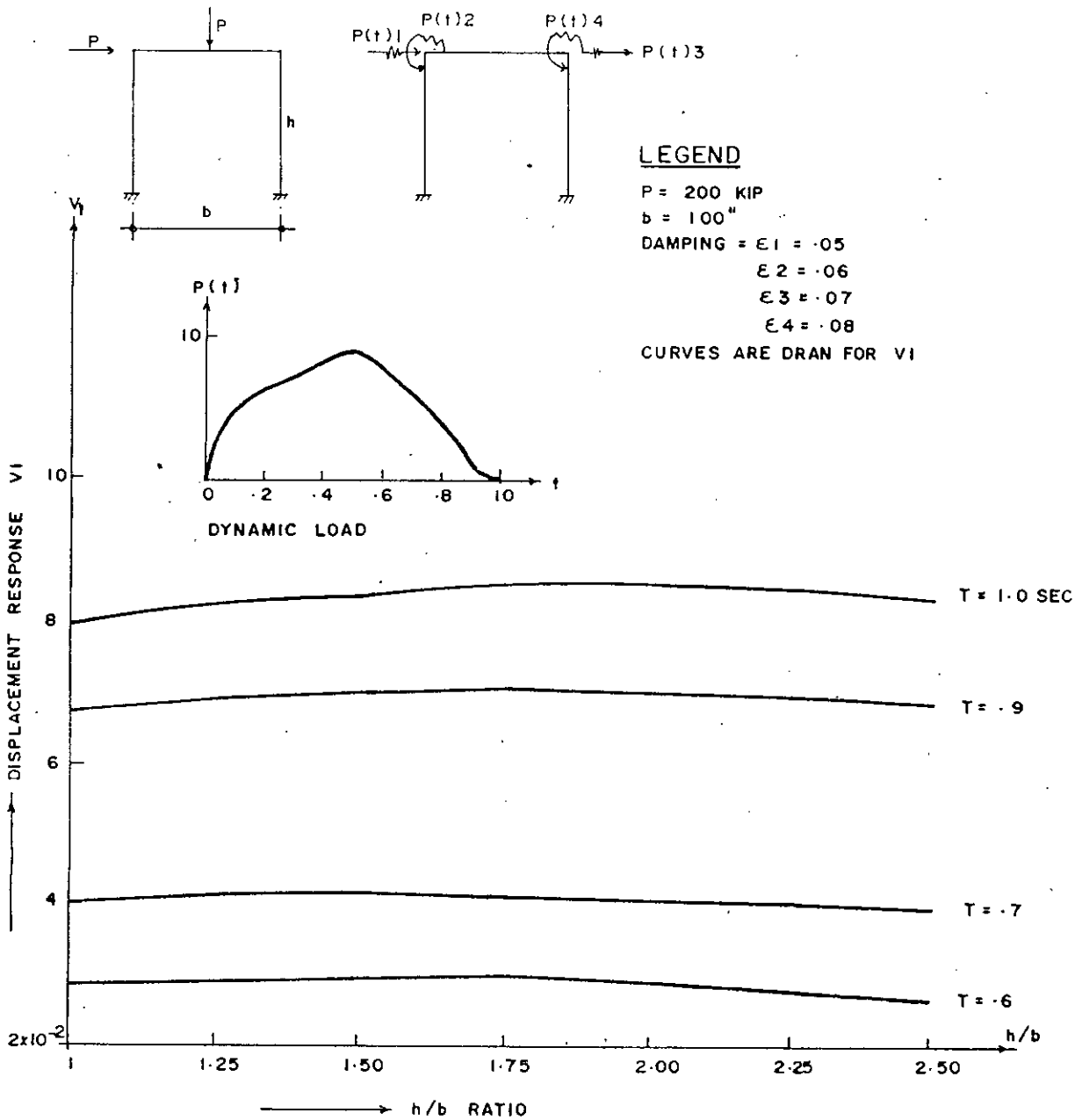

FIG. 4-18 : V VS. h/b CURVE FOR PLANE FRAME

increase in height to width ratio seems to increase the response insignificantly only at higher time.

4.7.2 Portal Frame with Degrees of Freedom Unrestrained in Three Dimensions.

A simple portal frame same as that in Fig. 4.16 is considered. The motion of the structure is assumed to take place in three dimensions as for a space frame. The displacement perpendicular to the plane of the frame is not restrained and this will differ the present problem from that considered in Art. 4.7.1. The base of the structure is fixed and bay width remains constant at 100 inch. The sectional properties are same for all members. Two static concentrated loads P=1 kip each, one horizontal and the other vertical, are shown in Fig. 4.19. The influence of change of height on different factors are studied and described below. The variation in result due to freedom of a plane frame in all dimensions is also studied.

The frequencies of the structure corresponding to different modes have been computed by standard eigen value solution as before. The frequencies of the structure with different heights and corresponding to different modes are determined. The variation of two lowest frequencies w_1 and w_2 with height h is shown in Fig. 4.19. It is observed that both the frequencies gradually decrease

with the increase in height. And at a certain height one of the frequency becomes zero. This may be termed as the critical height for this structure. For this particular problem, the critical height is found to be h=125 inch. So if the height is further increased beyond 125 inch the structure will not oscillate. However, from Fig. 4.16 the critical height was found to be 400 inch and at this height the static load p was 200 kip. So by comparing these two schemes of the same structure, it is evident that the structure considered to be restrained perpendicular to its plane is much stable and its critical load is very high compared to that for the structure free to move in three dimensions. It should be further noted that for a height of the structure exceeding some particular value, the frequency corresponding to one mode which was lower than another frequency corresponding to another mode at lesser heights, may now become higher. However, after the buckling of the structure in one or another mode, the nonzero value of a frequency in any other mode has little practical significance.

The critical load for the frame as earlier is computed as the load at which the frequency vanishes. Critical loads corresponding to different heights of the structure have been calculated and the variation of Pcr with height is illustrated in Fig. 4.20. It is observed that the nature of this curve is almost identical to that in Fig. 4.17, drawn for a portal frame

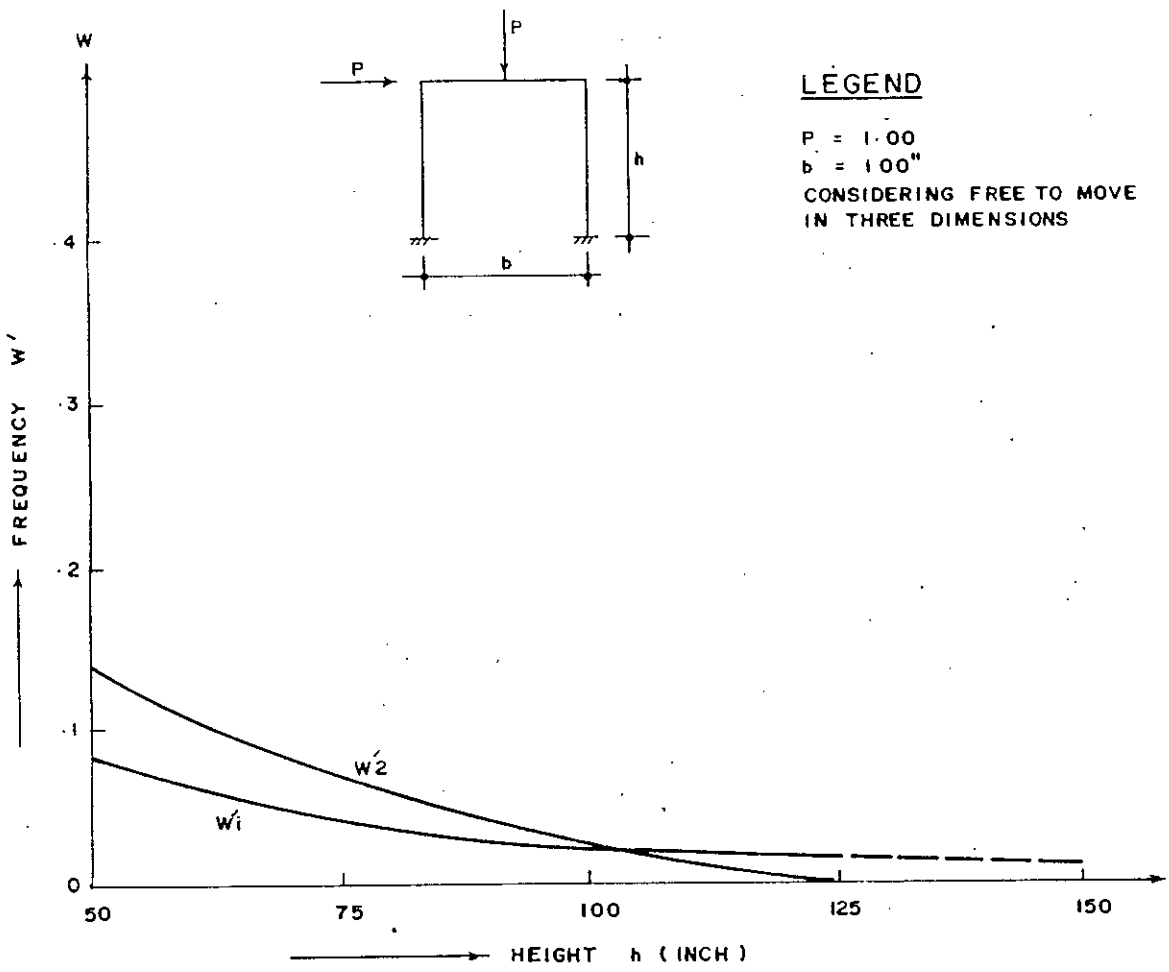

FIG. 4-19: W' VS. h CURVE

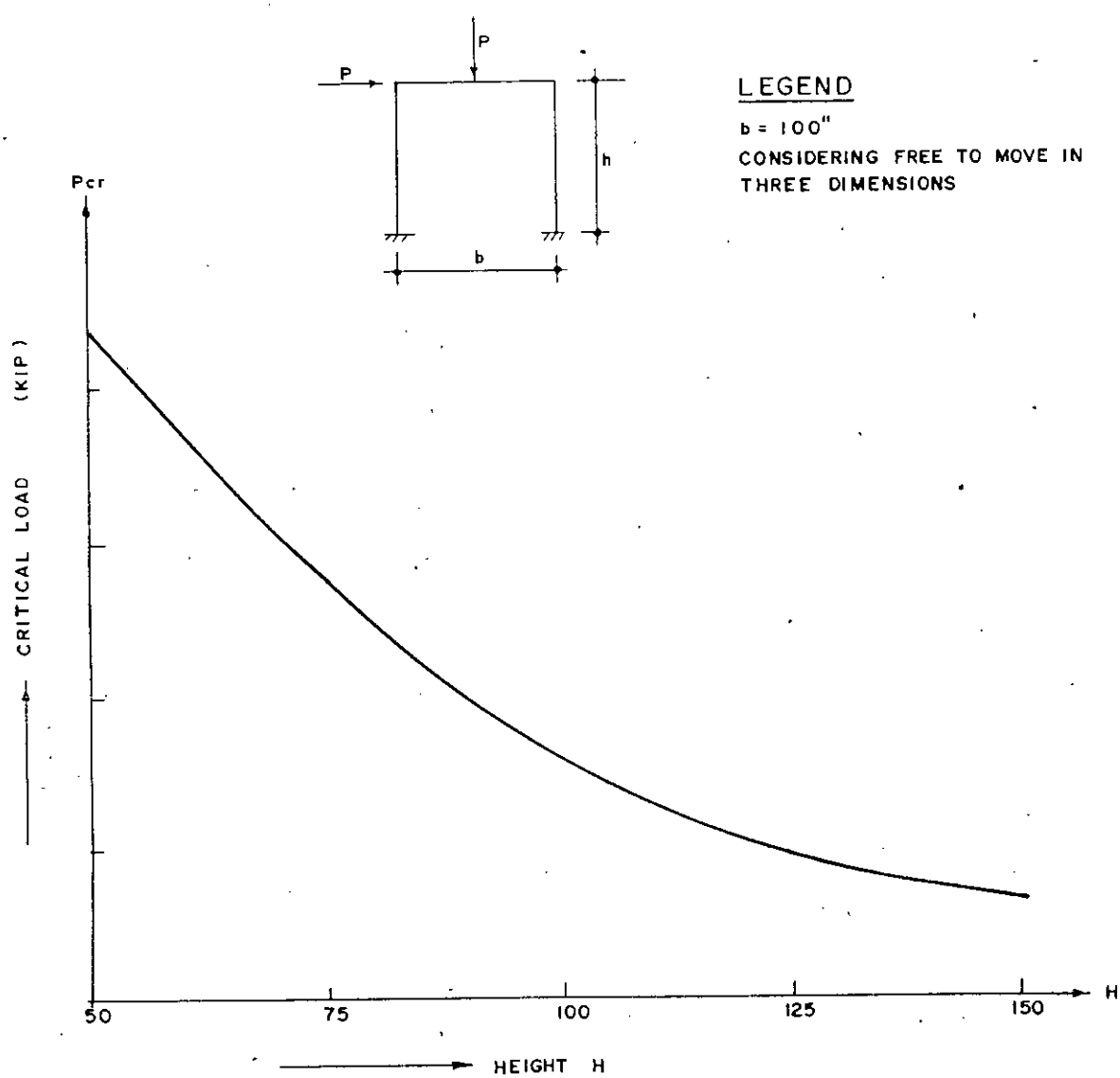

FIG.4-20 : Pcr VS. h CURVE

restrained to move in a direction normal to its plane. However, the level of critical load for the present problem is much lower than that corresponding to Fig. 4.17 for the same h/b ratio of the structure. In Fig. 4.20, the critical load factor decreases with increasing h/b ratio. The rate of decrease of the critical load factor however, diminishes with increase in h/b ratio.

4.7.3 Thin-Walled Space Framework

A thin-walled space framework with its legs fixed at the base as shown in Fig. 4.21, is selected for the present investigation. Both the base dimensions are taken constant and equal to 100 inch. The height of the structure is considered to be variable. All the degrees of freedom for the top four corner joints are unrestrained. The sectional properties of all members are assumed to be same as for the plane frame works discussed earlier. A static concentrated load P=5 kip is acting horizontally on the structure as shown in the figure. By changing the height of the structure as before, the influence of this factor on different quantities such as frequency, critical load, dynamic displacement etc. are studied.

The frequency of the space structure is computed by solving the eigen value problem. The frequencies corresponding to different modes for different height of the structure have been computed.

The variation of lowest three frequencies with height is plotted in Fig. 4.21. It is observed from this figure that all the frequencies gradually decrease with the increasing height of the structure. At a certain height h=400 inch, the frequency corresponding to first mode vanishes. This means that the corresponding height is the critical height for the structure at the applied static load. If the height of the structure or the static load is further increased, the structure will collapse and will no more be a system oscillatory. That is why the non-zero frequencies of the structure corresponding to other modes with load or height exceeding their critical values do not have any practical significance. The rate of change of all the frequencies is again observed to fall with increasing height.

As stated already, the load factor λ reaches its critical value, when the frequency vanishes. The λ cr for the structure changes with the change of its height and the critical load pcr for a given height can be calculated as the product of the static load and critical load factor. The critical load factor λ cr is computed for changing heights of the structure starting from a structure height of h= 100 inches. The variation of critical load factor with the variation of height is illustrated in Fig. 4.22. It can be observed that the load factor decreases gradually with increase in height h. At a certain height it is found that the load factor is unity. This means at this height the applied load

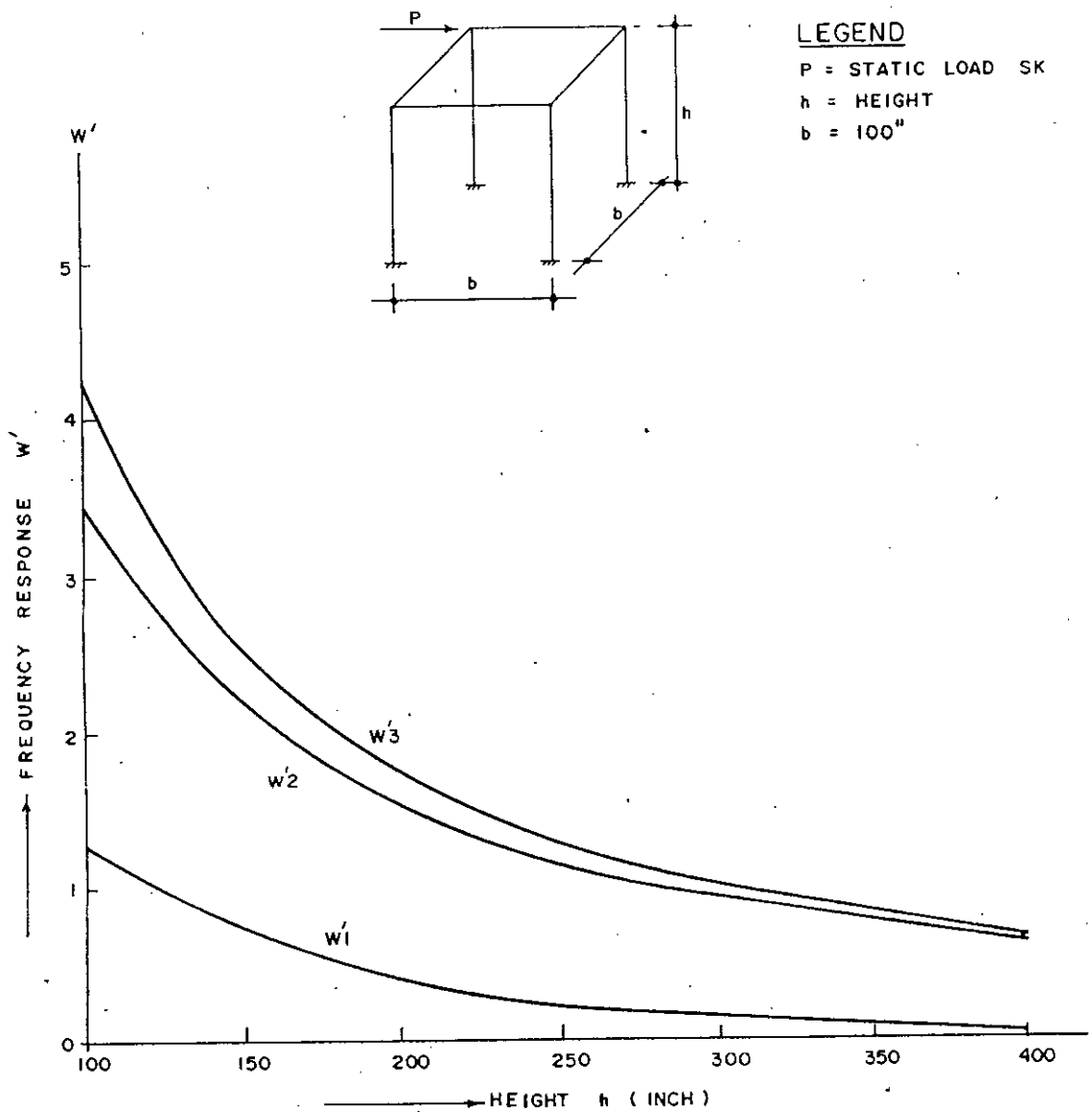

FIG. 4 - 21 : W' VS. h CURVE FOR SPACE FRAME

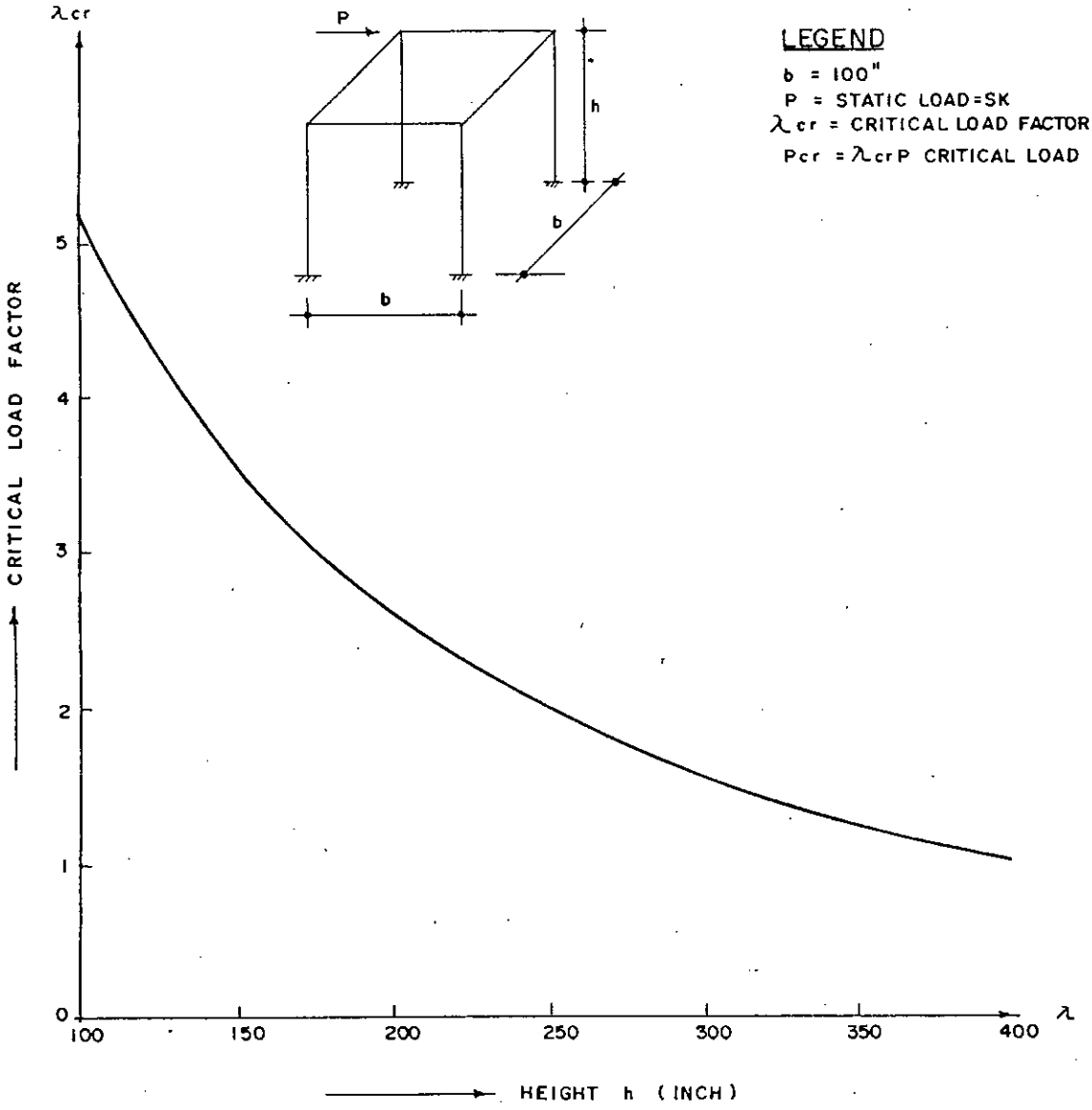

FIG. 4-22: λcr VS. h CURVE FOR SPACE FRAME

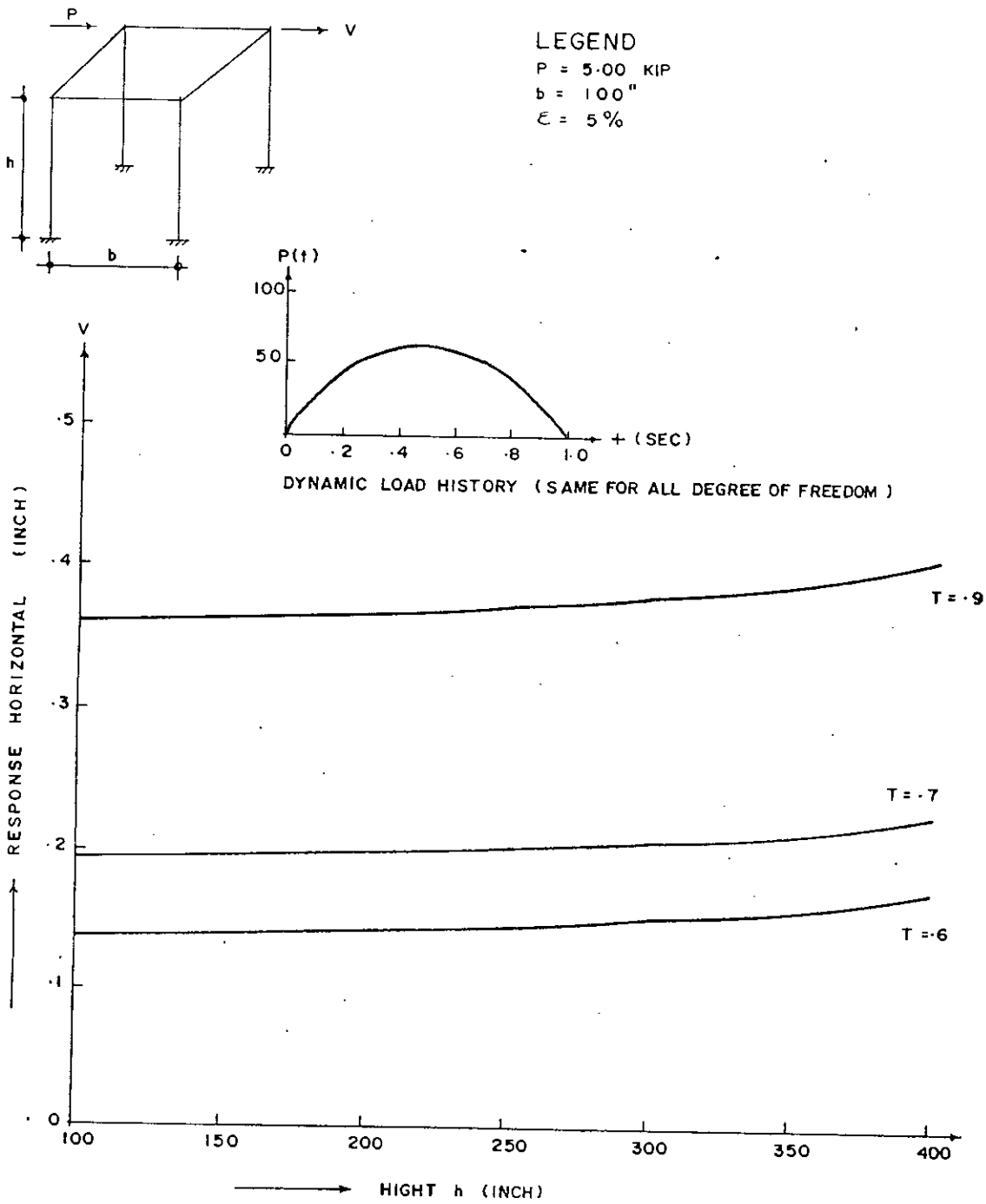

FIG.4 -23 : V VS. h CURVE FOR SPACE FRAME

is the critical and this height is the critical height for the applied load. It may be further observed that as for plane frames, the load factor height curve becomes almost asymptotic to some horizontal.This indicate again that for very high three dimensional systems the influence of height on critical load becomes less prominent.

To study the effect of height on dynamic response the dynamic load history is assumed same for all degrees of freedom corresponding to which it acts. The load history is shown in Fig. 4.23.The damping ratio is taken 5% for all modes.The dynamic displacement response v_1 along 'x' axis at node 1 for different values of structure height is computed. The variation of this response with height at different times is shown in Fig. 4.23. The response is found to increase gradually with height corresponding to all times concerned. However, the increase is not that significant and it should be remembered that the response may be highly dependent on the specific time history of the dynamic load selected for the analysis.

4.8 EFFECT OF SIMULTANEOUS VARIATION OF BAY WIDTH AND HEIGHT

In the preceding article, the variation of frequency, critical load etc. with height has been shown for thin-walled plane and space frameworks. The simultaneous variation of bay width and

height with constant b/h ratio may as well significantly influence these parameters. The aim of this article is to study the effect of this simultaneous variation of bay width and height on the above mentioned parameters. For this purpose, the structures analysed in Art. 4.7 are again selected and the variation of the quantities such as frequency, response etc. with bay width and height varying together are investigated. The result of this study are summarized in the following subarticles with graphical representations where necessary.

4.8.1 Effect on frequency

The frequencies are computed here by the standard eigen problem solution as before. It is evident from Eqs. 2.16 and 2.30, that the combined stiffness and mass matrices are functions of the bay width and height of a structure. Hence, the frequencies corresponding to different modes of vibration are to change with changing structure geometry. First, a simple portal frame is selected and it is considered as a plane frame by restraining its all out of plane degrees of freedom. The sectional properties of individual members are taken same as in Art. 4.7.1. Initially, the structure is assumed to be loaded by two static concentrated loads of equal value P = 200 kip each. At the beginning of the analysis, the load factor λ is taken to be unity. The ratio of bay width, b and height h is taken constant end equal to 1.0. The

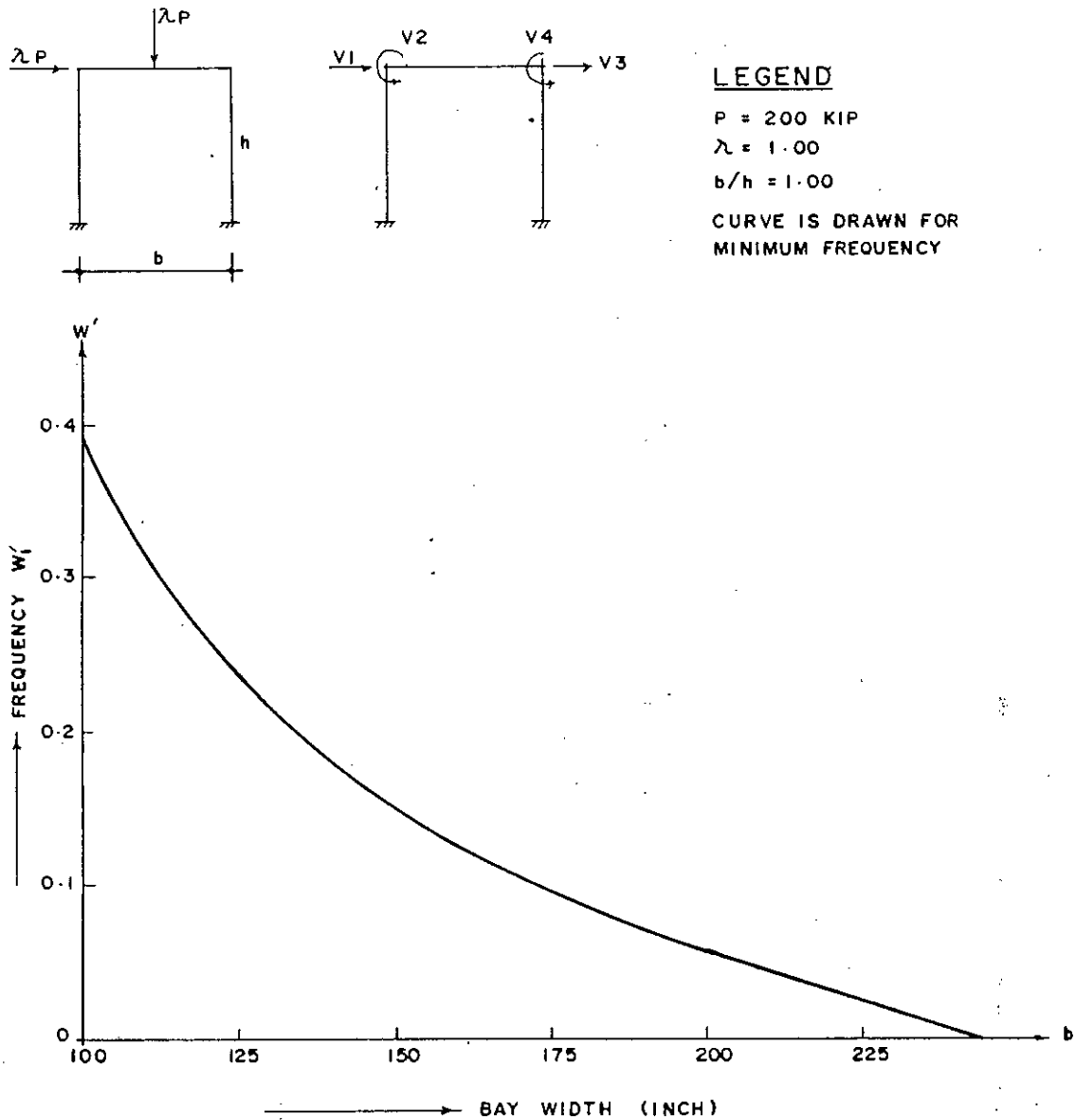

FIG. 4-24 : W′ VS b CURVE FOR PLANE FRAME

bay width and height are changed simultaneously keeping the ratio b/h = 1.00 constant and the frequencies corresponding to each mode are determined for changing b and h. The variation of the least frequency which corresponds to the first mode, with the varying bay width b is shown in Fig. 4.24. In this figure, the ratio b/h is equal to 1, which implies that the height of the structure changes and becomes equal to its bay width as soon as the bay width is changed. It is observed from this figure that the frequency diminishes with increasing bay width and height. It can be further observed that at a certain height and equal bay width the frequency vanishes altogether. This means that the structure lost its stability and if the height and bay width are increased further, it can no more vibrate in the corresponding mode about its original position of equilibrium. Hence, this height and bay width may be termed as critical for this structure at the corresponding static load.

Comparing Fig. 4.16 and 4.24, it is found that the critical height of a structure with fixed bay width is higher than that of a identical structure under same load but its bay width increased only. In other words, the critical height, when only height is changed, is more than the critical height when both bay width and height are changed with b/h ratio remaining constant unity. It is practically understood that the simultaneous increase in bay width and height makes the structure more flexible than that with

fixed bay width.

Again the above plane frame is considered to free to move in three dimensions and identical investigations are carried out. The static applied load p is assumed to remain constant at 1 kip. By changing the bay width b in steps while keeping b/h = 1.00, the frequencies corresponding to all modes are computed by similar manner as before. The variation of frequencies with bay width is shown in Fig. 4.25. It is found that frequencies decrease with increase of bay width and at a certain value of b, the least frequency vanishes . This condition determines the critical height and bay width of the structure for the applied load p. It is also seen that this critical height is smaller than the critical height obtained from Fig. 4.19 in which the bay width remains constant. This is practically understandable, because a structure in which both bay width and height are increased simultaneously becomes flexible faster compared to one in which the bay width is kept constant.

Identical investigations are carried out for a space frame, the loading conditions and sectional properties of which are taken to be exactly same as for the one considered in Art. 4.7.3. The ratio b/h is again kept one. By changing the bay width and height simultaneously, keeping b/h = 1.00, the frequencies corresponding to all modes are computed as earlier. The variation of

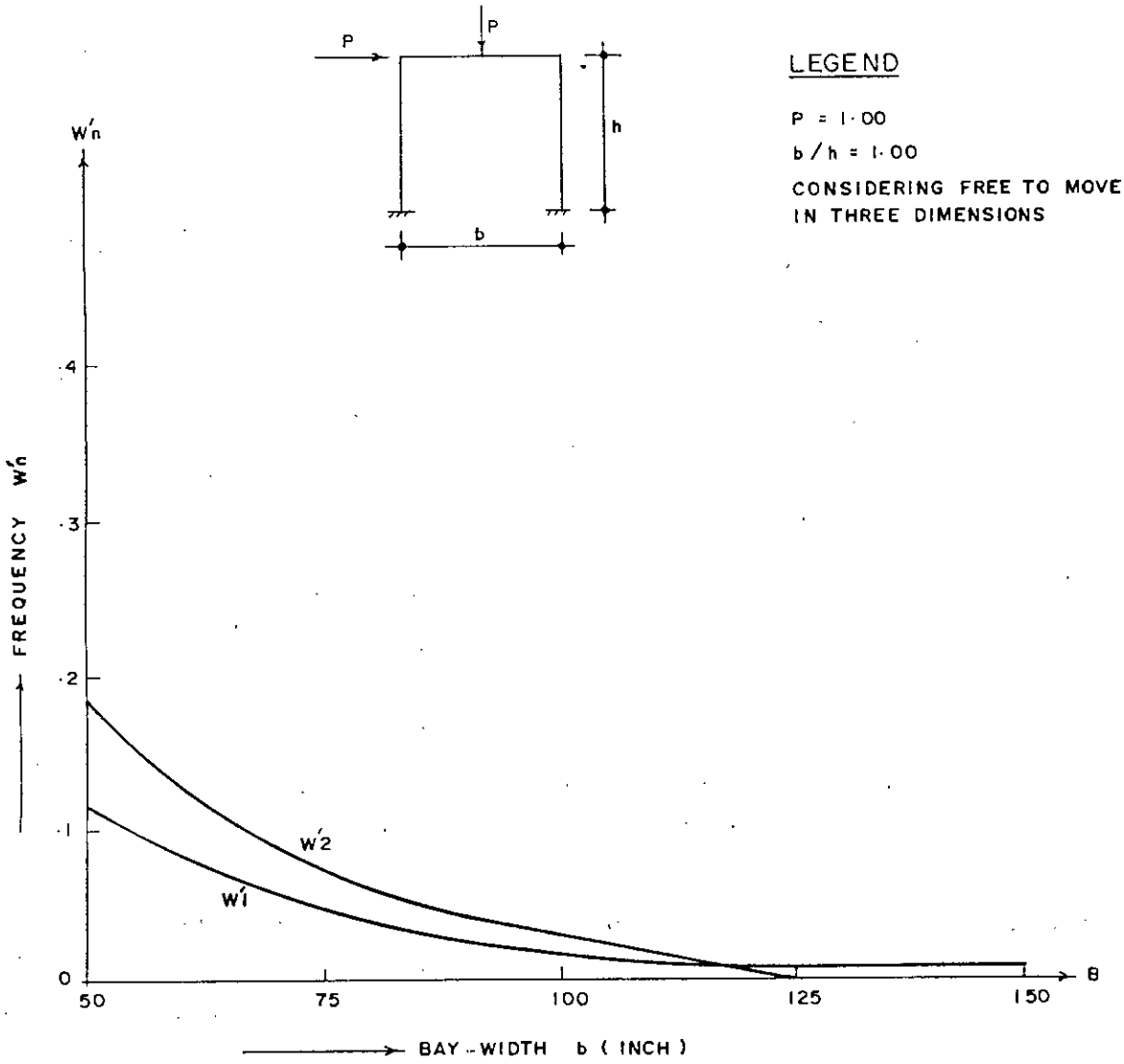

FIG. 4-25: W′ VS. b CURVE

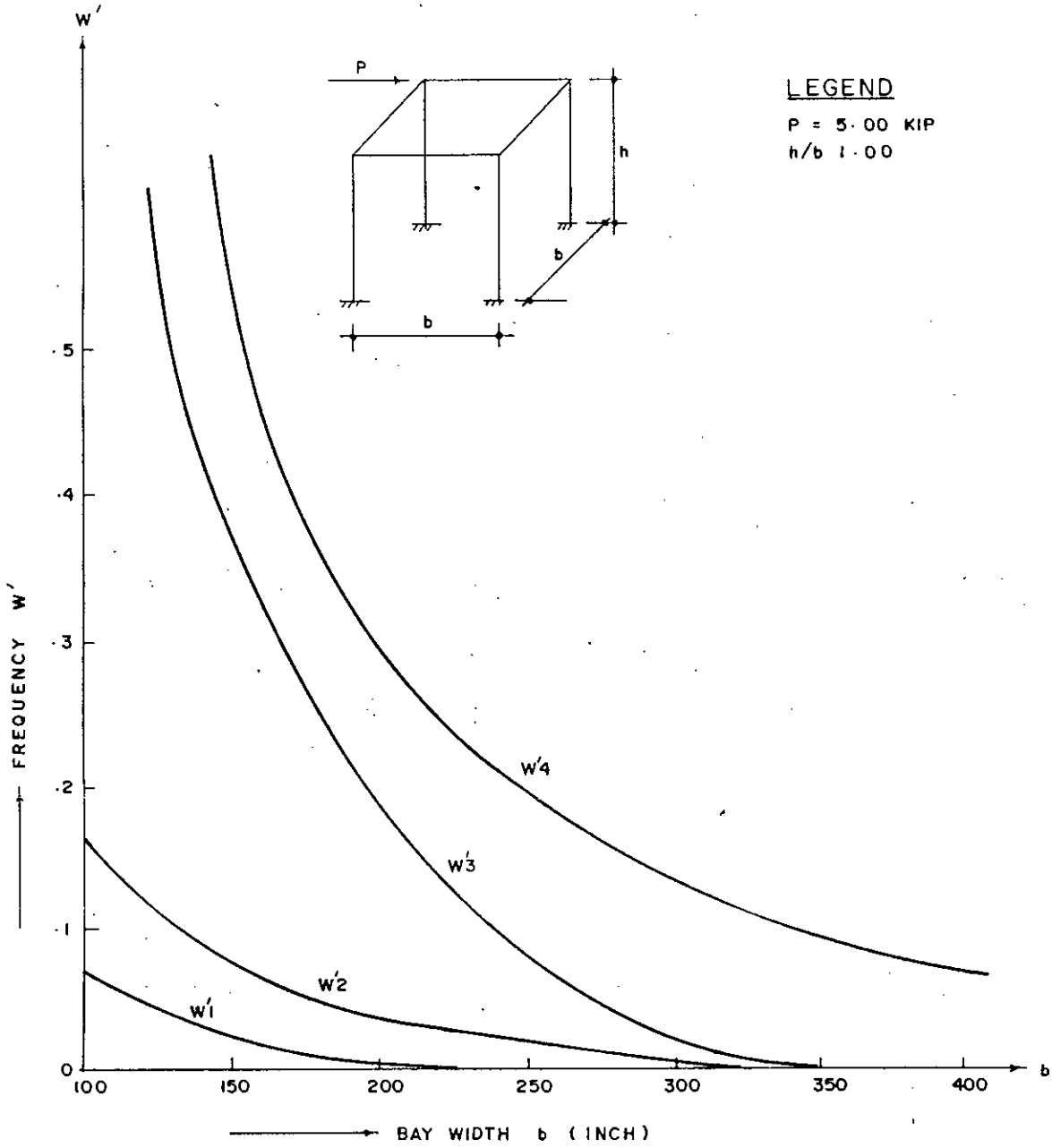

FIG. 4-26: W′ VS. b CURVE FOR SPACE FRAME

frequencies with bay width is illustrated in Fig. 4.26. It can be seen that the frequencies decrease with the increase in bay width and height. At a certain value of b and h, the least frequency vanishes. It is important to note that at higher values of b, the frequencies corresponding to higher modes of vibration may also vanish. It means the structure can loss its stability in different modes. However, the higher modes of buckling become practically significant if the primary mode is restrained some way or other. If b and h are increased beyond the value at which the least frequency vanishes, the structure can not vibrate about its original position of equilibrium. The corresponding b and h may be termed as critical width and height for the structure. This simultaneous value of critical height and bay width is again seen to be lower than the value of critical height if the bay width remaining constant.

4.8.2 Effect on Critical Load

The variation of critical load due to the simultaneous variation of bay width and height are investigated on the similar types of structures considered in the preceding article. Here the ratio of bay width and height is kept constant at unity. The critical load is computed when the least frequency vanishes. The variation of critical load with bay width b for constant ratio of b/h are shown for three different structures in Figs. 4.27, 4.28 and 4.29

respectively.

In case of plane frame, taking the initial value of static load P equal to 200 kips, it is found that the critical load factor decreases with the increase of height and width as shown in Fig. 4.27. And at a certain height and width the critical load factor is one. This indicates that the initially applied static loads are critical loads at this height.

For the portal frame, free to move in three dimensions, the variation of critical load with bay width and height is shown in Fig. 4.28. In this case also the critical load decreases with the increase of height and bay width. Comparing Figs. 4.27 and 4.28 it is seen that at a certain height of structure the critical load is higher for the plane frame than that for the structure free to move in three dimensions. It means the critical load in a structure can be increased if its out of plane motion can be restrained.

Fig. 4.29 illustrates the variation of critical load factor with bay width b for a space frame work. It is found from this figure that the critical load decreases with an increase in height and bay width. At very high values of bay width and height the effect of increase in bay width on the critical load factor is seen to be less prominent compared to structures with low bay

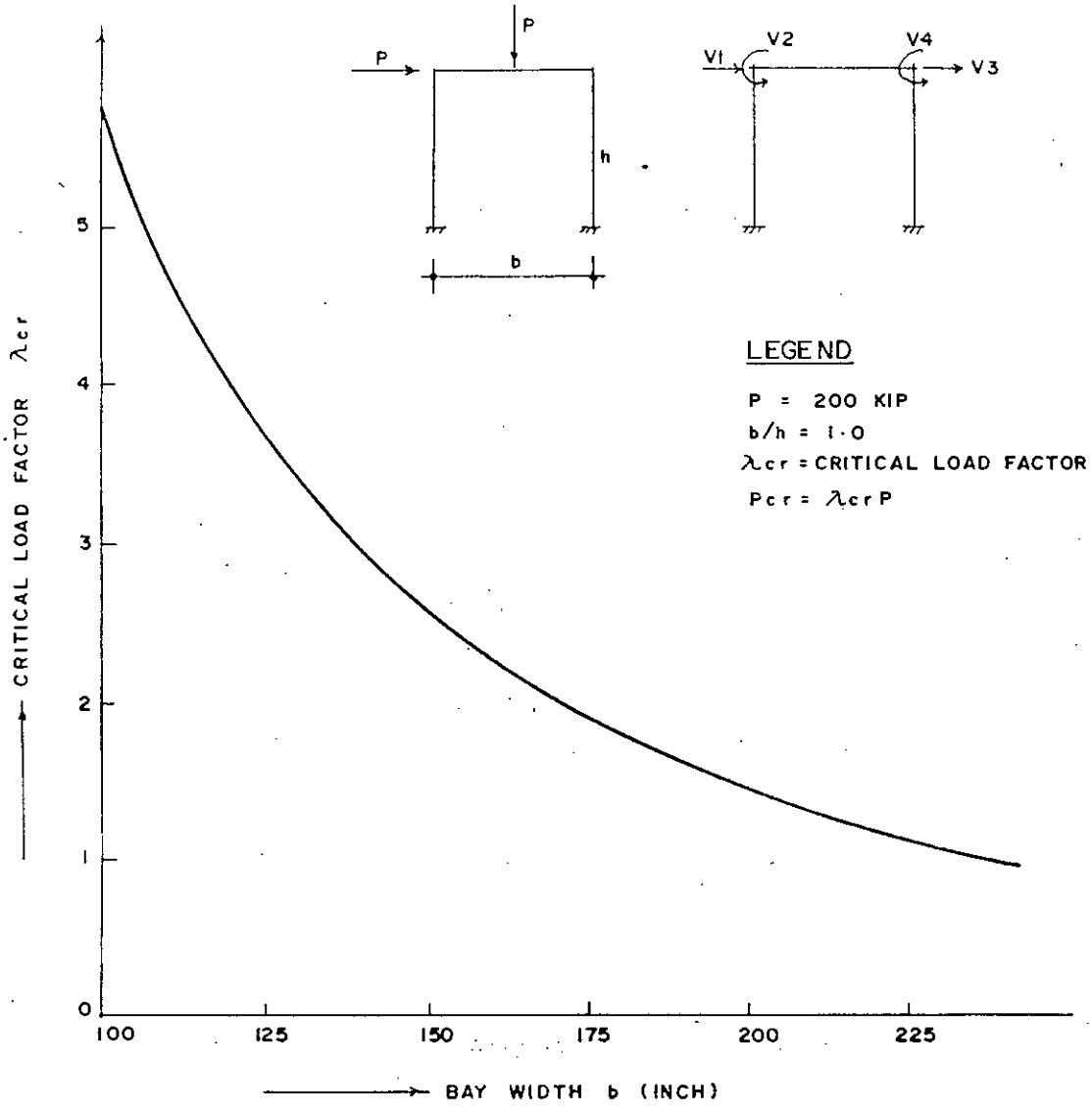

FIG. 4-27 : λ_{cr} VS. b CURVE FOR PLANE FRAME

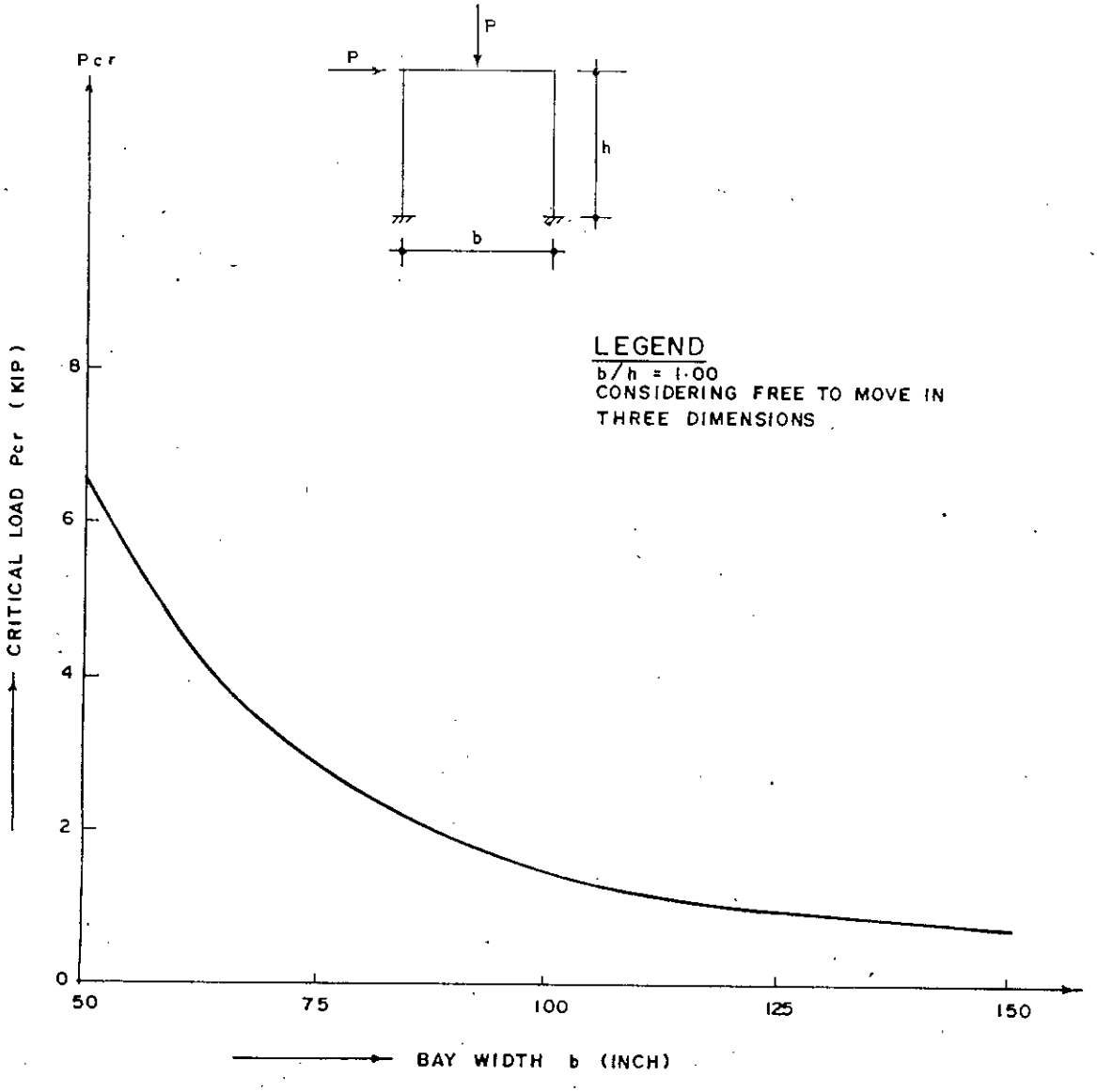

FIG. 4-28: Pcr VS. b CURVE

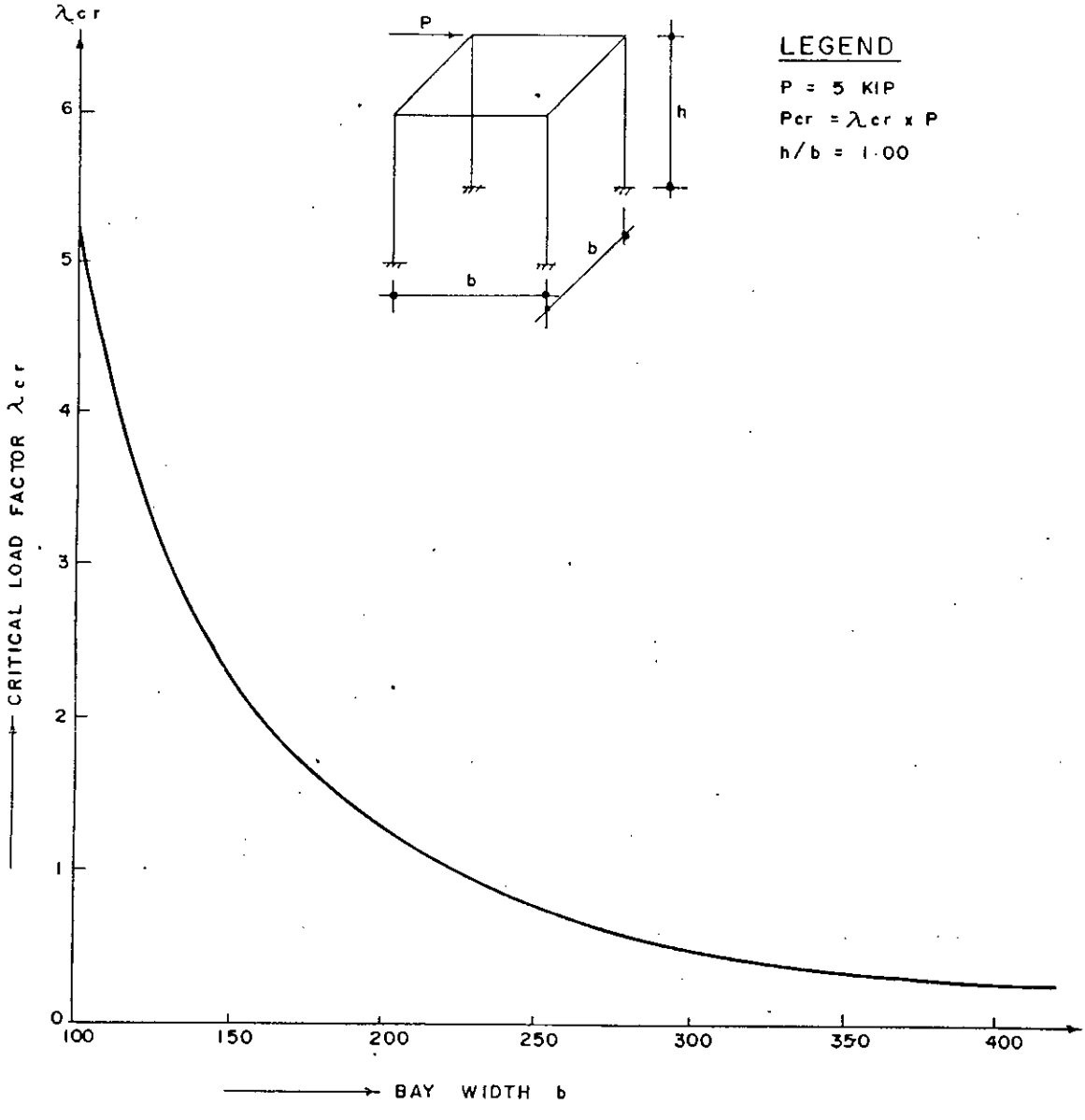

FIG. 4 -29 : λcr VS. b CURVE FOR SPACE FRAME

width and height.

4.8.3 Effect on Dynamic Response

To study the effect of structure geometry on dynamic response a plane frame is selected as shown in Fig. 4.30. Two static loads each equal to 200 kips are assumed to act on the structure. The dynamic load history remains identical corresponding to all degrees of freedom as shown in the figure. The damping ratios for all degrees of freedom are same and equal to 8%. The dynamic response is computed by step by step integration method. The variation of displacement v1 with the variation of height and width keeping b/h = 1.00, is illustrated in Figs. 4.30 and 4.31. Curves in Fig. 4.30 show the variation of response as a function of time at discrete by widths, while those in Fig. 4.31 represent response as a function of bay width at different times. It is observed that the dynamic response increases with the increase of height and width. It is also found to increase with the increase in time. It means if the bay width and height are increased, the structure becomes more flexible and the displacement at the same dynamic load history increases.

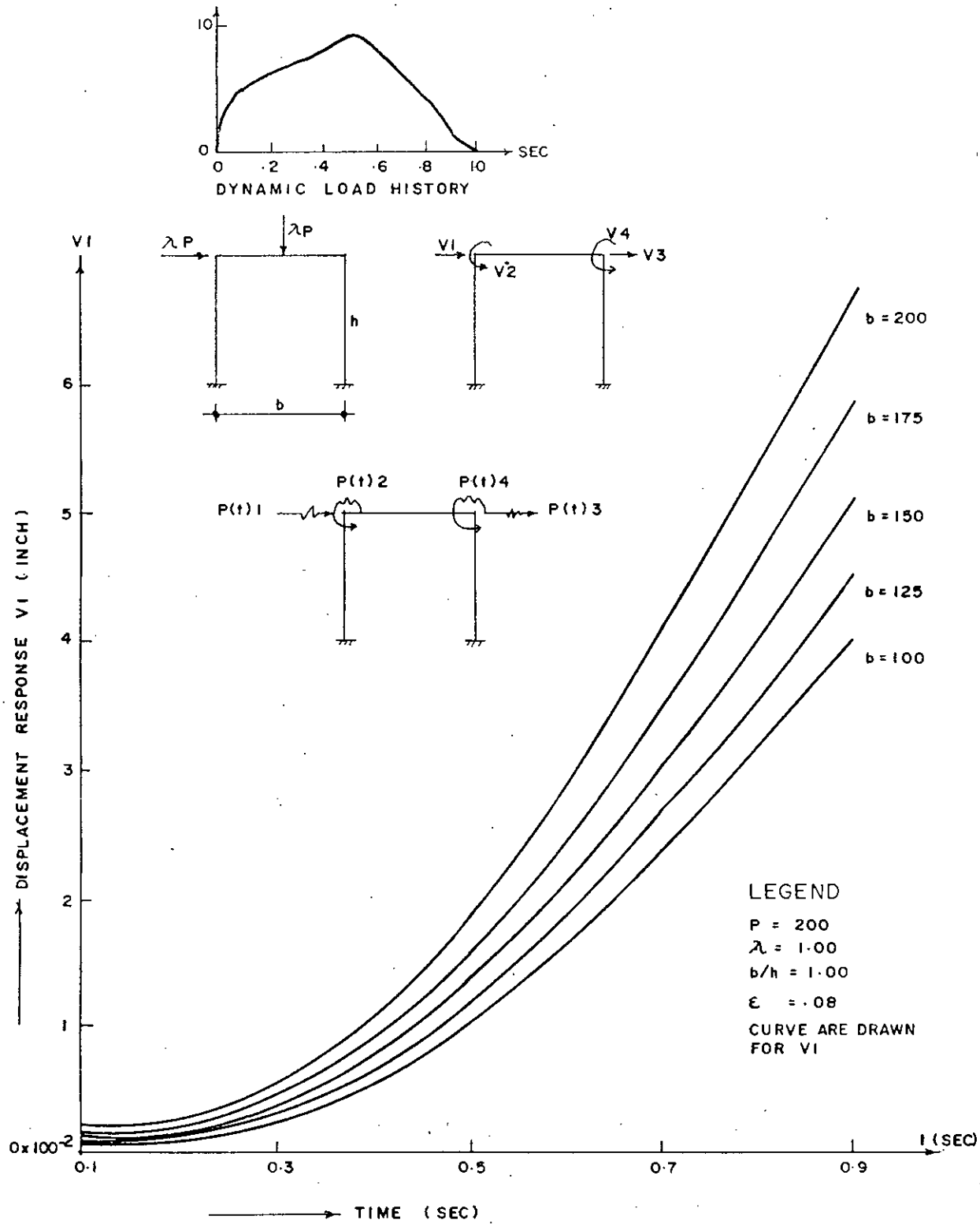

FIG. 4 - 30: EFFECT OF BAY WIDTH ON DISPLACEMENT

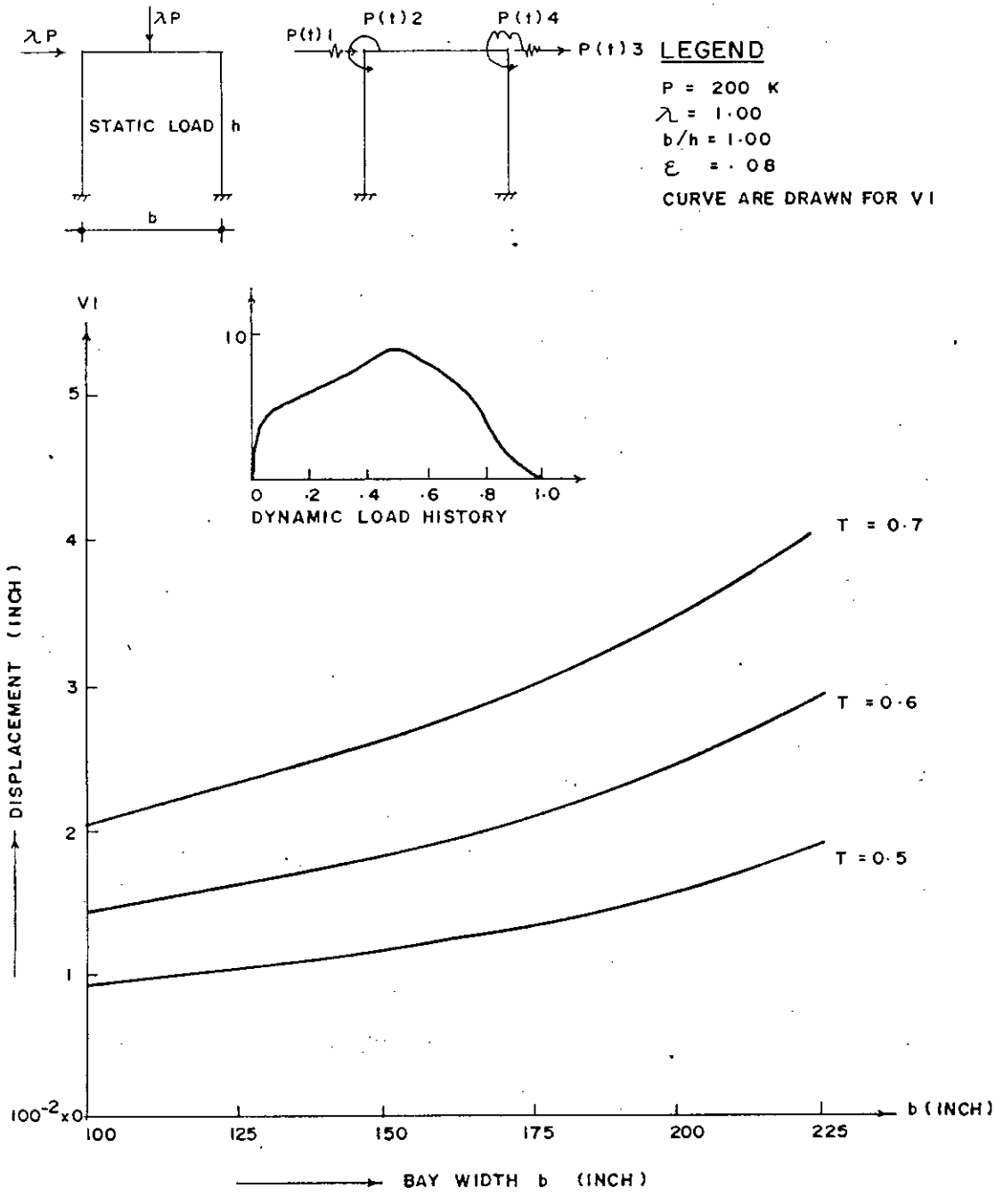

FIG. 4-31 : EFFECT OF BAY WIDTH ON DISPLACEMENT

4.9 EFFECT OF RELATIVE VERTICAL AND HORIZONTAL LOADING

In the preceding articles the effect of load factor λ , applied simultaneously to all static loads has been discussed. The influence of this factor on frequency, response etc. and the influence of structure geometry related parameters has been studied in detail. Most of the problems dealt with statically applied horizontal and vertical loads, both of which were changed simultaneously by increasing the load factor λ . However, the influence of the load factor related to a single load, keeping the other constant has not been given proper attention. In this article, the effect of the relative values of the vertical and horizontal loads on frequencies, critical load factor, displacement response etc. will be investigated. For this purpose, an identical portal frame, as used previously, has been selected. Both the height h and bay width b are taken to be 100 inch.The sectional properties of all the members are assumed same. Initial value of the smaller of the vertical and horizontal loads is taken equal to 200 kips. The position of the loads on the structure is shown in Fig. 4.32. A load factor k signifying the relative values of the horizontal and vertical loads has been used.The effect of the load factor k on different parameters is described in the following subarticles. The study is conducted separately for both the cases of vertical load exceeding

horizontal or vice versa.

4.9.1 Effect on Frequency

To investigate the variation of frequencies with the variation of horizontal and vertical loads separately, first the vertical load p is kept constant at 200 kips. The horizontal load p is changed by changing the horizontal load factor k, which also signifies the ratio of horizontal and vertical load. The vertical load factor remains constant at 1.00. The variation of lowest frequency w1 with the change of horizontal load is illustrated in Fig. 4.32. The frequency is computed following the same procedure as earlier. It is evident that the frequency decreases with the increase of k. The rate of decrease of frequency with the increase in horizontal load is not much significant. Next the horizontal load has been fixed at 200 kips and the vertical load is increased by gradually increasing load factor k. Now k signifies the ratio of vertical to horizontal loads. The variation of lowest frequency w1 with the variation of vertical load is computed by changing the vertical load factor k. The corresponding curve showing the influence of k on w_1 has been plotted in Fig. 4.33. It is observed from this figure that w_1 decreases with the increase of k. However, comparing Figs. 4.32 and 4.33, it is found that the frequency diminishes at a lower rate for k relating to horizontal load than that when k relates

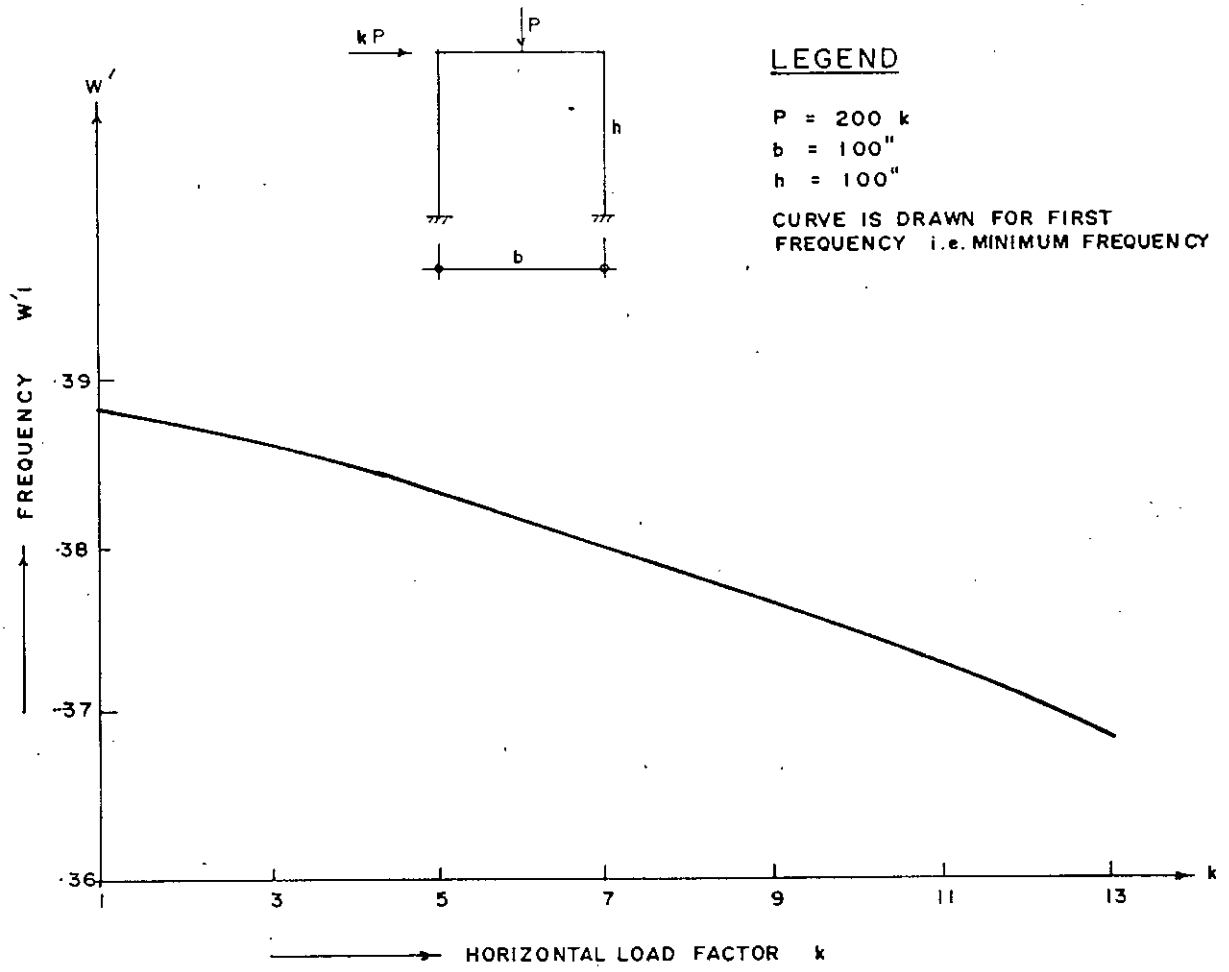

FIG. 4-32 : EFFECT OF HORIZONTAL LOAD ON FREQUENCY

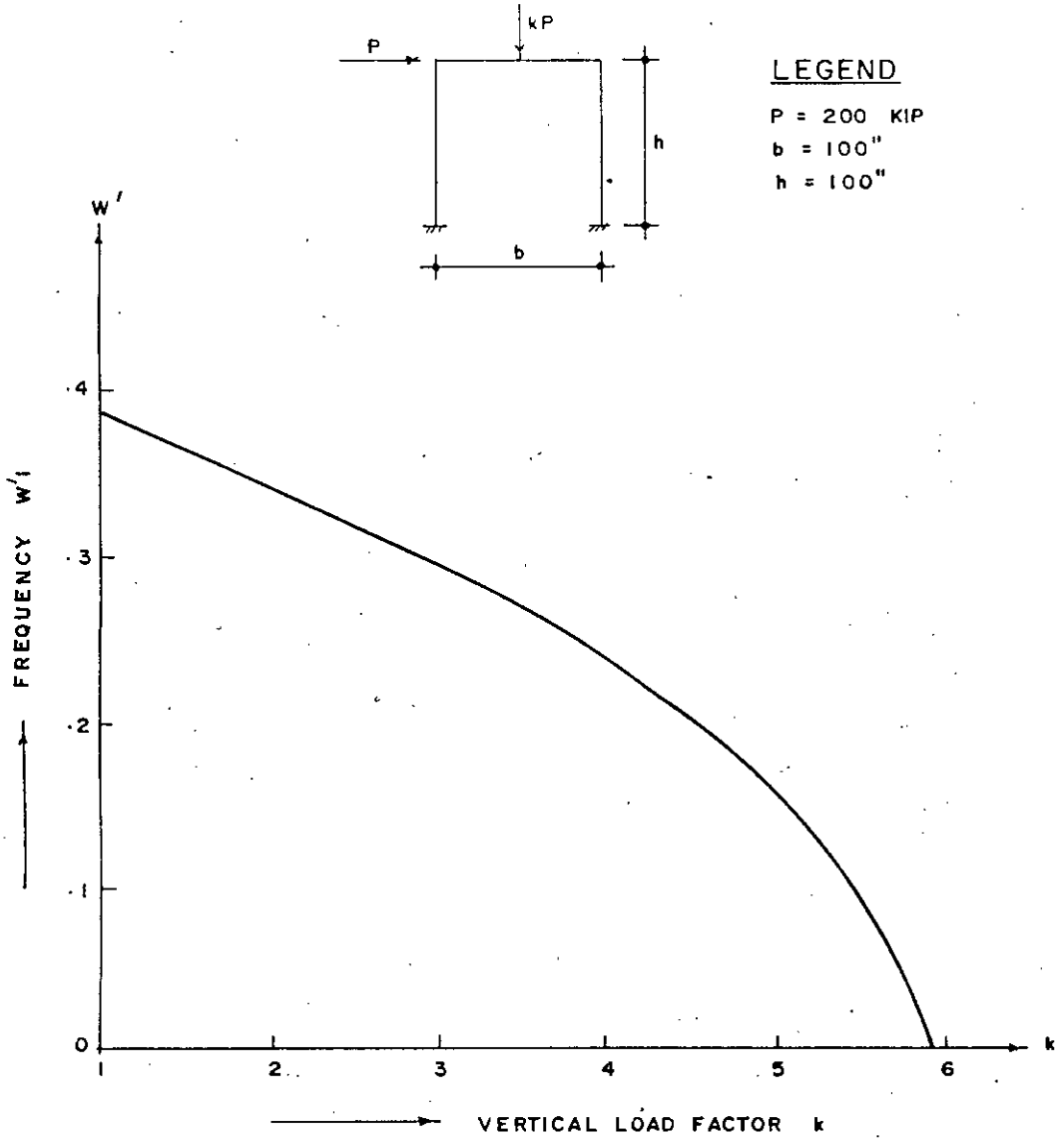

FIG. 4-33: EFFECT OF VERTICAL LOAD FACTOR ON FREQUENCY

to vertical load. This indicates that the structure is more sensitive to vertical load than to horizontal load. This is also practically understandable, as the vertical load certainly will increase the axial force effect in a much more significant way than horizontal load.

4.9.2 Effect on Critical Load

The influence of the relative values of vertical and horizontal loading on the critical load factor are illustrated graphically on Figs. 4.34 and 4.35. In Fig. 4.34, keeping the vertical load p constant of 200 kips, critical load factors are calculated for different values of the horizontal load by changing the value of k. Here k is always greater than unity; or in otherwords, the horizontal load always exceeds the vertical load. The variation of critical load factor λ cr with the ratio of horizontal and vertical load is plotted. It is found that critical load constantly decreases with the increase in the ratio of horizontal and vertical loads. However, it is interesting to note the change in curvature of the curve at a certain value of ratio k. It means that the rate of change of λ cr is not same for all values of k, rather the rate becomes maximum at a certain value of k. In Fig. 4.35 the variation of λ cr with the ratio of vertical to horizontal loading is plotted. Here the horizontal load is kept constant at 200 kips and the critical load factor is computed for

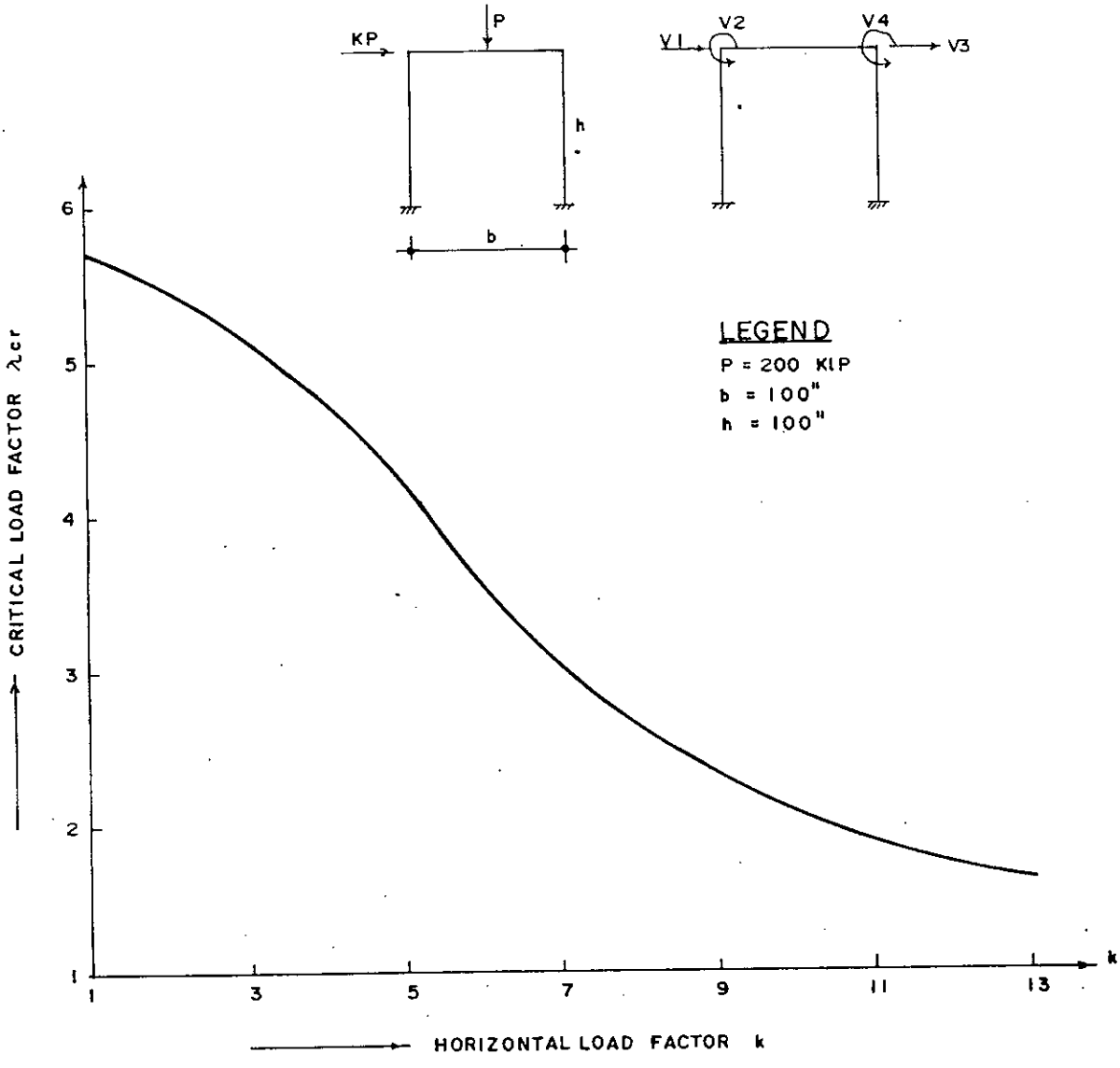

FIG. 4-34 : λ_{cr} VS. HORIZONTAL LOAD FACTOR k CURVE

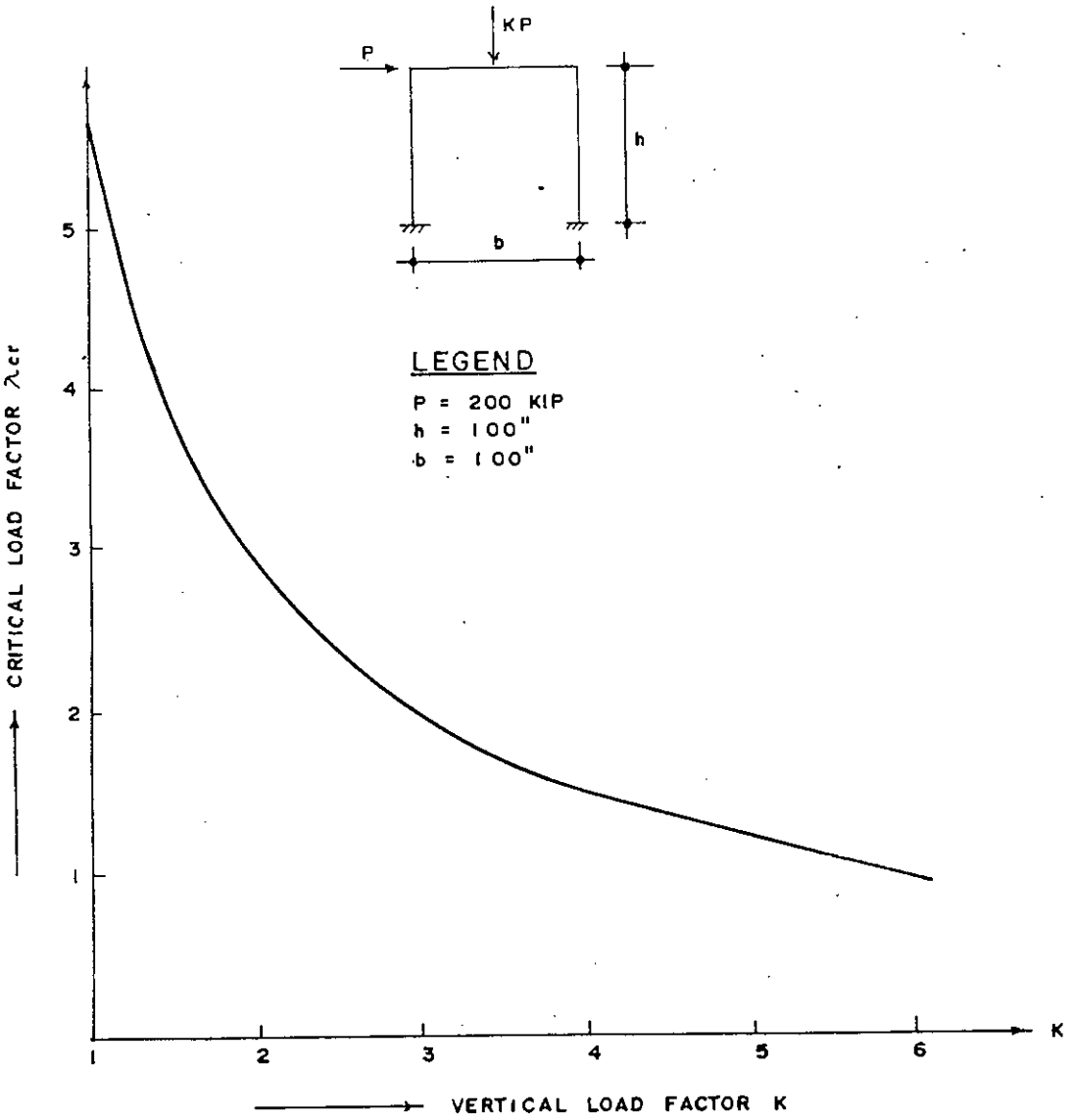

FIG.4-35 : λcr VS. VERTICAL LOAD FACTOR (k) CURVE

different loads by changing the vertical load factor k. Here k is assumed greater than unity or in otherwords vertical load is always greater than the horizontal load. The critical load in both the cases of Figs. 4.34 and 4.35 are computed by standard eigen value solution as earlier. It is found from Fig. 4.35, that the critical load factor λ_{cr} decreases with the increase of vertical load. The rate of decrease of λ_{cr} gradually reduces with increasing k and this rate is higher at lower value of k. Or as it should be, the structure is more sensitive to vertical loading than to horizontal loading. The validity of this conclusion becomes clear from a comparison of Fig. 4.34 and 4.35. Thus for any particular value of k, the load factor λ_{cr} obtained from Fig. 4.35 is always lower than that from Fig. 4.34. It can be concluded therefore to increase the stability of the structure, the vertical load should be kept minimum possible.

4.9.3 Effect on Displacement Response

To compare the effect of the relative values of horizontal and vertical loads on dynamic response, the dynamic load history is assumed same corresponding to all degrees of freedom as shown in Fig. 4.36 to Fig. 4.38. The damping ratios corresponding to all degrees of freedom is assumed same and equal to 0.08. By changing the horizontal and vertical load factor k separately, the dynamic response for both these cases is computed by step by

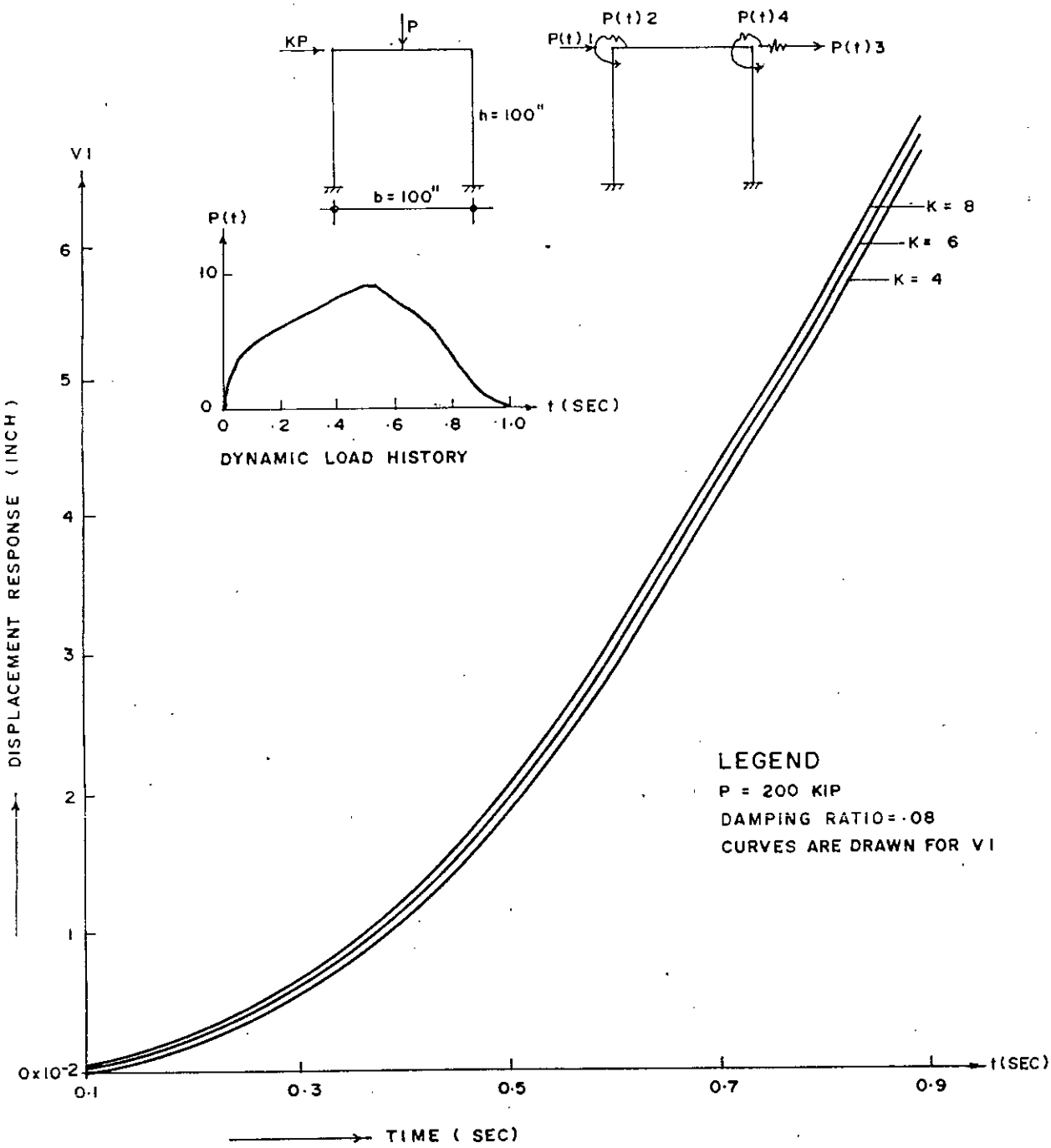

FIG.4 - 36 : EFFECT OF HORIZONTAL LOAD FACTOR ON DISPLACEMENT

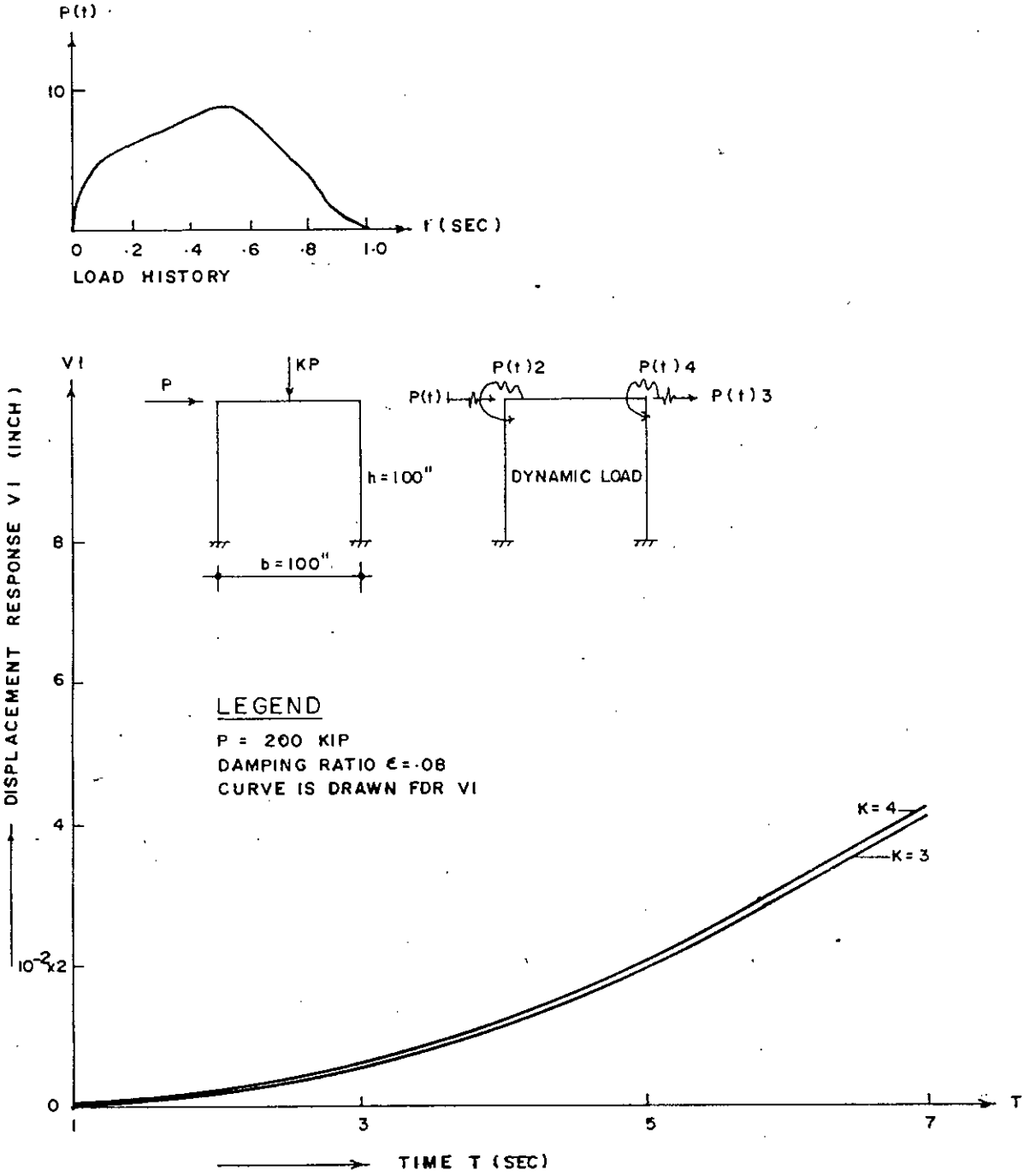

FIG. 4 -37 : EFFECT OF VERTICAL LOAD FACTOR ON DISPLACEMENT

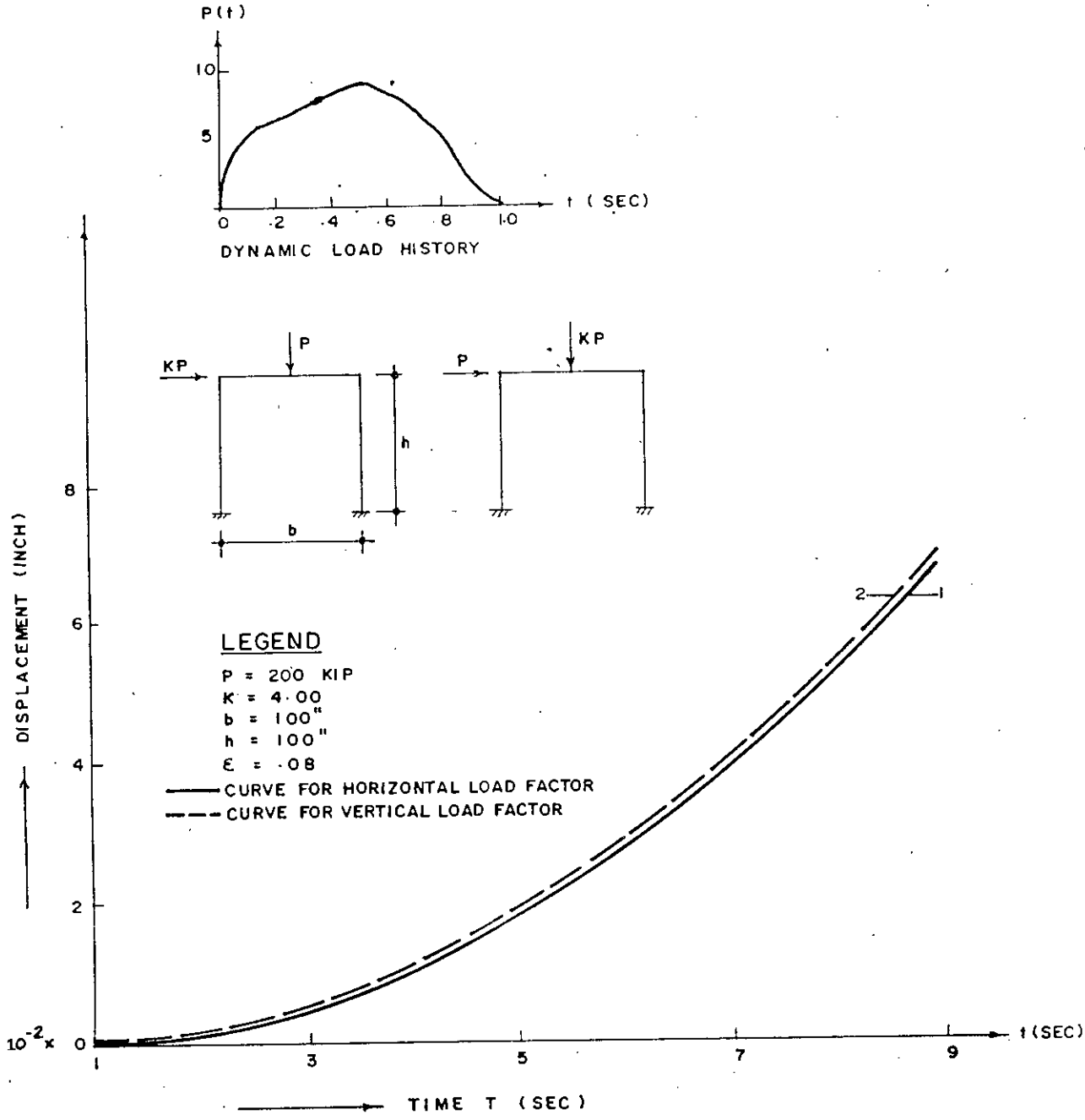

FIG.4-38 : EFFECT OF RELATIVE VERTICAL AND HORIZONTAL LOADING ON DISPLACEMENT

step integration method. The influence of horizontal load factor k on displacement response v_1 is plotted in Fig. 4.36, while the variation of v_1 with vertical load factor k is shown in Fig. 4.37. From these two figures, it is found that the dynamic response increase with increase of load factor k. For a closer comparison of the influence of vertical and horizontal load factor on displacement response the corresponding response verses time curves are plotted for k=4 in Fig. 4.38. It is evident that the dynamic response is higher for the same time increase of vertical load over horizontal than vice versa at any time t. Although the difference in response is not that significant for the value of k taken in Fig. 4.38, it may be quiet significant for greater values of k.

4.10 INFLUENCE OF WARPING ON DYNAMIC RESPONSE

To study the influence of warping on dynamic response a simple portal frame subjected to combined action of static and dynamic load is considered (Fig. 4.39). The width and height of the frame are taken same and equal to 100 inch. The load history for each dynamic load is assumed same and shown in Fig. 4.39. The displacement response v_1 has been calculated by step by step integration method and plotted against time in Fig. 4.39. The solid curve in this figure shows dynamic response when warping is free at joints 2 and 3; the broken curve correspond to the case

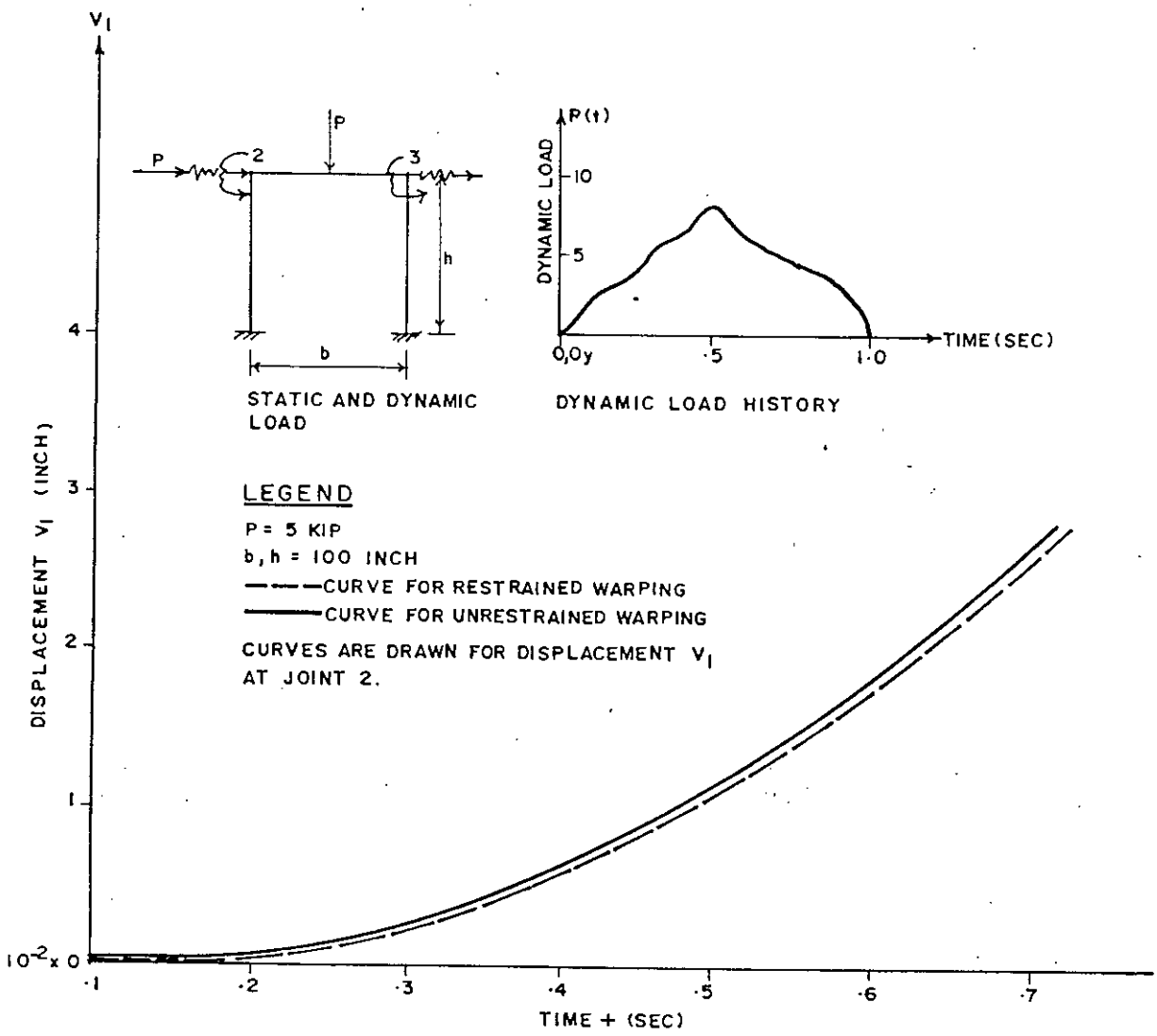

FIG. 4-39: INFLUENCE OF WARPING ON DYNAMIC RESPONSE

of restrained warping at the two joints. These curves show that the dynamic response increases for the case of free warping. This indicates that by restraining warping at joints of a frame, the dynamic stability may be improved.

CHAPTER 5

CONCLUSIONS AND RECOMMENDATIONS FOR FUTURE STUDY

5.1 CONCLUSIOSNS

The followings are the conclusions drawn from the study conducted in this work:

1. The dynamic displacement response increases if the axial force effect is included.

2. The dynamic response of thin-walled frames decreases with the increase in damping ratios and vice-versa.

3. The critical load can be conveniently obtained using the dynamic model incorporating 7 degrees of freedom.

4. Decrease in dyanic stiffness of a structure results due to an increase in static load factor.

5. The critical load capacity of a framed structure decreases and the dynamic displacement response increases with the increase of its height.

6. The simultaneous variation of bay-width and height is found to influence a structure more significantly compared to that when a single parameter is varied. Effect of vertical load on structure instability and frequency modification is more pronounced then that of horizontal load.

5.2 RECOMMENDATIONS FOR FUTURE STUDY

The program developed in this work for the dynamic analysis of geometrically nonlinear thin-walled frames can be modified to consider the physical nonlinearity. Initial imperfection consideration may also be catered by appropriate modification of the program. The nonlinear effect of time varying dynamic load may also be included for future research.

REFERENCES

1. Arthur,N.L.,'Response of Structures to Time Varying Wind Load', Journal of the Structural Divisoon, ASCE, Vol. 96 No. ST2, February, 1970, pp. 381-392.

2. Arthur,C.H., Sing,L. and, Johon,F., 'Dynamic Analysis of Elastic Plastic Frame', Journal of the Structural Division, ASCE, Vol. 90 No. ST2, April, 1964, pp. 315-343.

3. Archer, J.S.,'Consistent Mass Matrix for Distributed Mass System', Journal of the Structural Division, ASCE, Vol. 89 No. ST4, April,1963, pp. 161-178.

4. Bailey, H.R.,'Dynamic Bending of Elastic Columns', Journal of the Structural Division, ASCE, Vol. 89, ST4, August, 1963, pp. 95-114.

5. Barsoum, R.S. and, Gallagher, R.M.,'Finite Element Analysis of Torsional and 'Torsional-Flexural Stability Problems', International Journal for Numerical Methods in Engineering, Vol. 2, 1970, pp. 352-355.

6. Basu, A.K., Nagpal, A. K. and, Nagar, A.,'Dynamic Characteristics of Frame wall System', Journal of the Engineering Mechanics Division, ASCE, Vol. 108, No. ST6, June, 1982.

7. Bathe, K.J. and, Wilson, E.L., 'Numerical Methods in Finite Element Analysis', Prentice Hall, Inc. New Jersy, 1978.

8. Biggs, J.M.,'Structural Dynamics', McGraw Hill Book Company, 1975.

9. Bleich, F.,'Buckling Strength of Metal Structures', Engineering Society Monographs, McGraw-Hill, New York 1952.

10. Burch, G.T.,'Digital Computer Solution for the Dynamic Analysis of Rigid Frames', Journal of the Structural Division, ASCE, Vol. 89, 1963.

11. Charles,B. and, Jerome,S.B., 'Factors Influencing Frame Stability', Journal of the Structural Division, ASCE, Vol. 106, No. ST2, February, 1980, pp. 491-504.

12. Clough, R.W. and, Penzien, J., 'Dynamics of Structures', McGraw-Hill, New York 1975.

13. Cook, R.D.,'Concept and Application of Finite Element Analysis', John wiley and Sons, New York 1974.

14. Fenits, D.G.,'Dynamics and Vibration of Structures', John Wiley and Sons, New York, 1972.

15. Gear, J.M. and, Weaver,W. Jr., 'Analysis of Framed Structure', D. Van Nostrand Company Inc. 1965.

16. Gold berg,J.E.,'Lateral buckling of Braced Multistory Frames', Journal of the Structural Division, ASCE, Vol. 94, 1968.

17. Halldorsson,P. and, Wang,C.,'Stability Analysis of Framework by Matrix Method', Journal of the Structural Division ASCE, Vol. 94, No. ST7, July, 1968.

18. Hancock, G.J.and, Trahair, N.S.,'Finite Element Analysis of the Lateral Buckling of continuously Restrained Beam Columns', The Institution of Australia, May, 1978.

19. Hassan, A.,'A Study on the Torsional Flexural Stability of Restrained Thin-Walled Beams', M.Sc.Engg. thesis, BUET, 1985.

20. Hurty, W.C. and, Rubinstein, M.F., 'Dynamics of Structures', Prentic Hall, New York 1965.

21. Irons, B. and, Ahmad, S., 'Techniques of Finite Element', John Wiley and Sons, 1980.

22. Khalifa, M.K. and, Elgaaly, M.A.,'Stability of Ponny Truss Bridge', Institute of Structural Engineers, U.K. June, 1970.

23. Kitipornchal, S. and, Ritcher, N.J., 'Elastic Lateral Buckling of I-beams with Discrete Intermediate Restraints', The Institution of Australia, July, 1978.

24. Krajcinovic, D., 'A Consistent Discrete Elements Techniques for Thin-walled Assemblages', Int. Journal of Solids and Structures, Vol. 5, 1969.

25. Krajcinovic, D.,'Matrix Force Analysis of Thin-walled Structures', Journal of the Structural Division, ASCE, Vol. 96, No. ST1, January, 1970, pp. 107-122.

26. Leimbach,K.R. and, Donald,Mc., 'Free Vibration of Two Dimensional Framework', Journal of the Structural Division, ASCE, Vol.96, No. ST2, February, 1970, pp. 267-290.

27. Levien, A.M. and, Hartz, B.J., 'Dynamic Flexibility Matrix Analysis of Frames', Journal of the Structural Division, ASCE, Vol. 89, No. ST4, August, 1963, pp. 515-536.

28. Le-Wa-Lu, 'Inelastic Buckling of Steel Frames', Journal of the Structural Division, ASCE, Vol. 91, No. ST6, December, 1965, pp. 159-184.

29. Maison,F. and, Neuss, C.F., 'Dynamic Analysis of Forty-Four Story Building', Journal of the Structural Division, ASCE, Vo. 111, No. ST7, July, 1985, pp. 1559-1574.

30. Powell, G. and, Klinger, R., 'Elastic Lateral Buckling of Steel Beams', Journal of the Structural Division, ASCE Vol. 96, No. ST9, September, 1970, pp. 1919-1932.

31. R. Emilio, 'Slenderness Effects in Buildings', Journal of the Structural Division, ASCE, 1965.

32. Rao, S.S., 'The Finite Element Method in Engineering', Pergamon Press, U.K. 1982.

33. Rawlings,B.,'Dynamic plastic Analysis of Steel Frames', Journal of the Structural Division, ASCE 1964.

34. Razzaq,A. and, Mossa,M., 'Elastic Instability of Unbraced Space Frame', Journal of the Structural Division ASCE, 1980.

35. Snitko, N.K.,'Dynamics of Structur', Moscow 1960.

36. Sulata, K., 'Finite element Analysis of R.C. Frames', Journal of the Structural Division ASCE, Vol. 110, 1984.

37. Timoshenko S.P. and, Gere, T.M., 'Theory of Elastic Stability', 3rd Edition, Mcgraw-Hill Book Company, New York, 1961.

38. Torkamoni, A.M.,'Dynamic response of tall Buildings to Wind Excitation', Journal of the Structural Division, ASCE, Vol. 111, No. ST4, April, 1985, pp. 805-825.

39. Trahair, N.S., 'Elastic Stability of Continuous Beams', Journal of the Structural Division, ASCE. Vol. 95, No. ST6, June, 1969, pp. 1295-1312.

40. Vasquer, J. and, Riddell, R.,'Thin-walled Core Element for Multistory Buildings', Journal of the Structural Division, ASCE, May 1984.

41. Vlassov, V.Z., 'Thin-walled Elastic Beams', Second Edition. Israel Program for Scientific Translations, Jerusalem, 1961.

42. Weaver, W. Jr., 'Computer program for Structural Analysis', D. Van Nostrand Company. Princeton, N.J, 1967.

43. Wang, P.C.,'Numerical and Matrix Methods in Structural Mechanics', John Wiley and Sons, New York, 1966.

44. Zienkiewicz, O.C., 'The Finite Element Method', 3rd Edition, McGraw-Hill Book Company, 1977.

বাংলাদেশ প্রকৌশল বিশ্ববিদ্যালয়
নং 75709
তাং 24-10-89
লাইব্রেরী, ঢাকা